Review article

Recent development in multizonal scaffolds for osteochondral regeneration

Le Yu [a],[1], Sacha Cavelier [a],[1], Brett Hannon [b], Mei Wei [b],[c],[*]

[a] Department of Chemical and Biomolecular Engineering, Ohio University, Athens, OH, 45701, USA
[b] Biomedical Engineering Program, Ohio University, Athens, OH, 45701, USA
[c] Department of Mechanical Engineering, Ohio University, Athens, OH, 45701, USA

ARTICLE INFO

ABSTRACT

Osteochondral (OC) repair is an extremely challenging topic due to the complex biphasic structure and poor intrinsic regenerative capability of natural osteochondral tissue. In contrast to the current surgical approaches which yield only short-term relief of symptoms, tissue engineering strategy has been shown more promising outcomes in treating OC defects since its emergence in the 1990s. In particular, the use of multizonal scaffolds (MZSs) that mimic the gradient transitions, from cartilage surface to the subchondral bone with either continuous or discontinuous compositions, structures, and properties of natural OC tissue, has been gaining momentum in recent years. Scrutinizing the latest developments in the field, this review offers a comprehensive summary of recent advances, current hurdles, and future perspectives of OC repair, particularly the use of MZSs including bilayered, trilayered, multilayered, and gradient scaffolds, by bringing together onerous demands of architecture designs, material selections, manufacturing techniques as well as the choices of growth factors and cells, each of which possesses its unique challenges and opportunities.

1. Introduction

Osteochondral (OC) tissue engineering has attracted considerable interests of researchers over the past decade due to the rapid increase of osteoarthritis (OA) patients. OA is a musculoskeletal condition described as loss of articular cartilage within synovial joints [1]. It was estimated that 80% of individuals over the age of 65 have signs of osteoarthritis development in at least one joint of their bodies [2]. This condition is characterized by joint pain, tenderness, crepitus, limitation of movement, stiffness, and inflammation, most commonly in the hand, spine, knee, hip, and foot [3]. One of the causes of OA is the progression of OC defects [4]. Defects in OC tissue are organized into five categories: normal chondral tissue (Grade 0), swelling and softening of chondral tissue (Grade I), partial thickness chondral defects (Grade II), full thickness chondral defects (Grade III), and OC defects (Grade IV) [5,6]. A partial thickness chondral defect only extends into cartilage; a full thickness chondral defect extends across cartilage and into the junction of the calcified cartilage and subchondral bone layers, commonly known as an OC defect [7–9]. Such a defect remains challenging to be treated due to the complex composition, spatially arranged multizonal architecture, and varied functionalities of each region of the OC tissue.

Current practices for OC repairs depend on the severity of the defect. For instance, for articular cartilage lesions less than 2.5 cm, subchondral bone is penetrated and fractured to create a full thickness of chondral defect [10]. Once a fibrin clot forms over the subchondral bone surface, native stem cells differentiate into chondrocytes and osteocytes [11]. However, this technique, although convenient, affects the quality of the repair as fibrocartilage tissue, rather than the functional hyaline cartilage, is typically formed [12,13]. Further, the mechanical properties of fibrocartilage were found inferior to native cartilage tissue [14], which limits the application of the technique even in small lesions. Cartilage can also be replaced via transplantation of another non-load bearing or low-bearing joint of the body (autograft) or from a donor's joint (allograft). Autografting procedures for OC repair are however restricted by limited supplies of available cartilage sites, site morbidity, postoperative rehabilitation, and fixation of graft into defect sites [6,15]. When conducting an autograft transplantation, concerns of the donor site damage, donor tissue long-term stability, and integration with native cartilage arise [16]. Due to the greater availability, allograft transplantation has been a more common approach for cartilage repair. Studies have shown

---

that hyaline cartilage regeneration is feasible using fresh and frozen allografts [17]. However, immunogenetic responses from the host and graft preservation issues arise because of the lack of adequate testing for bacterial and viral infections in donor allografts [18–20].

Tissue engineering strategies have emerged as outperformed alternatives, among which multizonal scaffolds (MZSs) have been regarded as a preferred design for the repair of OC defects as they exhibit superior performances than single-phased scaffolds [21]. The structure and composition of the extracellular matrix (ECM) of the OC tissue vary in the superficial, transition, deep, and subchondral bone zones [22]. Creating a multilayered scaffold mimicking the structural variations appears to be a feasible approach to reproduce the spatial organization of OC tissue, and addition of corresponding growth factors and cells further generates suitable microenvironments for cartilage and subchondral bone formation [23,24]. Still, it remains a challenge to attain such a structure with optimal osteochondral regeneration potential. For instance, the bonding between multiple layers is generally weak. The porosity and pore distribution within the cartilage and bone transitional layer are difficult to control but they are crucial for maintaining the integrity of the scaffolds, preventing the zonal migration of differentiated cells, preventing the unwanted invasion of blood vessels and nerves from the subchondral bone to cartilage, and allowing for sufficient flow of nutrients and wastes [25]. The design of such an interface remains a challenge when the cartilage and bone layers are created separately. Despite of all the challenges, MZSs have demonstrated superior in vivo performances, and have generated growing interest in using this type of architecture for OC repair [26,27]. The outcome of MZSs in repairing OC tissue largely depends on the synergistic action of the following factors: scaffold material selection, architectural design, fabrication technique, and growth factors (GFs) and cells loaded (Fig. 1).

OC tissue engineering is a fast-growing field where innovative methods, advanced biomaterials and novel architectures have rapidly emerged over the last a few years. Such developments have addressed partially the limitations of earlier practices, but new challenges have also risen. This review aims to focus on the most recent reports that have provided efficient replicates of OC tissues, particularly those with the use of MZSs. It will begin with an overview of the function and hierarchical architecture of OC unit and then focus on the biomimetic architectures of MZSs, material selections, the latest fabrication techniques, and the impact of cells and growth factors incorporated in the MZSs. At the end, challenges and future perspectives of the field will be discussed.

2. Hierarchical structure of osteochondral tissue

2.1. Overview

Osteochondral tissue consists of articular cartilage, calcified cartilage, and subchondral bone. Among them, articular cartilage is hyaline cartilage, which is the most abundant type of cartilage found in human body [28,29]. Unlike bone, articular cartilage is avascular, aneural, and lacks lymphatic vessels [28,30]. It is composed primarily of 65–80 wt% water, 10–20 wt% collagen (predominantly type II), and 10–20 wt% proteoglycans (predominantly aggrecans) [31,32]. Other types of collagen and proteoglycans are also found in articular cartilage but less abundant [32–35]. Collagen is organized in fibers that are oriented specifically to withstand forces acting on the cartilage tissue. In addition, these fibers provide mechanical support to the ECM and residence to the chondrocytes for each zone in articular cartilage [33]. Fig. 2 summarizes the morphologies of chondrocytes and orientations of collagen fibers in each zone of the OC tissue. At the surface of the unit, the superficial zone of articular cartilage acts as a lubricant that transmits mechanical loads and aids in bone movement in an efficient low-friction manner [29,36]. Notably, aggrecan, a negatively charged elastic proteoglycan, binds to hyaluronic acid (HA), and works with collagen fibers to resist compressional stresses [37,38]. To explain the compressive viscoelastic behaviors of cartilage, a mechanical model that considers cartilage as a solid matrix with interstitial fluid (biphasic poroelastic theory) was proposed by Mow et al. [37,38], where two articular cartilage properties were characterized: the aggregate modulus (stiffness of the tissue at an equilibrium state) [39] and the permeability (resistance of the interstitial fluid through the solid matrix) [40]. The aggregate modulus of cartilage is measured between 0.5 and 0.9 MPa [39,41], and a decreasing trend of the permeability is observed from the superficial to the deep zones [42]. The porosity of cartilage is in the range 60–85% with a mean pore size of 2–6 nm [43]. Subchondral bone has a porosity ranging from 5 to 90% and a pore size of 0.1–2000 μm, each increasing from the cortical bone layer to the trabecular bone layer [43,44]. Besides the depth-dependent porosity and pore size distributions, the compressive modulus as well as the tensile moduli in the directions of both perpendicular and parallel to the cartilage surface also demonstrate a depth-dependent manner. The compressive modulus exhibits an increasing trend while the tensile modulus shows a decreasing trend from the superficial to the deep zone [43]. Between the articular
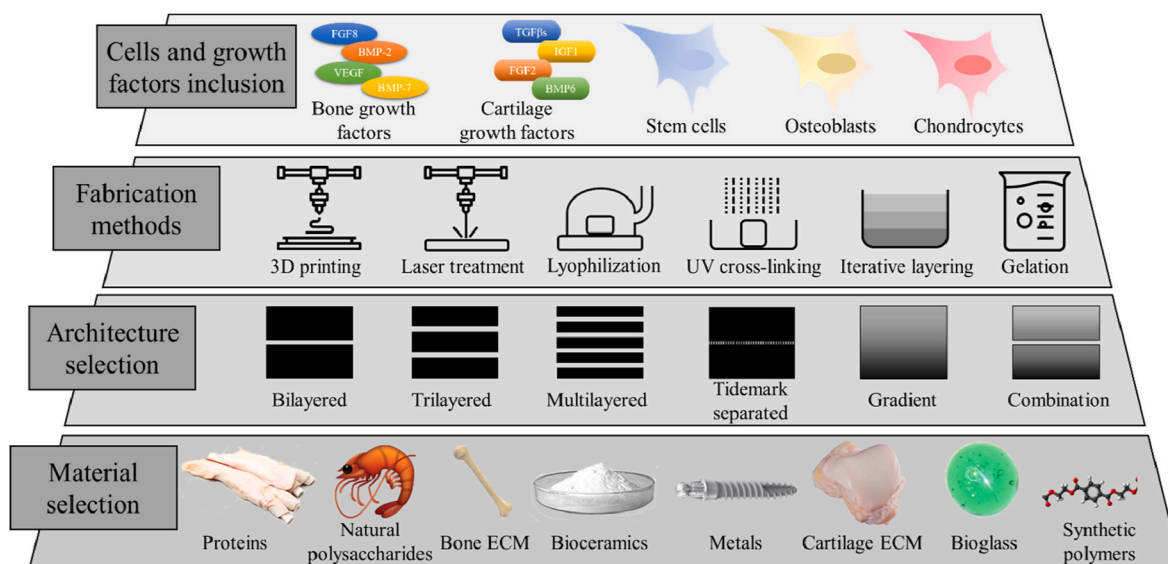
Fig. 1. Decision-making process in fabrication of a novel MZS. Choices of materials and architectures are crucial for the biological and mechanical performances of the MZS. Fabrication methods need to be adapted to increase the degree of control on the structural and composition parameters. Loading GFs and/or cells are add-on strategies to adjust the chondrogenic and osteogenic properties of corresponding regions by providing biological and environmental cues.
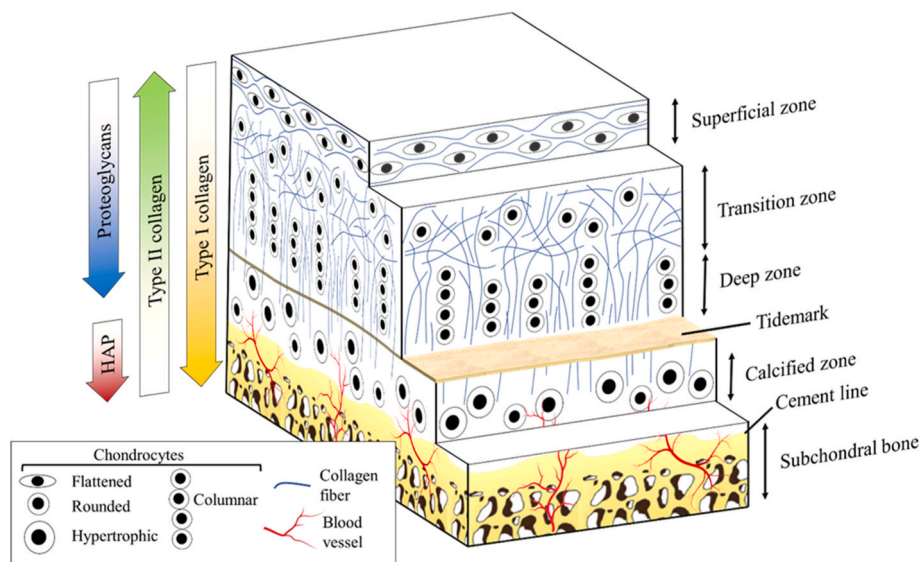
Fig. 2. Schematic illustration of the multilayered structure of osteochondral tissue and its main individual components, including collagen fibers, chondrocytes, and extracellular matrix composition.

cartilage and the subchondral bone, there is an interfacial layer known as the calcified cartilage zone, which is responsible for force transmission, nutrition and waste transportation, and microenvironment stabilization. Notably, a thin 3D tidemark representing the junction of calcified and uncalcified cartilage is important to maintain the complexity of osteochondral tissue, for instance, by preventing blood vessel and nerve invasions from the subchondral bone to the cartilage tissue.

2.2. Anatomical hierarchies and zonal functions

Superficial zone - The superficial zone (SZ) is the outermost layer of articular cartilage. Consisting of approximately 10–20% of the overall thickness, the collagen fibers arrange parallelly to the articular surface in the SZ [40]. This orientation is optimal for resisting in shear and tensile stresses that occur at the articular surface [45]. These collagen fibers are tightly packed and surrounded by flattened chondrocytes, as shown in Fig. 2. The chondrocytes synthesize high concentrations of collagen, up to 86% dry weight, and low concentrations of proteoglycans in the SZ [29,36], which confers the highest water concentration of all the zones in articular cartilage [32]. The collagen fibers in this zone primarily consist of type II and type IX collagen [43,46]. The articular surface consists of lamina splendens, a thin membrane composed of synovial fluid [47].

Transition zone - Following the superficial zone, the transition zone (TZ), or the middle zone, represents approximately 40–60% of the overall thickness. Type II collagen fibrils in this layer are thicker compared to those in the SZ and are organized obliquely, as shown in Fig. 2 [40]. The collagen fibers compose of 67% dry weight of the tissue [43]. Its main functions include serving as the first line of defense to compression stresses and deformation to loads [36,48]. The chondrocytes are rounded and surrounded by the abundant ECM [29] and the concentration of proteoglycans is higher compared to the SZ [36].

Deep zone - Beneath the transition zone, the deep zone (DZ) accounts for approximately 30% of the articular cartilage thickness [46] and exhibits type II collagen fibrils with the largest diameter. The fibrils are oriented perpendicularly to the articular surface and play a crucial role in resistance to compressive forces [40]. The chondrocytes in this layer are arranged in a columnar structure as shown in Fig. 2 [49]. Notably, the cell density decreases by 59% and 67% from the superficial zone to the transition and deep zones, respectively [50], while the proteoglycan concentration is at its highest and the water content is the lowest in this

zone [4,36].

Calcified cartilage zone –Tidemark distinguishes the non-calcified zone from the calcified zone. This structure maintains a specific geometric pattern that counters articular shearing [36]. The calcified cartilage zone is then located beneath the tidemark and can be characterized as the transition from cartilage to subchondral bone by calcification of the ECM. It consists of chondrocytes with hypertrophic phenotype as depicted on Fig. 2. These chondrocytes produce type X collagen and calcify the ECM to provide an excellent structural integration with the subchondral bone [28]. This zone has many hollows, protrusions, and interlacing that resist shear stresses from separating cartilage and subchondral bone [40].

Subchondral bone zone - The subchondral bone zone is separated from the calcified cartilage zone by a cement line, as shown in Fig. 2. The subchondral bone is composed of two primary components: trabecular bone and subchondral bone plate (cortical bone) [6]. The subchondral bone plate lies just beneath the calcified cartilage zone and is marked with porosity demonstrated as channels populated by blood vessels and nerves [6]. The trabeculae bone supports cartilage and acts as a shock absorber. The bone tissue consists primarily of type I collagen and hydroxyapatite (HAP) [51–54]. Notably, unlike normal bone tissues which consist of about 60% dry weight of hydroxyapatite, HAP constitutes 85.8 ± 3.4% dry weight of the subchondral bone [43]. Cell population in subchondral bone consists mainly of osteoblasts, osteocytes, osteoclasts, and bone lining cells, which are differentiated from local mesenchymal stem cells (MSCs) [55,56]. Osteoblasts form new bone tissue via HAP synthesis, while osteoclasts activity is responsible for bone resorption to optimize the stiffness-to-mass ratio of bone. Finally, osteocytes regulate interactions between bone cells [56].

3. Biomimetic architectures in MZS

Cartilage injuries usually extend to the subchondral bone zone. Full-thickness repairs are therefore required to increase the long-term functionality of the OC tissue [57]. Mechanical, biological, and physico-chemical differences across the OC structure, from cartilage to subchondral bone, pushes the exploration of novel MZS designs to better mimic the complexity of natural OC tissue. Regenerating the cartilage layer appears to be a huge challenge given the absence of neural and vascular networks and limited presence of chondrocytes [58,59]. The subchondral bone, although less challenging to be repaired [60], remains a key structural element as it is the foundation of the OC tissue

and its incomplete restoration is problematic for the long-term functionality of the implant [61].

The creation of multizonal scaffolds aims to address these issues by exhibiting gradient mechanical properties that are compatible with the stresses in human joints [1], promoting zonal-specific cell homing, proliferation, and differentiation, allowing nutrient flow via interconnected pores [62], providing integration between the regenerated tissue and native tissue, and maintaining sufficient adhesive strength between the zonal interfaces [59,63–65]. Design strategies with various levels of complexity (bilayered, multilayered, or gradient) have been developed, each with its own set of advantages and drawbacks.

3.1. Bilayered scaffolds

A simple way to mimic OC architecture is to combine a cartilage and a subchondral bone layer with tailored physical and chemical properties into a bilayered scaffold (Fig. 3A). The ideal structure of OC scaffolds must exhibit (i) a chondrogenic microenvironment for cartilage formation; (ii) an osteogenic microenvironment for subchondral bone regeneration; (iii) a cartilage layer – bone layer interface; (iv) a good integration with the native tissue [23,66]. This last point is typically facilitated by pressing fit the scaffold into the subchondral bone defect for better integration [18].

While monophasic scaffolds have failed to simultaneously combine chondrogenicity and osteogenicity [67], recently developed bilayered scaffolds tend to address this issue. A common strategy for the design of bilayered scaffolds with both chondrogenicity and osteogenicity is to use

polymers as the cartilage layer and polymer-embedded bioceramics as the bone layer [21,57,59,69–77]. Studies reported bilayered scaffolds coupling polymer-camphene [78], two different polymers [68], polymer-bioglass [79], and decellularized cartilage matrix-decalcified bone matrix [66,80] to promote both osteogenesis and chondrogenesis. In some cases, osteoconductive metals are used for the bone layer [81–85]. Specifically, HAP (further discussed in Section 4) has been embedded in the bone layer due to its remarkable osteoconductive property. For instances, zonal-specific osteogenic and chondrogenic differentiation of BM-MSCs was obtained due to the inclusion of HAP in the bone layer of chitosan [59], gelatin [70] or silk fibroin-chondroitin sulfate based bilayered scaffolds [57].. The incorporation of HAP is also a useful strategy to improve the mechanical properties and decrease the biodegradation rate of the layer [59].

Currently, the main issue in bilayered scaffolds is the poor bonding strength between the two layers [86,87]. Adhesion at the interface must be high enough to allow surgical manipulation of the scaffolds and avoid delamination. Previous studies evidenced that a superior adhesive strength at the interface increased the chance of tissue integration and repair [56,88]. A strong interface could be achieved via controlled crosslinking of scaffolds [59]. Particularly, in this study, the subchondral bone layer was partially crosslinked using genipin before the second cartilage layer was cast. Then the bilayer structure was further crosslinked and freeze-dried. After the incorporation of nHAP, the composite scaffold was crosslinked one more time. Such prepared scaffolds have controlled degree of crosslinking, and they demonstrated good integration between the two layers and failed in tension away from
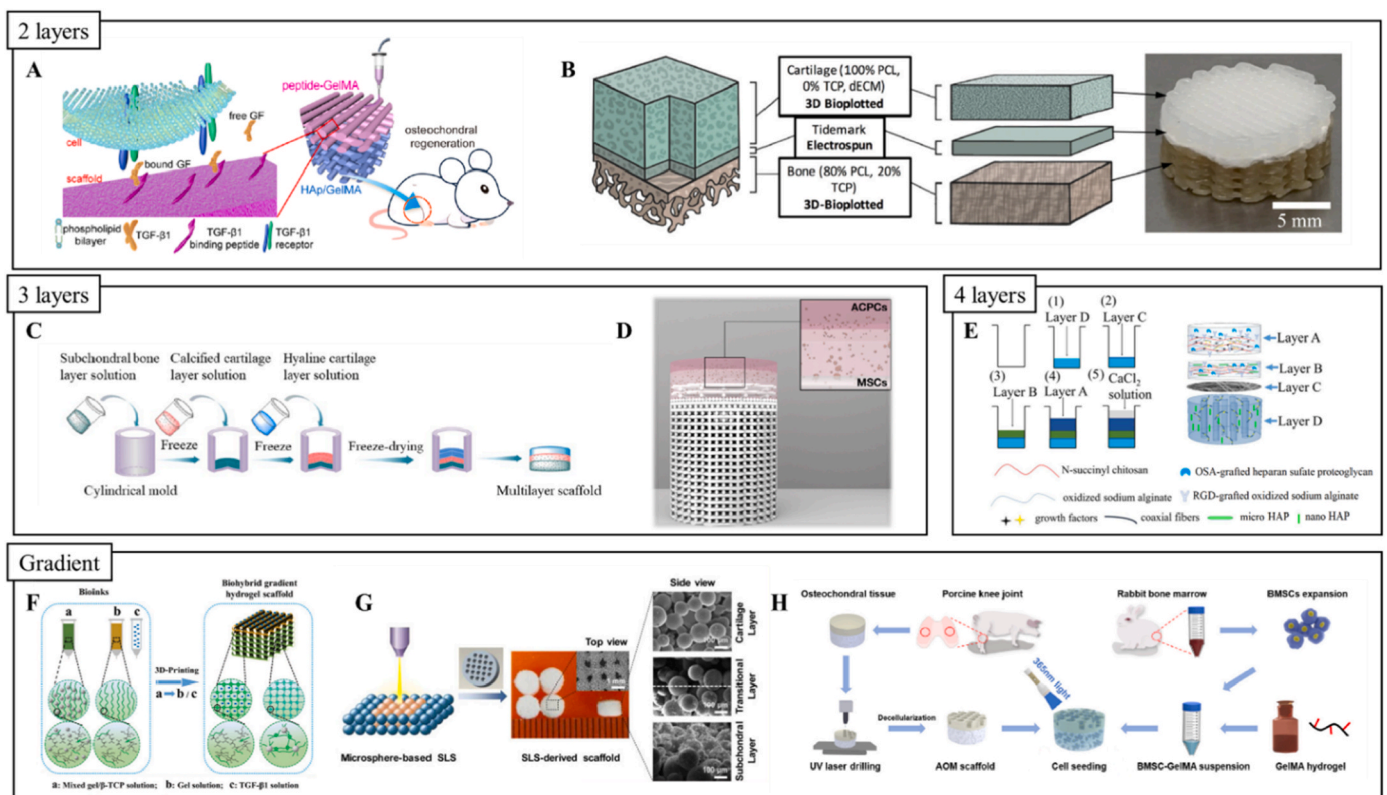

Fig. 3. A. A bilayered scaffold consisting of a 3D printed gelatin-based matrix with HAP in the bone layer (BL), and growth factors (GFs) in the cartilage layer (CL). Adapted with permission from Ref. [76]. B. Bilayered scaffold with BL and CL separated by a thin electrospun PCL tidemark. Adapted with permission from Ref. [94]. C. A category of trilayered scaffolds used bioceramics in the middle layer (calcified cartilage layer, CCL) in addition to BL. Adapted with permission from Ref. [96]. D. In another version of trilayered scaffolds, a non-mineralized middle layer (ML) was used. Adapted with permission from Ref. [58]. E. A high degree of complexity can be achieved with multilayered scaffolds, with more than three layers, multiple polymeric materials, bioceramics, and GFs. Adapted with permission from Ref. [65]. F. A category of gradient scaffolds used gradient porosity to reproduce the structure features of the OC tissue (the pore size was in the range of 360–700 μm). Adapted with permission from Ref. [72]. G. Gradient composition scaffolds usually involve progressive HAP contents with a higher HAP content (30 wt%) in the BL. Adapted with permission from Ref. [97]. H. Gradient scaffolds fabricated from ECM take advantage of the gradient porosity and composition naturally present in the OC tissue but require a decellularization process and/or in combination with other materials. Adapted with permission from Ref. [66].

the interface. Another example using controlled crosslinking to achieve strong integration between the bone and cartilage layers of bilayered scaffold was reported by Lin et al. [79], where a novel solvent-free urethane crosslinking method was developed to produce porous poly (glycerol sebacate) (PGS) scaffolds with controllable crosslinking degrees. Guo et al. [89] have also utilized a gentle pre-cross-linking strategy on a loosely cross-linked cellulose network to retain a strong integrality of a bilayered osteochondral scaffold. In the case of ECM-based bilayered scaffolds, laser drilling was an effective approach to achieve both ideal pore size and strong adhesive strength of the bilayered scaffold [66,80]. . Besides crosslinking and laser drilling, binding the bone and the cartilage layers with a bioglue showed some success in terms of its interfacial mechanical responses of the scaffolds [93], but the low permeability at the interface hindered cell migration and differentiation, leading to poor integration between the newly regenerated bone and cartilage layers [25]. Recent studies further confirmed that inserting a dense tidemark layer at the interface (Fig. 3B) prevented cell migration within bilayered polymeric scaffolds and eventually delayed the integration of the cartilage layer [74,84,94]. Another approach to diminish mechanical weakness at the interface between the two layers was to fabricate bilayered scaffolds using one single polymeric material but two different pore size distributions. . Notably, Duan et al. [68] tailored the size of pores in cartilage and bone layers of poly(lactide-coglycolide) acid (PLGA) bilayered scaffolds in order to promote chondrogenic and osteogenic differentiations (average pore size of 100–200 μm for the cartilage layer and 300–450 μm for the bone layer). This approach produced scaffolds with tensile and compressive mechanical properties close to those of native tissues, but limited tissue repair in vivo [68]. In addition, a computational investigation has been conducted recently at the interfaces of bilayered polymeric scaffolds, and the results showed that polycaprolactone (PCL)/gelatin methacrylate and PCL/polyethylene glycol diacrylate (PEGDA) scaffolds exhibited the best tensile, compressive and shear properties among various polymer scaffolds produced by 3D printing [92]. This insight could guide future studies on construction of polymeric bilayered scaffolds by selecting appropriate biomaterials (discussed in Section 4).

Despite extensive attention has been paid to enhance the interfacial strength of bilayered scaffolds and zonal chondrogenicity and osteogenicity, the oversimplification of the anatomical architecture of OC tissue into a bilayered structure limits the performance in regenerating OC defects using bilayered scaffolds. For instance, abrupt changes in Young's modulus between the two layers could eventually lead to unstable structure at the interface and poor integration [95]. A transition layer, also called middle layer (ML) or calcified cartilage layer (CCL, Fig. 3C), can be inserted at the interface, forming a trilayered scaffold.

3.2. Trilayered scaffolds

In addition to addressing the aforementioned inter-layer instability, the intermediate layer in trilayered scaffolds can support an additional compressive load [65]. The CCL also contributes to vascular development in the neobone tissue while facilitating an avascular environment in the cartilage layer [90]. Like the tidemark in bilayered scaffolds, a CCL acts as a physical barrier that maintains low oxygen levels and avascular environment, which is beneficial for chondrogenic differentiation [98]. To fulfil these requirements, the CCL must exhibit a specific microstructure. In human OC tissue, the porosity of the CCL is only 1.6–9.7%, with pores ranging from 11 to 39 nm. Such an architecture not only blocks nutrients larger than 10 nm, but significantly delays their migration. Indeed, the interconnectivity of the porous network is poor, and according to a recent simulation [99], the diffusion of solute transport was estimated to be 2000 times lower than that of subchondral pores. In such an environment, the cell density is three times lower than that of hyaline cartilage [100]. The composition of the human CCL is between those of the uncalcified and the calcified tissues. Within its

thickness of ~100 μm, the collagen content in CCL is three times lower than that in hyaline cartilage, and the mineral content is slightly inferior to that of the subchondral bone [96]. The regeneration of such a structure and composition is therefore a challenge for tissue engineering. To address this issue, cell-based approaches have been attempted using chondrocytes to form a CCL by secreting type II collagen and a mineral phase, but the degree of control of this technique remains low [101]. On the other hand, scaffold-based strategies have been made with their structure, composition, and mechanical and biological properties exquisitely tailored through various chemical modifications such as by incorporating inorganic bioceramics or bioglasses [102,103]. More importantly, a CCL barrier allowing the transportations of oxygen and nutrition while minimizing cell passage can be obtained by both densifying the layer and reducing the pore size [98].Recent studies on trilayered scaffolds with an intermediate dense layer exhibited not only superior regeneration of hyaline-like cartilage and subchondral bone tissue in vivo [104–106], but also improved mechanical properties of the neo-formed tissues compared to bilayered scaffolds [64,104].

Despite these promising results with a denser CCL to regulate the flow of nutrient and cell migration, most of the trilayered scaffolds exhibit an architecture with progressive pore sizes [96,107,108] and/or compositions [23,96,107–111]. For example, Hu et al. [108] fabricated chitosan-gelatin based scaffolds with 0, 10, and 30 wt% of HAP in the cartilage, CCL, and bone layers, respectively, and gradient pore diameters ranging from 153.5 μm to 325.3 μm were observed across the cartilage zone and the bone zone. The scaffolds exhibited matching compressive properties with those of natural cartilage and appropriate degradation rate. Adipose derived mesenchymal stem cell (AD-MSCs) differentiated into either chondrogenic or osteogenic lineage and the differentiation was particularly promoted by a dynamic mechanical stimulation in an in vitro setting. Unfortunately, tissue regeneration was relatively poor in vivo without dynamic stimulation. Similarly, Zhou et al. [96] created collagen I-sodium hyaluronate based trilayered scaffolds with gradient HAP contents and pores sizes, and observed appropriate biodegradation rate, excellent cell adhesion and proliferation but low compressive properties (Fig. 3C).

Besides the aforementioned architectures, more features have been added to the trilayered scaffold designs, forming multilayered scaffolds. Qiao et al. [112] highlighted the importance of lubrication at the surface of a cartilage layer As a result, their design conststsd of a gelatin matrix reinforced with PCL and poly(ethylene glycol) (PEG) oriented fibers mimicking the orientations of collagen fibrils in the superficial, deep, and subchondral bone zones. Such configuration was beneficial for in vitro chondrogenic and osteogenic differentiations of BM-MSCs, and in vivo cartilage and subchondral bone regenerations. In another study by Gegg and Yang [109], gelatin matrix was reinforced by chondroitin sulfate microribbons. The resulting trilayered scaffolds exhibited strong interfacial bonding and enhanced cartilage matrix production. When the microribbons were aligned, collagen deposition in superficial zone was improved. A 4-fold increase in glycosaminoglycans (GAGs) production was observed, and the compressive modulus of the neo-formed cartilage increased to a level matching that of the native tissue. However, due to the complexity of such designs, only a few recent studies have adopted oriented fibers in constructing multilayered scaffolds [58,78,104].

Although trilayered architectures exhibit better biological performances compared to bilayered scaffolds, multiple issues were raised. For instance, the facts that the biodegradation rate and mechanical property mismatch between adjacent layers [6,19] are the major limitations causing poor tissue integration and even the collapse of the newly formed tissues. Moreover, multilayered scaffolds bring unwanted complexity, such as long fabrication process and low reproducibility [110,113]. Chen et al. [65] reported that the highest histological score (24.2 based on the O'Driscoll scoring system 12 weeks post implantation in rabbits) for OC repair was obtained with a 4-layer scaffold involving 5 different materials and growth factors: an alginate-chitosan cartilage layer, an alginate-chitosan-HAP CCL, a PCL-PEG fibers electrospun

membrane, and an alginate-HAP bone layer loaded with growth factors (Fig. 3E). Further, concerns of weak interfacial mechanical properties and delamination rise as stratification of MZSs increases. They generally exhibit poor long-term performances (e.g. weak integration with the native tissue, loss of mechanical properties etc.), which negatively impact their translation to long-term clinical studies [56]. A better way to mimic the OC tissue structure and address the issues related to the discrete scaffold properties lies in the development of continuous gradient scaffolds.

3.3. Gradient scaffolds

Although multilayered scaffolds exhibit phases with different structures and properties inspired by the zonal structure of native OC tissue, gradient scaffolds may effectively address the issues of poor integration at interfaces [114] while demonstrating strong capability in regenerating subchondral bone, cartilage, and the bone-cartilage interface [115]. These gradient scaffolds better mimic the structural and compositional transitions in native OC tissue [116] and minimize shear stresses between two adjacent zones [117]. The challenges in constructing gradient scaffolds reside in the presence of a mechanical gradient that supports the compressive stress [72,108], an interconnected pore network that reflects that of OC tissue [118,119] and the ability to promote cell differentiation in osteogenic and chondrogenic lineages. Recent developments led to investigations of gradient hydrogels [72,118, 120–122], MZSs with gradient porosity (Fig. 3F) [27,63,72,86,97,119, 121,123] and/or composition (Fig. 3G) [96,97,116,119,124], and decellularized cartilage ECM (Fig. 3H) [125]. Notably, it is also possible to simply achieve gradient properties in homogeneous structures by applying external triggers to redistribute the prefabricated uniform constructs, forming a "fake" gradient MZS for osteochondral regeneration (to be discussed in Section 5.4).

3.3.1. Gradient compositions

Creating a gradient composition in MZSs is a common strategy to mimic the features of OC tissues where the fraction of collagen and HAP, which confers strength and stiffness to subchondral bone, varies and creates different cell environments [96]. As a result, constructing gradient composition in MZSs improves their mechanical properties [126], bone-cartilage interface integration, and tissue regeneration [63] compared to single-layered or bilayered scaffolds [96]. In order to produce compositional gradient, the majority of the recent studies combined HAP particles with PCL or gelatin. HAP volume fraction ranging from 7 to 50 wt% in the bone layer to 0 wt% in the cartilage layer demonstrated positive impacts on chondrogenic and osteogenic differentiation [116], tissue regeneration [97] and/or improvement of mechanical properties [97,119,127]. Although MZSs with only gradient compositions achieved one or more of the above advantages, they still require further adjustments to achieve desired overall performances.

3.3.2. Gradient structures

The gradient porosity and interconnectivity in the OC tissue play essential roles in nutrient and oxygen transportation, cells adhesion and migration, and vascular ingrowth [128,129]. Scaffolds with a single pore diameter are prone to have insufficient mechanical support, metabolism malfunction, or cell degeneration [130]. Small pores (100–200 μm) tend to limit nutrient transportation, vessel formation and osteogenesis, and promote chondrogenesis [131]. In contrast, a highly porous structure with interconnected pores ranging from 300 to 500 μm is ideal for nutrients transportation [128], bone cell migration [132] and subchondral bone restoration [133]. Pore sizes and distributions are therefore key factors for restoration of OC tissue that have been addressed by many recent reports of gradient MZSs [63,72,86,96, 97,115,119,121,123]. In these studies, pore size gradients ranging from 75 to 360 μm in the cartilage layer and 153–900 μm in the bone layer were used with success. Pores in the bone layer are usually larger than

those of the cartilage layer by a factor of 2–5. Tailoring pore size and its distribution in gradient scaffolds also improves their mechanical properties to better match those of the native tissue [63,98,120,122] and promotes cell differentiation and tissue formation [72,97,121]. Nevertheless, this strategy alone is not sufficient to obtain all these characteristics [96,115]. For instance, Gao et al. [72] proposed a bilayered hydrogel with β-tricalcium phosphate (β-TCP) added to the bone layer and pore-size-gradient structure (360–700 μm). Excellent osteogenic differentiation of BM-MSCs was observed in the bone layer, along with chondrogenic differentiation in the upper part of the hydrogel. Tissue restoration was also evidenced. Unfortunately, the tensile and compressive resistances, although high for a hydrogel, were still too low for OC repair. One of the most promising repairs was reported by Sun et al. [121], where PCL fibers reinforced MSCs-laden hydrogel scaffolds with gradient pore size ranging from 150 to 750 μm. The scaffolds exhibited compressive properties similar to those of native tissue, and excellent cell differentiation, neocartilage formation, and vessels ingrowth in the bone layer. PCL fibers were also used in another study to reproduce the orientational features of collagen fibers in each OC region, and thereby generating a scaffold with gradient stiffness mimicking that of OC tissue. This particular design positively impacted its osteointegration [134]. However, potential drawbacks of the MZSs with gradient structures include poor spatial distribution of differentiated cells and low reproducibility [86] that can be related to the lack of control on the porous structure. To address these drawbacks, gradient scaffolds with both architectural and compositional gradients may provide a better solution.

3.3.3. Gradient compositions and structures

By selecting PCL, a readily printable polymer for melt extrusion 3D printing [135], Bittner et al. [119] fabricated porosity- and composition-gradient scaffolds with high fidelity and reproducibility. Scaffolds were 3D printed with vertical gradients mimicking both the composition (0, 15 to 30 wt% HAP) and the microstructure (pore size of 200–900 μm) of OC tissue. They observed that the mechanical properties of both the single (porosity) and dual (porosity and composition) gradient scaffolds were similar to those of uniformed scaffolds with the highest porosity. The ceramic content was however insufficient to counterbalance the loss of mechanical properties caused by the weakest section of the scaffolds (area with the highest porosity) [119]. A similar study using PCL-based scaffolds fabricated via selective laser sintering (SLS) was reported by Du et al. [97]. Both HAP content (0–30 wt% with 5% increments) and pore size (400–500 μm) gradients were shown in the scaffolds, exhibiting high compressive modulus and strength. Moreover, robust in vitro MSCs adhesion and proliferation, and in vivo neocartilage and neobone formations were observed (Fig. 3G). Future attempts on gradient MZS should therefore be focused on material selection in order to achieve both excellent mechanical and biological performances.

3.3.4. Gradient hydrogels

Because of their physicochemical properties, such as adjustable water content, permeability, and mechanical properties, hydrogels are a unique category of material for fabricating gradient architectures for OC tissue repair [136–138]. However, the mechanical properties of these hydrogels remain low, and crosslinking or densification are typically required, which may affect cellular activities, degradation rate, permeability, and nutrient transportation of the material [139,140]. Increasing the stiffness of hydrogels also impacts cell differentiation, which eventually leads to more osteoconductive materials even in the cartilage layer [141]. To address these issues, additions, such as polymeric fibers [91], nano HAP [120], or chondroitin microribbons [109] (see Section 3.2), were used to successfully increase the mechanical properties of hydrogels while guiding tissue restoration. In the perspective of developing hydrogels with simple structures and ease of production, Gao et al. [72] demonstrated that the choice of polymers

was crucial for fabricating functional hydrogels. In this study, a high-strength thermoresponsive supramolecular copolymer hydrogel was synthesized by copolymerization of N-acryloyl glycinamide and N-[tris(hydroxxymethyl)methyl] acrylamide. The resulted 3D printed gradient hydrogel demonstrated excellent tensile/compressive strengths and stretchability as well as rapid thermoreversible sol-gel transition behavior.

Finally, even if the concern for weak interfaces is addressed by constructing gradient scaffolds or hydrogels, the complexity of their manufacturing process is increased when a combination of mechanical, biological, and physicochemical properties needs to be optimized. For instance, it was reported that the manufacturing process of gradient bilayered [66,72] or gradient trilayered [96,142] scaffolds had a higher degree of complexity compared to non-gradient structures. Also, architecture control and material selection are challenging and time-consuming as they are often conducted through trial-and-error approaches. To broaden material selection, decellularized and/or decalcified xenogeneic OC tissues were proposed [66,80,125]. Articular cartilage matrix requires laser modification to achieve complete decellularization of the tissue and exhibit ideal porous structure for cell loading. Although time-consuming, this technique allowed to preserve the structure and mechanical properties of the tissue, as opposed to the cartilage grinding-freeze-drying technique. As a result, decellularized cartilage or bone matrix had similar gradient porosity and composition to those of OC tissue. The cartilage layer exhibited good compressive properties, in vitro chondrogenic and osteogenic differentiations of BM-MSCs, and mature OC tissue formation in vivo with the production of GAGs and type II collagen [66,125]. However, the use of xenogeneic, allogenic or autogenous materials is accompanied by a set of limitations, such as immunoreaction (xenogeneic and allogenic grafts) or tissue availability, and donor site morbidity (autologous grafts) [143]. Such limitations are discussed further in Section 4.

Table 1 summarizes major findings, fabrication techniques, material selections, and GFs, and cells used in a selection of the most promising recent studies on MZSs. It depicts the complexity of the types of MZS structures through studies of bilayered, trilayered, bilayered with tidemark, 4-layered, and gradient/multilayered-gradient architectures.

4. Recent biomaterial selections for fabrication of MZSs

To respond to multiple requirements of MZSs, increasingly complex designs have been created with a suitable microenvironment favorable for cell activities, ideal biodegradation rate, and good mechanical properties. Property mismatch between two adjacent layers must be addressed structurally and compositionally. Regarding the compositions of recent MZSs, polymers, including synthetic, natural, and ECM-based, generally act as a matrix for both the cartilage and the bone layers. Bioceramics/bioglasses are added to the subchondral bone layer, mimicking the high mineral content in bone tissue, and rarely, metals are also included [151].

4.1. Polymers

The wide range of polymer properties has provided rich options for material selections for MSZs, especially those with a stiffness or toughness similar to cartilage tissue [152]. In addition, it has been reported that materials demonstrating a viscoelastic, rather than a purely elastic behavior, play crucial roles in cartilage matrix formation [153], cell activity [154,155]. With the fast-developing of 3D printing, printable polymers with improved structure fidelity are preferred, but balanced composition must also be in place to provide a suitable environment for embedded cells [156]. Recently used polymers in MZSs construction can be divided into three categories: proteins, natural polysaccharides, and synthetic polymers.

4.1.1. Proteins

4.1.1.1. Collagen and gelatin.
The advantages of natural polymers over synthetic materials are their excellent biocompatibility [14,49]. Collagen, the building block of cartilage and bone, is the main component in OC tissue [157]. The gel-forming capability of collagen makes it a promising candidate for scaffolds with controllable properties [158]. However, its fast degradation at body temperature has diminished researchers' interest in the material unless its degradation rate is prolonged by crosslinking [97,159]. Collagen is frequently combined with other polymers, such as chitosan [43], sodium hyaluronate [96] or PLGA [82], to increase its chondrogenecity, or with bioceramics to confer its osteogenicity and mechanical properties: for instance, Amann et al. [111] used collagen as a matrix in a trilayered scaffold with different chitosan: collagen ratios, and bioceramics were included in the bone layer (Fig. 4H). Efficient proliferation and successful chondrogenic and osteogenic differentiations of MSCs were observed in the respective cartilage and bone layers. Parisi et al. [116] obtained similar results by constructing collagen-HAP scaffolds with a gradient composition. A drawback of collagen is its capacity to self-assemble into fibrils due to its telopeptide terminal ends, which reduces its gel forming ability [160]. This issue was addressed in a work by Cao et al. [161], where telopeptide-free collagen, or atelocollagen, was combined with HAP to fabricate trilayered MZSs. The resulting scaffolds exhibited simultaneous cartilage, calcified cartilage, and bone restauration along with superior resistance to interfacial delamination.

Gelatin is a partially hydrolyzed form of collagen with good biocompatibility and biodegradability [162]. The structure of the molecule possesses fragments that activate cell functions and ECM production [163], and promote chondrogenic differentiation [164]. Despite poor printability and mechanical properties [162,165], gelatin remains a common bioink for tissue engineering because of its low cost and ease of preparation [76,163,165,166]. Studies have shown that the viscosity of gelatin hydrogels could be improved by mixing it with hyaluronic acid and therefore to be used as bioinks to 3D print MZSs [164]. Gelatin exhibits weak mechanical properties in both tension [118] and compression, especially in its hydrogel form [109,110] which restricts its use to cartilage layers only. However, crosslinking of gelatin with methacrylamide or methacrylate [66,70,112,164] has been proven to be an effective strategy to increase the mechanical properties of MZSs to the levels close to those of native tissue. In addition, recent studies have successfully used gelatin to release growth factors to maintain an anti-inflammatory environment and improve cartilage and bone regeneration in MZSs, [70,73,76,112].

4.1.1.2. Silk fibroin.
Silk fibroin (SF) is widely available in the textile industry. It is a biocompatible natural polymer with flexibility, and it has therefore emerged as an attractive material for cartilage tissue engineering [167–169]. The advantages of SF-based scaffolds are their controllable porosity [71] and tunable mechanical properties [170]. SF also exhibits good biological properties as recently evidenced by Luo et al. [99], where SF-based trilayered MZSs with growth factors in the CL and HA in the BL (Fig. 4G) showed excellent in vitro MSC adhesion, proliferation, migration, and differentiation, in vivo neocartilage tissue formation at 24 weeks, and high expression of type II collagen. The main limitation of SF hydrogel resides in its poor mechanical properties when it is not combined with other materials. Despite of crosslinking, the mechanical properties of SF hydrogels remain low [171,172]. Additional strategies are required to address this. For instance, 3D printed bilayered scaffolds composed of a mixture of SF, cartilage and bone ECM exhibited superior mechanical properties [173]. Other recent investigations reinforced SF matrix using another polymer, such as chitosan, peroxidase, or chondroitin sulfate. The resulting composites reached a compressive modulus of 350 KPa (with chitosan) [115], 600 KPa (with peroxidase) [71], and 6.7 MPa (with chondroitin sulfate),

Table 1

Summary on the selections of materials, structures, fabrication techniques, growth factors, cell-laden, and major outcomes of the recent multizonal scaffolds for osteochondral regeneration.

Materials	Structure	Main Outcomes	Fabrication technique	Growth factors	Cell-laden for in vivo	Ref.
PLGA	Bilayered: CL: pore size 100–200 μm. BL: pore size 300–450 μm. 85/15 M ratio of lactide/glycolide.	In vitro: cell adhesion. In vivo: hyaline cartilage formation and bone regeneration. Compressive modulus of the repaired tissues was 50% of that of normal cartilage.	Porogen leaching/compression molding.	–	BM-MSCs seeded in CL for 7 days before transplantation.	[68]
PCL, TCP, cartilage ECM	Bilayered: CL: PCL-cartilage ECM hydrogel. Tidemark: PCL. BL: 80% PCL-20% TCP.	In vitro: osteogenic differentiation of AD-MSCs due to TCP, chondrogenic differentiation due to ECM. Tidemark inhibited cell migration between layers.	CL and BL: 3D printing/bioprinting. Tidemark: electrospinning.	–	3D-bioplotted BL and CL with AD-MSCs.	[74, 94]
Gelatin methacrylate, PCL, HAP	Bilayered: CL: Gelatin methacrylate. BL: PCL-HAP. Radially oriented.	In vivo: MSCs attachment, proliferation, migration, and osteogenic differentiation due to HAP. Neobone formation and integration, cartilage regeneration due to GFs. Compressive modulus: PCL: 75 $\pm$ 3 MPa, PCL-HA: 73 $\pm$ 1 MPa[b].	CL: digital light processing printing, UV light cross-linking. BL: FDM. GFs were loaded by co-printing.	CL: Interleukin-4 (IL4).	–	[70]
SF, chondroitin sulfate, nHAP (nanowires)	Bilayered: CL: SF-chondroitin. BL: nHAP.	In vitro: osteogenic/chondrogenic differentiation of MSCs in BL/CL. In vivo: mineralized tissue and cartilage like tissue formation. Young's modulus 5.26–5.62 MPa[a,c], tensile strength 0.83–0.77 MPa[e], compressive modulus 6.7 MPa[b,d].	Ethanol dissolution, molding, drying, alcohol-induced β-sheet cross-linking.	–	–	[57]
PEG-co-PGS, MBG	Bilayered: CL: PEG-co-PGS. BL: MBG.	In vitro: chondrogenic differentiation, maintained chondrocyte phenotype and enhanced cartilage matrix secretion. In vivo: articular hyaline cartilage and subchondral bone formation and integration in 12 weeks. Matrix secretion enhanced by low cross-linking and viscoelasticity (Young's modulus 0.6 MPa[a,c]).	CL: crosslinking and foaming method. BL: sol-gel, foam templating process. Combination: foaming and crosslinking in a Teflon mold.	–	–	[79]
Bovine cartilage ECM and decalcified bone ECM	Bilayered: CL: cartilage ECM (134 μm pores). BL: bone ECM (336 μm pores).	In vitro: biocompatible, MSC adhesion and proliferation. DCM promoted chondrogenic differentiation of MSCs and GAG secretion. DBM promoted osteogenic differentiation. In vivo: regeneration of superficial cartilage and subchondral bone. Young's modulus of cartilage ECM: 70 KPa[c], and bone ECM: 190 KPa[a].	CL: iterative lyophilization of ground cartilage ECM. BL: hydrochloric acid decalcification of bone ECM.	–	–	[80]
Chitosan, nHAP	Bilayered: CL: porous chitosan. BL: porous chitosan −70 wt% HAP with pore size gradient 160–275 μm.	In vitro: MSC adhesion and proliferation, and enhanced in BL. Osteogenic/chondrogenic differentiation in BL/CL. Chitosan supported chondrogenesis and GAGs production. Compressive strength: 4.81 KPa[f]. Compressive modulus: 34.2 KPa[b,d]. Low degradation rate, 5% mass loss after 21 days in PBS.	PCL-porogen microspheres leaching, lyophilization, genipin crosslinking.	–	–	[59]

Table 1 (*continued*)

Materials	Structure	Main Outcomes	Fabrication technique	Growth factors	Cell-laden for in vivo	Ref.
Porcine osteochondral ECM, gelatin-methacryloyl	Gradient bilayered: Decellularized osteochondral ECM filled with gelatin hydrogel	In vitro: chondrogenic/osteogenic differentiations of MSCs in CL/BL. In vivo: smooth cartilage and bone repair, relatively mature OC tissue. Young's modulus: 8.3 MPa (63% of the native level). Growth of the blood vessels in CL prevented by interface.	Ultraviolet (UV) laser drilling decellularization (ECM), gelatin-methacryloyl solution gelation (hydrogel).	–	BM-MSCs seeded in GelMA hydrogel before surgery.	[66]
PLGA, β-TCP, cartilage ECM	Trilayered:	In vitro: Cell adhesion and proliferation, biocompatibility.	CL: Temperature-gradient induced phase separation and crystallization of ground cartilage ECM, lyophilization, physical dehydrothermal cross-linking.	–	–	[64, 144]
	CL: cartilage ECM, 30 μm pores.	In vivo: hyaline cartilage-like and bone formation in CL and BL.	ML and BL: 3D printing, lyophilization.			
	CCL: dense PLGA-1% TCP, no pore. BL: porous PLGA-1% TCP, 400–500 μm pores.	Tensile strength: 48% of native cartilage tissue. Shear strength: 51% of native cartilage tissue. Enhanced properties due to the presence of CCL.	Assembled by dissolving-bonding process.			
Poly(ethylene glycol)-diacrylate (PEGDA) and N-acryloyl 6-aminocaproic acid (A6ACA) hydrogel, CaP	Trilayered:	In vitro: chondrogenic differentiation of MSCs and formation of cartilage-like tissue in CL and ML.	CL, ML and BL: polymerization, cryogelation.	–	BL acellular, top two layers were loaded with MSCs and cultured in chondrogenic medium for 1 week before implantation.	[21]
	CL: PEGDA. ML: PEGDA-CaP (anisotropic pore architecture). BL: PEGDA-A6ACA-CaP.	In vivo: MSCs differentiation, BL mineralization, formation of OC tissue with lubricated cartilage surface.	ML and BL: incubation with a Ca^{2+} and HPO_4^{2-} solution.			
Gelatin hydrogel, aligned chondroitin sulfate microribbons (μRBs)	Trilayered:	In vitro: stronger interfaces, higher cartilage ECM production, 4-fold increase in GAGs production due to μRBs.	Iterative layering in Teflon mold and UV light crosslinking.	–		[109]
	CL: 100% gelatin/0% μRBs.	Increased compressive modulus (CL 60 KPa[d], ML 250 KPa, BL 460 KPa[b]) due to μRBs.				
	ML: 90% gelatin/10% μRBs. BL: 75% gelatin/25% μRBs.	Enhanced collagen deposition in superficial zone due to μRBs alignment.				
Gelatin methacrylamide, PCL, PEG, PLGA	Trilayered:	In vitro: MSCs differentiation into chondrogenic/osteogenic lineages in CL/BL.	GFs were loaded into PLGA microspheres before printing.	CL: TGFβ1 and BMP7.	BM-MSCs were 3D bioprinted into each layer.	[112]
	All layers: gelatin hydrogel reinforced with PCL-PEG fibers with specific orientation/fiber spacing, GF-loaded PLGA microspheres.	In vivo: Simultaneous cartilage and subchondral bone regeneration.	All layers were prepared by a combination of MEW, FDM and	ML: TGFβ1.		
	BL: Addition of HAP.	Superficial layers created a regenerated lubricating and wear-resistant surface. Compressive modulus similar to native tissue for certain fiber orientations.	UV light crosslinking.	BL: BMP2.		
Chitosan, gelatin, nHAP, decellularized bone	Trilayered:	In vitro: MSCs adhesion and differentiation into chondrogenic and osteogenic lineages.	CL (SZ, MZ, DZ): Iterative layering, lyophilization and chemical crosslinking.	–	AD-MSCs were seeded within scaffolds for 14 days before implantation.	[108]
	SZ: chitosan-gelatin-0% nHAP.	In vivo: regeneration of bone and cartilage tissues in dynamic conditions.	BL: decellularization, deproteinization, decalcification, and degreasing of porcine femur.			
	MZ: chitosan-gelatin-10% nHAP.	Compressive modulus similar to native cartilage. Reinforcing effect of nHAP.				
	DZ: chitosan-gelatin-30% nHAP. Pore size 153.5–325.3 μm.	Biodegradation rate ~10%/week.				

Table 1 (*continued*)

Materials	Structure	Main Outcomes	Fabrication technique	Growth factors	Cell-laden for in vivo	Ref.
SF, HAP	BL: decellularized porcine femur. Trilayered:	In vitro: MSCs adhesion, proliferation, migration, and differentiation due to the presence of GF. High biocompatibility.	CL and ML: freeze-drying.	PDGFs.	–	[98]
	CL: 5% SF, 60–177 µm pores. ML: 20% SF, 27–171 µm pores. BL: 5% SF-HAP, 96–845 µm pores.	In vivo: cartilage regeneration, and at an earlier stage if GF. Hyaline cartilage-like structure at 24 weeks, high expression of type II collagen and cartilage ECM.	BL: HAP sintering, SF solution soaking. GFs were loaded by soaking polydopamine (PDA)-modified scaffolds into GFs-containing solution.			
Titanium, PLGA, autologous bone	Trilayered: CL: 100 µm pore size PLGA. ML: 30 µm pore size PLGA. BL: Titanium lattice structure filled with autologous cancellous bone.	Cost-effective and time-saving fabrication. Good integration with tidemark area between neocartilage subchondral bone. CL: enhanced neocartilage formation due to the stiffness of the Ti structure. BL: enhanced regeneration due to the presence of cancellous bone. Early neovascularization.	CL and ML: 3D printing (extrusion-based). BL: 3D printing (selective laser melting).	–	Chondrocytes were seeded onto the CL for 28 days before implantation.	[84]
Alginate, chitosan, PCL, PEG, HAP	4-layered: CL: alginate-chitosan. CCL: alginate-chitosan-HAP. Membrane: PCL-PEG fibers. BL: alginate-nHAP.	In vivo: formation of hyaline cartilage and integrated bone. Biodegradation of scaffold matched the reconstruction rate of bone and cartilage. Sequential delivery of GF. Early vascularization due to GF.	CL, CCL, and BL: oxidized sodium alginate-chitosan gelation, lyophilization. Membrane: electrospinning.	CL: FGF2, BMP2 and TGFβ1. CCL: wnt/β-catenin. BL: BMP2.	–	[65]
N-acryloyl glycinamide, and N-[tris (hydroxymethyl) methyl] acrylamide copolymers, TCP	Gradient bilayered CL: copolymer hydrogel. BL: copolymer hydrogel-TCP. Gradient pore size (360–700 µm).	In vitro: attachment, spreading, chondrogenic and osteogenic differentiation of MSCs. In vivo: regeneration of subchondral bone cartilage with GAGs and type II collagen production. Tensile strength: 0.41 MPa[e], compressive strength: 4.59 MPa[f], compressive modulus 0.12 MPa[b,d], large stretchability (up to 860%).	Copolymer gelation, 3D printing, TCP cross-linking. GFs were co-printed.	TGFβ1.	–	[72]
Type I collagen, sodium hyaluronate, nHAP	Gradient trilayered: CL: 50% collagen-50% hyaluronate. ML: 33% collagen-33% hyaluronate-33% nHAP. BL: 40% collagen-10% hyaluronate-50% nHAP. Gradient pore structure (61–158 µm) and uniform porosity (>85%).	In vitro: conductive to cellular adhesion. Proliferation of chondrocytes in CL/ML, osteoblasts in BL. Biodegradation rate: 25–50% after 30 days. Compressive modulus: 14.1–26.1 KPa[b,d].	Solution mixing, chemical crosslinking, lyophilization.	–	–	[96]
PCL, HAP	Gradient: Gradient HAP content (0–30 wt% with 5% increments) and pore size (400–500 µm).	In vitro: MSCs adhesion and proliferation. Osteogenic differentiation promoted by HAP. In vivo: smooth cartilage-like tissue formation. High degree of neobone formation due to HAP. Compressive modulus: 8.7 MPa[b,d]. Compressive strength: 4.6 MPa[f].	SLS of PCL and HAP-PCL microspheres prepared by emulsion solvent evaporation.	–	–	[97]
Decellularized porcine cartilage ECM	Gradient:	In vitro: cell adhesion, cartilage-like tissue on surface, GAGs and type II collagen production.	Cartilage harvesting, laser surface modification, detergent-enzymatic decellularization.	–	Autologous chondrocytes were seeded on the scaffolds for 1 week before implantation.	[125]

Table 1 (*continued*)

Materials	Structure	Main Outcomes	Fabrication technique	Growth factors	Cell-laden for in vivo	Ref.
MSC-laden hydrogel, PLGA, PCL	Lattice-arranged conical micropores.	In vivo: mature neocartilage with high contents of DNA, GAGs, type II collagen. Compressive modulus: 5 MPa[b,d].				[121]
	Gradient:	In vitro: MSCs proliferation, spreading, differentiation into chondrocytes, and cartilaginous matrix formation.	3D bioprinting.	Deepest layer: BMP4.	BM-MSCs were 3D bioprinted into each layer.	
	Gradient fiber spacing (150–750 μm). PCL hydrogel with GF-loaded PLGA microspheres.	Compressive modulus is similar to native tissue. In vivo: functional neocartilage, microvessels ingrowth.	GFs were loaded into PLGA microspheres and then co-printed.	All other layers: TGFβ3.		

[a] Subchondral bone tensile modulus: 98–270 MPa [145].
[b] Subchondral bone compressive modulus: 155–480 MPa [146].
[c] Cartilage tensile modulus: 2–25 MPa [147,148].
[d] Cartilage compressive modulus: 1.36–39.2 MPa [149].
[e] Cartilage tensile strength: 7–15 MPa [148].
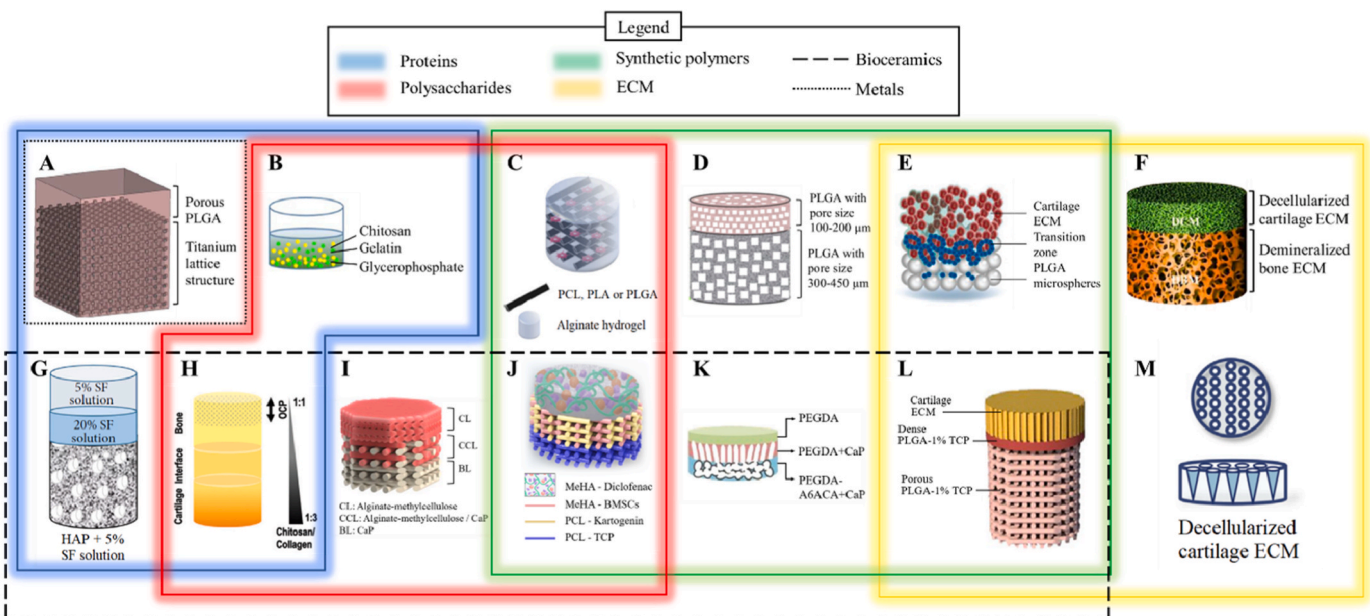[f] Cartilage compressive strength: 14–59 MPa [150].

Fig. 4. Map of the materials and their combination used in recent MZSs. Polymeric materials, especially chitosan, PCL and PLGA, are the most popular materials used as a matrix. Bioceramics are used as mineral additions in the BL. A. Trilayered scaffolds with metal in the BL and polymeric materials in the CL. Adapted with permission from Ref. [81]. B. Trilayered scaffolds composed of chitosan, glycerophosphate, and gelatin at various ratios and gradient porosities (86–95%). Adapted with permission from Ref. [108]. C. Bilayered scaffolds with alginate and agarose hydrogel reinforced by PCL, PLA, or PLGA fibers in the bone layer. Adapted with permission from Ref. [91]. D. Pure PLGA scaffolds divided into two regions with different pore sizes (100–200 μm and 300–450 μm). Adapted with permission from Ref. [68]. E. Cell seeded trilayered scaffolds with alginate hydrogel and cartilage ECM in the CL, addition of PLGA microspheres in the ML, and PLGA microspheres in the bone layer. Adapted with permission from Ref. [23]. F. Bilayered scaffolds made of decellularized cartilage ECM (134 μm pores) in the CL and decalcified bone ECM (336 μm pores) in the BL. Adapted with permission from Ref. [80]. G. Trilayered scaffolds with varying volume fractions of SF and HAP inclusion in the BL. Adapted with permission from Ref. [98]. H. Trilayered scaffolds with different chitosan:collagen ratios and embedded OCP in the BL. Adapted with permission from Ref. [111]. I. 3D printed bilayered and trilayered scaffolds with alginate-methylcellulose (MC) and alginate-MC-CaP inks. Adapted with permission from Ref. [190]. J. Trilayered scaffolds with a top layer made of methacrylated hyaluronic acid (MeHA) hydrogel embedding Diclofenac to regulate inflammation, and 3D printed PCL-MeHA and PCL-TCP layers. Adapted with permission from Ref. [188]. K. Trilayered scaffolds with PEG-diacrylate and N-acryloyl 6-aminocaproic acid (A6ACA) cryogel matrix and CaP in the BL, PEGDA-CaP in the CCL and pure PEGDA in the CL. Adapted with permission from Ref. [21]. L. Trilayered scaffolds combining oriented cartilage ECM, compact PLGA-TCP, and porous PLGA-TCP. Adapted with permission from Ref. [64]. M. Decellularized porcine articular cartilage ECM scaffolds with gradient lattice-arranged conical micropores added by laser. Adapted with permission from Ref. [125].

respectively [57].

4.1.2. Natural polysaccharides

4.1.2.1. Chitosan. Chitosan is a polysaccharide naturally derived from chitin, the main component of shrimp shells, upon deacetylation [159].

It is highly biocompatible, osteoconductive, and osteoinductive, with a structure similar to that of GAGs [174,175], another polysaccharide from the cartilage tissue. Because of its high degree of deacetylation, chitosan degrades at a slow rate (5 w% reduction after 3 weeks) [176]. In addition, chitosan possesses an ability to promote cell differentiation [177,178], which makes it a promising candidate for constructing both

cartilage and bone layers in MZSs [59,65,69,108,111,115,123,127]. In the bone layer, chitosan promotes the growth of calcium phosphate crystals and alkaline phosphatase, which are markers of osteogenesis [179,180]. Chitosan is responsible for superior adhesion at the interface of bone-cartilage layers and spreading of osteoblasts [174]. Recent studies reported that the presence of chitosan in the bone layer of MZSs enhanced osteogenic cell proliferation [59,69,108,111]. Also known as a promoter of adhesion and proliferation of chondrocytes [175], chitosan has been used for the construction of cartilage layer of recent MZSs to promote chondrogenic differentiation [108,111]. For instance, Pitrolino et al. [59] showed that pure chitosan was the preferred medium for chondrogenesis and was responsible for increased GAGs production. Chitosan-based MZSs were also correlated with high compression modulus (4–8.2 MPa) [69,127]. To achieve enhanced integrity and stiffness, chitosan could be mixed with proteins, such as SF [27], gelatin (Fig. 4B) [123], collagen [111] or combined with other polysaccharides to form polyelectrolyte complexes (chitosan-alginate [181] or chitosan-hyaluronic acid [182]). The biodegradation rate of chitosan-based MZSs can also be tailored by varying the compositions of the scaffold [69] and thereby reach an appropriate value matching the reconstruction rate of OC tissue [65,108,115]. Crosslinking techniques also successfully reduced the degradation rate of chitosan-based MZSs with a gradient composition [127], but this approach could lead to cell toxicity and low cartilage matrix production [183].

4.1.2.2. Hyaluronic acid. Hyaluronic acid (HA), the major component of the cartilage tissue, is a GAG that provides support to chondrogenesis [184,185]. HA is advantageous in MZS fabrication, and more particularly for the design of the CL, because of its good biocompatibility, appropriate degradation rate [186], and high printability [187]. In a bilayered scaffold fabricated by Liu et al. [75], HA hydrogels exhibited a high level of differentiation of MSCs into chondrocytes in the cartilage layer, and into osteoblasts in the HAP-HA bone layer. HA can be combined with other polymers to further improve its properties. For instance, HA is normally mixed with chitosan to enhance cell differentiation [69] or with PCL (Fig. 4J) to increase the production of cartilage matrix, type II collagen and GAGs [58,188]. Mixing with polyglycidol polymers is also a good strategy for tailoring the chondrogenicity of HA [189], although the resulting compressive properties of the scaffold remain low [58].

4.1.2.3. Plant-derived polysaccharides. The most abundant polysaccharides on earth are plant-derived polysaccharides, among which alginate and methylcellulose are commonly used for constructing MZSs [23,65,69,91,107,118,190,191]. Cellulose and its derivative (methylcellulose) are the main structural component of vegetal cell walls [192] and exhibit a hierarchical structure leading to high mechanical properties [192]. Alginate is a polysaccharide extracted from brown and red seaweeds [144,193] that has been widely used over the last a few years because of its fast gelation capability, low cost, and potential to support chondrogenesis. A limitation of alginate is its poor support to cell adhesion and cell proliferation [23]. Interestingly, Nie et al. [23] used this characteristic of alginate in a MZS to force chondrocytes migrating from the top alginate layer to the bottom PLGA porous region with better cell adhesion capability. As a result, the migrated cells secreted ECM across the cartilage region and the top subchondral bone region, forming a biological bonding between the two zones. The use of alginate alone is limited by its low viscosity that is undesirable for 3D printing [196]. Alginate is often required to mix with another polymer, such as methylcellulose (Fig. 4I) [190], or incorporated with particles, such as cellulose nanocrystals [118] or laponite (a clay mineral) [191], as thickeners to improve its viscosity. Besides viscosity, Sultan and Mathew [118] took advantage of the orientation of cellulose nanocrystals embedded in an alginate matrix to direct cell growth, control pore structure and density, and promote cell proliferation. . Alginate can also

be mixed with chitosan to improve its mechanical properties by forming polyelectrolyte complexes [65,69]. To this end, our group has designed a novel alginate-polyvinyl alcohol (PVA)-HAP hydrogel with optimal rheological properties for 3D printing tissue engineering scaffolds [194, 195]. Another example is provided by Critchley et al. [91], where formation of hyaline-like cartilage repair was observed in vivo in the cartilage layer of bilayered scaffolds made of alginate hydrogels and reinforced by a series of 3D printed synthetic polymers (PCL, PLA, or PLGA).

4.1.3. Synthetic polymers

4.1.3.1. Polycaprolactone. PCL is a biocompatible polymer with a low printing temperature that makes it suitable for various fabrication techniques [134], especially 3D printing [197] and electrospinning [74, 94]. It has good mechanical properties [198] that can be tailored by adjusting its molecular weight [199]. Notably, BM-MSCs were successfully co-printed with PCL hydrogel ink into scaffolds with gradient spacing [121]. PCL is widely used as fiber reinforcements in MZSs [58, 65,91,112] to achieve compressive properties matching those of native tissues [112,121]. Recent investigations on MZSs with load-bearing PCL-based matrix have reported high compressive moduli in the range of 8.2–220 MPa [70,97,119,127]. It has been found that PCL is efficient in facilitating chondrogenic differentiation, cartilage matrix production, and cartilage-like tissue formation [74,94,97,121,188], but osteogenic differentiation or neobone formation was only achieved in the presence of bioceramics in the bone layer [70,74,94]. PCL is nonetheless a versatile material that can be used as a main component in both cartilage and bone layers, as demonstrated by Steele et al. [134]. In this study, four manufacturing methods, electrospinning, porogen leaching, directional freezing, and melt electrowriting (MEW), were considered to fabricate PCL-only scaffolds with gradient stiffness and porosity. A limitation of PCL is its low biodegradation rate as it takes nearly 3 years for PCL to completely degrade in vivo, which significantly obstructs matrix from deposition [200]. Fortunately, the biodegradation rate of PCL can be tailored by modulating its molecular weight [198]. Notably, the degradation time can be shortened to as short as six months [201].

4.1.3.2. PLA and PLGA. PLGA is a copolymer of polylactic acid (PLA) and polyglycolic acid (PGA), a family of FDA-approved biocompatible polyesters [202]. Its biodegradation rate is higher than that of PCL and can be easily tailored via various routes, such as by modulating the ratio of lactic acid to glycolic acid in the PLGA chain [203]. The good processing properties of PLGA make it an attractive candidate for 3D printing [204], or to be added to a polymeric matrix to control the biodegradation and biological performances of scaffolds [205]. Recently, PLGA has been used to fabricate the bone layer [23,64,104], the cartilage layer [82–84] or the entire MZS [63,73,77,78,86,205]. In these studies, PLGA supported cell attachment [206], high subchondral bone regeneration [23,78,104], and simultaneous chondrogenic and osteogenic differentiations [86]. More interestingly, it has been found that PLGA scaffolds can regenerate both cartilage and subchondral bone tissues by simply adjusting the zonal-specific pore size or porosity of scaffolds [207,208]. Similarly, a recent study on poly(ʟ-lactic acid) (PLLA), a stereoisomer of PLA, evidenced that this material could support both osteogenic and chondrogenic differentiations upon the generation of a gradient piezoelectric field [209]. Although PLGA could promote cell activities, a study has shown that it also initiated de-differentiation of chondrocytes upon adhesion, and eventually led to the deposition of type I and type X collagen impurities in the neo-formed cartilage [23]. Reduction of chondrogenic expressions and GAGs production were also observed in PLA-based scaffolds although osteogenesis was improved in the bone layer [78]. The use of PLA or PLGA-only matrixes is also limited by their high melting temperatures, which challenges the use of live cells in 3D bioprinted MZSs [210]. In

addition, PLGA creates an acidic environment while degrading, causing inflammation and cell death [91,121]. As such, PLA and PLGA have been mainly used as reinforcing fibers [91]. PLGA was also used for slow release of bioactive molecules [211] and growth factors in MZSs [112, 121].

4.1.3.3. Other polymers. A combination of natural polymers with a growing non-exhaustive list of synthetic molecules have also been explored, such as PEG dimethacrylate [205], polyethylene oxide (PEO) [142], polyacrylamide [191], PEG-poly(glycerol sebacate) (PGS) [79] or polyethersulfone [212]. Usually, a specific property of the synthetic polymer motivated its use in MZSs. For instance, polyacrylamide was combined with laponite to fabricate gels with electrostatic interactions that are capable of self-healing and redirecting the macrophage phenotype [191]. PEG is also a popular synthetic polymer for constructing MZSs due to its high solubility in water, excellent biocompatibility, and adjustable degradation rate [213,214]. In MZSs, PEG was combined with PCL to form reinforced fibers, resulting in a significant increase of mechanical strengths [65,112]. Additionally, Kang et al. [21] used synthetic copolymer of PEG-diacrylate and N-acryloyl 6-aminocaproic acid copolymer to encapsulate cells in a controlled porous architecture (Fig. 4K) and observed chondrogenic differentiation, osteochondral tissue reconstruction, and lubrication of the cartilage surface (lubricin). As a biocompatible polymer with tunable mechanical properties, PGS has also been used in cartilage engineering. However, it is usually associated with a long high-temperature crosslinking process that can take for several days [215]. Generally, PGS is rarely used alone due to its undesirable processing properties that complicate the fabrication of porous scaffolds [189]. For instance, Lin et al. [79] fabricated a bilayered scaffold with a cartilage layer matrix composed of PEG-PGS copolymer. The viscoelastic behavior and the chondrogenicity of the copolymer were modulable using a significantly shorter urethane crosslinking. Similarly, Gao et al. [72] copolymerized N-acryloyl glycinamide and N-[tris(hydroxymethyl)methyl] acrylamide to synthetize a high-strength copolymer hydrogel that is suitable for 3D printing. The hydrogel was used as a matrix in a bilayered scaffold with HAP in the bone layer. Besides its excellent mechanical properties, the scaffold demonstrated improved chondrogenic and osteogenic differentiation of MSCs and excellent cartilage and subchondral bone tissues formation. Another study also reported that functionalized multizonal hydrogels made of conjugated PGA-PEG-PGA terminated by cartilage-specific or bone-specific peptide sequences improved the histological scores of the newly formed tissues in vivo compared to non-functionalized hydrogels [216]. Besides this work, conjugated systems of co-polymers remain, however, rarely used. The complete scheme of their physicochemical properties still needs to be depicted by further exploration, especially regarding their biodegradation rate.

4.2. Bioceramics and bioglasses

Calcium phosphates (CaPs) constitute a large family of bioceramics in bone tissue engineering because of their similarity to the chemical composition of bone minerals. In general, they are resorbable and can promote cell differentiation into osteoblasts [217–219]. However, when CaPs are used as a matrix, high sintering temperatures are required to bind CaP particles [220]. This may limit many materials from being used jointly with CaPs. As such, CaPs are often used as additives to the bone layer of MZSs. Among them, HAP is the most commonly used. Despite remarkable mechanical properties, bioinert ceramics, such as alumina or zirconia, do not interact with surrounding tissues [19], which strongly limited their usefulness in OC repairs. Instead, bioglasses, another class of bioceramics, were used. However, due to a few serious concerns (discussed in a later section), they are used less popularly for preparation of MZSs.

4.3. HAP

HAP ($Ca_{10}(PO_4)_6(OH)_2$), the main component of natural bone, demonstrates excellent in vivo biocompatibility and osteoconductivity [221]. It can differentiate MSCs into osteoblasts [70], and to promote their proliferation by increasing the local Ca^{2+} ion concentration [222]. HAP also plays an important role in the integration of neo-formed cartilage and subchondral bone [223]. It is therefore the most preferred mineral addition in the bone layer of MZSs for supporting osteogenesis [57,59,65,69,70,73,75,86,96,97,107,108,110,115,116, 119,161]. HAP has been consistently reported to support in vitro differentiation of MSCs into bone cells and/or in vivo subchondral bone regeneration. The amount of HAP incorporation in recent MZSs ranged from 0.5 wt% [69] to 70 wt% [59], and it was normally embedded in a polymeric matrix, such as gelatin [70,73,109,111,143] and chitosan [59,65,69,108,115]. The size of the HAP addition can impact the rate of in vivo scaffold resorption and tissue ingrowth [224]. In general, nanoparticles are easily digested by osteoclasts and reused by osteoblasts to form new bone tissue [225], which makes them excellent additions for enhancing osteogenicity and in vivo bone ingrowth [57,59, 96,107,108,110,115,142].

4.4. TCP, OCP

Other CaPs formulations used in MZSs are TCP ($Ca_3(PO_4)_2$) and octacalcium phosphate (OCP, $Ca_8H_2(PO_4)_6$), which have similar physicochemical properties as HAP except that they are less stable than HAP [226]. TCP and OCP were used in a few recent studies to construct MZSs [64,71,74,77,94,104,111,188]. For instance, they were precipitated in the bone layer of MZSs upon incubation in solutions containing Ca^{2+} and HPO_4^{2-} ions [77]. Such prepared bone layers promoted osteogenic differentiation [77], mineralization, and osteochondral bone tissue formation [190]. When a bone layer made of pure TCP was used in bilayered scaffolds, good cell adhesion and proliferation along with mineralized matrix production were observed in vitro despite that the layer was too brittle [71]. TCP is preferred over OCP for supporting cell proliferation [64,72,104,188], osteogenic differentiation of MSCs [72, 74,94] and neobone formation [72,104] in MZSs. In addition, OCP has a lower Ca/P ratio (1.33) compared to that of HAP (1.67) or TCP (1.5), which demonstrates a faster resorption rate in vivo [227].

4.5. Bioglasses

Bioglasses are a class of ceramics containing a bioactive component (CaO, Na_2O, SiO_2, or P_2O_5) that generates a calcium-phosphorous layer on its surface upon contacting to body fluid [228]. This layer is highly osteoinductive, osteoconductive and osteointegrative [229], and supports new bone formation [230]. Bioglasses also have good antimicrobial properties [231]. In a work by Lin et al. [233], a technique to fabricate mesoporous bioactive glass MZS was developed by dissolving tetraethyl orthosilicate and triethyl phosphate in ethanol, followed by evaporation in vacuum conditions and calcination. As a result, a bilayered scaffold with a bone layer composed of pure bioglass was fabricated, and it regenerated subchondral bone 12 weeks post implantation in vivo. However, despite their high strength and stiffness, bioactive glasses have drawn limited interest in OC tissue engineering due to their brittleness [232]. In addition, a series of other drawbacks, such as the difficulty to process into porous scaffolds, poor biodegradation properties of some bioglasses, or concerns of toxic ion release (borate bioactive glass), further restricted their usefulness in biological applications [232].

4.6. Cartilage and bone extracellular matrix

Cartilage and bone ECMs exhibit physicochemical properties and natural architecture ideal for OC tissue engineering upon

decellularization and decalcification [80]. The anisotropic and gradient architecture of cartilage ECM creates an ideal chondro-inductive environment for chondrocytes spreading and cartilaginous tissue regeneration [234]. When transitioning from the superficial to the deep zone, higher nutrient concentrations, increased mechanical properties, lower level of GAGs [235], and enhanced support for vascularization were observed [236]. As an emerging candidate for OC tissue engineering, decellularization of articular ECM needs to be further improved to better preserve its chondroinductivity, osteoconductivity and mechanical properties [66,125]. Particularly, decellularization of the cartilage region is challenging and time-consuming and has been rarely complete because of its extremely high matrix density [23,125]. As a result, limitations, such as immunoreaction [143], stress shielding [237], poor integration with the areolar tissue [238], and implant failure [143], have been reported.

ECMs can be extracted from an animal source [80,125] or obtained from culturing chondrocytes on a substrate material, such as alginate hydrogels (Fig. 4E) [23]. In a study by Cao et al. [80], decellularized cartilage ECM scaffold was combined with bone ECM that was pre-decalcified. The bilayered MZS exhibited both neocartilage and trabecular bone regeneration in vivo (Fig. 4F). However, cell migration occurred at a very small scale in the scaffold because of the high density of the collagen network [239]. A technique to improve both cell spreading and decellularization of cartilage ECM was proposed by Li et al. [125], where a lattice-arranged microporous architecture was laser-drilled to create ideal dimensions for cell migration (Fig. 4M). Cell spreading was substantially enhanced compared to untreated ECM and functional restoration of the cartilage tissue was observed in vivo after 8 weeks of implantation. A similar ultraviolet laser drilling technique was used by Wang et al. [66] and it was found that such a treatment was beneficial for in vivo tissue regeneration.

To facilitate the decellularization process, lyophilized cartilage or/and bone ECMs were also ground into powders and then digested by pepsin in acid [64,74,94,104,240]. The resulting solutions were further processed into hydrogels [74,94], or mixed with polymers to eventually form a bioink suitable for 3D printing [173], or directionally freeze-dried to obtain a OC-like anisotropic architecture (Fig. 4L) [64,104]. In a recent study by Browe et al. [240], ground cartilage and bone ECMs were used to fabricate bilayered scaffolds with aligned collagen fibers by modifying the freeze-drying kinetics to direct differentiations of MSCs. In this study, the control of the pore size and alignment improved cellular spreading and GAGs deposition. Overall, the use of autologous cartilage and bone ECMs circumvents the limitations associated with imperfect decellularization, limited tissue availability, and donor site morbidity [241].

4.7. Metals

Metals remain scarcely used in MZSs because most of them are not biodegradable. A few metals, such as titanium (Ti) and its alloys, have excellent biocompatibility, resistance to corrosion, low density, high toughness, and high stiffness [242–246]. Printing Ti lattice structures with selective laser sintering (SLS) is considered a cost-effective and time-saving approach to prepare scaffolds [84]. It was used to construct a stiff supporting bone layer in MZSs, which is usually combined with a polymeric chondro-inductive cartilage layer [84]. Interestingly, studies have shown that a stiff Ti subchondral layer supported neocartilage growth in both cartilage and middle layers, and improved the integration of the regenerated bone and cartilage tissues with the adjacent host tissue [82–84,246].Besides its non-degradability, a drawback of Ti, paradoxically, is its high stiffness (103 GPa) [247] that exceeds that of natural bone by a large margin [37]. Ti implants can therefore transmit more stress compared to the surrounding bone tissue, which eventually causes the tissue to resorb under the action of the osteoclasts, and loses its mechanical properties [248]. This phenomenon, called stress shielding, has pushed researchers to explore other metals with elastic

modulus comparable to that of bone tissues. For instance, tantalum (Ta) has sufficient strength [249], but an elastic modulus between those of cortical and cancellous bone, which completely avoids stress shielding [250]. In addition, Ta is biocompatible, corrosion resistant, and it promotes osteogenic differentiation [251]. In a study on a bilayered MZS composed of porous Ta (BL) with BMSCs seeded collagen membranes (CL), Wei et al. [85] evidenced that Ta did not inhibit BMSCs spreading, but instead played an important role in their osteogenic differentiation and bone-Ta integration. Ta–Ti alloy has also been used to improve the performances of metal-based MZSs. Ta–Ti alloys exhibit similar biocompatibility to Ti, but a higher resistance to corrosion, along with an elastic modulus matching that of natural bone [252]. For instance, Sing et al. [81] fabricated Ti–Ta lattice structures embedded in collagen hydrogels (Fig. 4A), which supported cartilage formation without causing stress shielding.

Table 2 summarizes various materials used in constructing specific layers of MZSs. Besides the variety of materials used, it shows that combination of materials is often necessary to reach desired properties. The biological performances of MZSs largely depend on a combination of careful material selection, architecture design, and appropriate fabrication techniques.

5. Novel fabrications techniques

The overall biological performance of MZSs in OC repair is not only determined by its composition and structure, but also their fabrication technique as it is a key that impacts the mechanical, physicochemical, and biological properties of the MZSs. Single usages of traditional scaffold manufacturing techniques, such as freeze-drying, gas-forming, phase separation, template leaching, and sol-gel method, are no longer considered facile strategies to make non-monophasic scaffolds that better mimic the complex zonal architecture of natural osteochondral tissue [26,255]. To this purpose, combining a few classic processes or using several novel fabricating approaches provides feasible routes to fulfill the need for MZS fabrication. This section summarizes the strategies that are commonly used nowadays to manufacture MZSs, including the traditional lyophilization-based, electrospinning-based techniques, the most recent emerged 3D printing, and other approaches such as those involved the formation of naturally cell-derived structures.

5.1. Lyophilization

The basic principle of lyophilization (freeze-drying) is sublimation, through which the solid-state frozen water is sublimated directly into gas phase under a negative chamber pressure at a low temperature, forming a 3D scaffold. The morphology and size distributions of pores within the scaffold are simply a replica of those of ice [256,257]. Therefore, the microstructure of scaffold is controlled by the nucleation and growth of ice crystals during the freezing process of lyophilization. Kinetically, the growth of ice crystals prefers the direction perpendicular to the c-axis of its hexagonal lattice [51]. As a result, under homogeneous cooling, an equiaxed cellular structure is formed. In contrast, under a unidirectional freezing gradient, an anisotropic lamellar structure is formed along the c-axis of ice crystals (Fig. 5A). Overall, the freezing temperature, rate, and direction control the pore size, porosity, homogeneity, and pore orientation of the obtained structure, offering the possibility to design MZSs with zonal specific microstructures that replicate the collagen fiber orientations in each region of natural OC tissue [258]. Nevertheless, it is still challenging to engineer a multilayered scaffold to mimic the complex zonal architecture of natural OC using lyophilization alone. In other words, only a single layer of the MZSs can be produced at a time, and they have to be subsequently stacked to form a zonal structure. However, the poor adhesive strength between two adjacent layers has been a huge concern of such designs. To solve this problem, several groups including ours have worked to fabricate MZSs using multilayered lyophilization techniques or

Table 2

Comparison of the advantages and disadvantages of common materials used in constructing the bone layer and the cartilage layer of MZSs for OC regeneration.

Material	Types of layers	Pros	Cons	Ref.
Polymers - Proteins				
Collagen	CL	Gelation capability Controllable properties Chondrogenic	High degradation rate Self-assembly into fibrils	[96,111, 116,161]
Gelatin	CL	Chondrogenic	Poor printability Poor mechanical properties Low cost Ease of use	[24,70, 108–110, 112,118, 123,124, 253]
Silk fibroin	CL	Controllable porosity Controllable mechanical properties Chondrogenic	Poor mechanical properties Low degradation rate	[27,57, 71,98]
Polymers - Natural polysaccharides				
Chitosan	CL	Chondrogenic Superior CL-BL adhesion Promote GAGs production Polyelectrolyte complexes forming ability	Cell toxicity Low cartilage ECM production upon crosslinking	[27,59, 65,69, 108,111, 123,124]
	BL	Osteogenic Controllable degradation rate Controllable mechanical properties	Poor mechanical properties High degradation rate	[27,59, 69,108, 111,123]
Hyaluronic acid	CL	Chondrogenic Ideal degradation rate High printability Natural component of cartilage	Low compressive properties Better if mixed with other polymers	[58,69, 75,86, 188]
Alginate	CL	Fast gelation capability Low cost Chondrogenic	Low viscosity Better if mixed with other polymers or thickeners Poor cell adhesion and proliferation	[23,65, 69,91, 118,190]
Methylcellulose	CL	Improve structural control High mechanical properties	Preferred as inclusion	[118, 190]
Polymers - Synthetic				
Polycaprolactone	CL	Low printing temperature Chondrogenic Controllable mechanical properties	Poor biological properties Mostly used as reinforcing fibers	[65,74, 94,97, 119,121, 124,134]
	BL	Good mechanical properties	Requires mixing with bioceramics Low degradation rate	[58,70, 74,91,94, 97,119, 121,124, 133]
PLA and PLGA	CL	Ideal and controllable degradation rate Good processing properties Chondrogenic	Promotes differentiation of chondrocytes Induces type I and type X	[63,68, 83,86, 121,253]
	BL	Osteogenic	collagen impurities High melting temperatures	[23,64, 68,86,91, 104,112, 121,253]
		Controllable porosity	Creates acidic environment while degrading	[63]
PEG	CL	High solubility in water Controllable degradation rate Good mechanical properties Chondrogenic	Mostly used as reinforcing fibers	[21,65, 79,112]
PGS	CL	Controllable mechanical properties	Requires long crosslinking process Undesirable processing properties	[79,189]
Bioceramics - Bioglasses				
HAP	BL	Osteoconductive Osteogenic Promote osteointegration	Mostly used as additive	[57,59, 65,69,70, 73,75,86, 96,97, 107,108, 110,115, 116,119, 161]
TCP, OCP	BL	Osteogenic Promote mineralized matrix production Ideal degradation rate	Mostly used as additive Less stable than HAP	[71,74, 77,94, 104,111, 188,254]
Bioglasses	BL	Highly osteoinductive, osteoconductive and osteointegrative surface Antimicrobial properties High strength and modulus	Brittleness Poor processing properties Poor biodegradation properties Toxic ion release (borate bioactive glass)	[79]
ECM				
Cartilage ECM	BL, CL	Ideal physicochemical properties Ideal microstructure Chondrogenic	Requires challenging decellularization Requires laser-drilling to improve cell migration Limited tissue availability	[23,24, 74,80,94, 104,125, 240]
Bone ECM	BL	Ideal physicochemical properties Ideal microstructure Osteogenic	Requires decellularization Limited tissue availability	[24,80, 240]
Metals				
Titanium	BL	Corrosion resistant Low density High toughness	Not biodegradable Stress shielding	[82–84]

Table 2 (*continued*)

Material	Types of layers	Pros	Cons	Ref.
Tantalum	BL	Supports neocartilage growth Corrosion resistant High strength Ideal stiffness Osteogenic	Not biodegradable	[81,85]

lyophilization in combination with other approaches.

Levingstone et al. [113] developed a collagen-based layered construct for osteochondral repair through an iterative layering freeze-drying technique. As shown in Fig. 5B, a porous bone layer scaffold was first fabricated by freeze-drying a suspension consisting of type I collagen and HAP in a mold. The scaffold was crosslinked and rehydrated to facilitate the preparation of the subsequent layers. An intermediate layer was then engineered via a second freeze-drying process by pipetting a suspension made of type I collagen, type II collagen and HAP atop the rehydrated bone layer. Finally, a cartilage layer was prepared through a third time freeze-drying by adding a suspension made of type I collagen, type II collagen, and HA atop the first two layers. As demonstrated in Fig. 5C, such prepared MZS showed a seamlessly bonded layered structure, high level of pore interconnectivity and high porosity (97%) [113]. Their subsequent in vitro and in vivo studies indicated that such prepared MZSs exhibited excellent biocompatibility and promoted osteochondral repair potential in both a critical-size OC defect rabbit model [113,262] and a long-term caprine (12 months) OC defect model [263].

Our group managed to design a monolithic MZS that closely mimics the zonal microstructure, composition, and collagen fiber orientation of OC tissue through a lyophilization bonding process [22,264]. First, a unidirectional freeze casting mold (Fig. 5D) made of poly(methyl methacrylate) (PMMA) was developed to fabricate a SZ with lamellar structure. PMMA was used as an insulator while a copper cap was applied as an excellent thermal conductor to confer a thermal gradient along the length of the mold. A suspension consisted of type I collagen and HA was added to the mold to form a lamellar SZ upon lyophilization. Subsequently, a lamellar osseous zone (OZ; subchondral bone zone) scaffold was prepared by co-precipitation of type I collagen and HAP into a composite gel, followed by self-compression, unidirectional freezing, lyophilization, and crosslinking [265,266]. To create a seamlessly bonded scaffold mimicking the zonal composition and structure of OC tissue, a lyophilization bonding process was developed to join the SZ and OZ, as illustrated in Fig. 5E. As shown in Fig. 5F, these processes yielded a fully integrated multidirectional scaffold with four morphologically distinct zones: a lamellar SZ with highly aligned horizontal oriented collagen-HA fibers; a thick collagen-HA TZ with homogenously distributed isotropic pores; a lamellar OZ consisting of highly aligned vertically oriented collagen-HAP fibers; and a calcified cartilage zone (CCZ) in between the TZ and OZ with a combination of morphological and compositional characteristics of these two zones. Our subsequent in vitro and in vivo studies demonstrated that such prepared MZSs were able to induce osteogenic differentiation of BM-MSCs, maturity of chondrocytes, and neo-OC tissue formation [267].

Stuckensen et al. [260] has also utilized unidirectional freeze-drying to produce a monolithic MZS with highly aligned lamellar structure in each zone. Briefly, a custom-built cryostructuring device (Fig. 5G) was designed to create a temperature gradient along the long axis of the device to guide the solidification of precursor materials. After the addition of the precursor comprising of type I collagen and brushite for the subchondral zone (SC), the next precursor consisting of type I and type II collagen in chondroitin sulfate was added to build up the deep chondral zone (CD). The third precursor composed of type I and type II collagen in chondroitin sulfate with a lower concentration compared to CD was added atop the CD in the same manner to obtain the middle chondral zone (MZ). After the three-step solidification process, lyophilization and crosslinking were applied to generate a stable monolithic MZS as shown in Fig. 5H.

Overall, multilayer lyophilization was used to prepare MZSs in a layer-by-layer manner from bottom (subchondral bone layer) to top (cartilage layer) [113,260,262,263], or it can be applied at the end to serve as a bonding process to join all layers [22,264,267]. Besides these examples of multilayer lyophilization process, lyophilization is often used in combination with other techniques to fabricate MZSs. Huang et al. [105] recently used lyophilization to bond type II collagen sponge and acellular normal pig subchondral bone, where a natural CCZ was included by removing the hyaline cartilage above the CCZ of pig knee. Such prepared scaffold showed a well-integrated morphology with a trilayered structure and exhibited excellent in vivo OC repair in a minipig knee joint defect model. In another study, freeze-drying was used in combination with a porogen-leaching-out approach to produce multi-layered, chitosan-HAP scaffold with a distinct zonal specific gradient of pore sizes (Fig. 5I) [59]. In this study, PCL microparticles with different mean sizes were leached out from lyophilized chitosan-HA scaffold, forming a porous multilayered scaffold with zonal specific pore size gradient. Similarly, Mahapatra and coworkers [78] applied a combination of freeze-drying, salt-leaching, and phase-separation to generate a bilayered poly(L/D-lactide acid) (PLDLA) scaffold with a dense layer and a nanofibrous layer (Fig. 5J). The two layers had a similar level of porosity (~90%) and pore size (~150 μm) but different surface topographies which resulted in distinct surface areas and hydrophilicity. In particular, the nanofibrous layer demonstrated a larger surface area and higher hydrophilicity, which facilitated osteogenesis by enhancing cell-to-matrix interactions and in turn stimulated MSCs into elongated morphology, resulting in better osteogenic differentiation [268,269]. On the contrary, the dense layer with smaller surface area and lower hydrophilicity was able to promote cell-to-cell adhesion by enhancing the condensation and aggregation of MSCs, which are important steps for chondrogenesis [78,270,27]. Liquid phase synthesis has also been used to produce multiphasic scaffolds in combination with the freeze-drying technique [163,272]. Fig. 5K shows a good example combining these two processes [261], where liquid phase inter-diffusion was conducted to produce a gradient interface region to bond the subchondral bone layer with the cartilage layer before lyophilization. Other techniques, such as foam replication [273], thermally-induced phase separation (TIPS) [274], and microspheres-based syringe pump method [275,276], have also been used in conjugation with lyophilization to construct MZS.

5.2. Electrospinning

Electrospinning is a process used to produce nanofibers through an electrically charged jet of polymer solution or melt exerting electrostatic force [277]. The nanofibers produced by this process possess high specific surface areas and adjustable mechanical properties suitable for a wide range of applications [278,279]. More importantly, the fiber arrangement is tunable to simulate the hierarchical architecture of natural ECM [26]. As a result, it has been applied extensively in fabricating tissue engineering scaffolds [280,281]. More specifically, the cartilage layer of osteochondral MZSs manufactured using electrospinning technique is of potential to have a flexible and elastic structure that mimics the morphology of hyaline cartilage ECM; the interfacial layer of MZSs constructed through electrospinning can act as a tidemark to prevent cell migration between cartilage and bone zones while allowing for nutrition and waste transport; and such prepared bone layer of MZSs possess good mechanical properties and bioactivity that simulate ECM production of subchondral bone [282,283]. Although it is hard to use electrospinning alone to construct MZSs due to the low
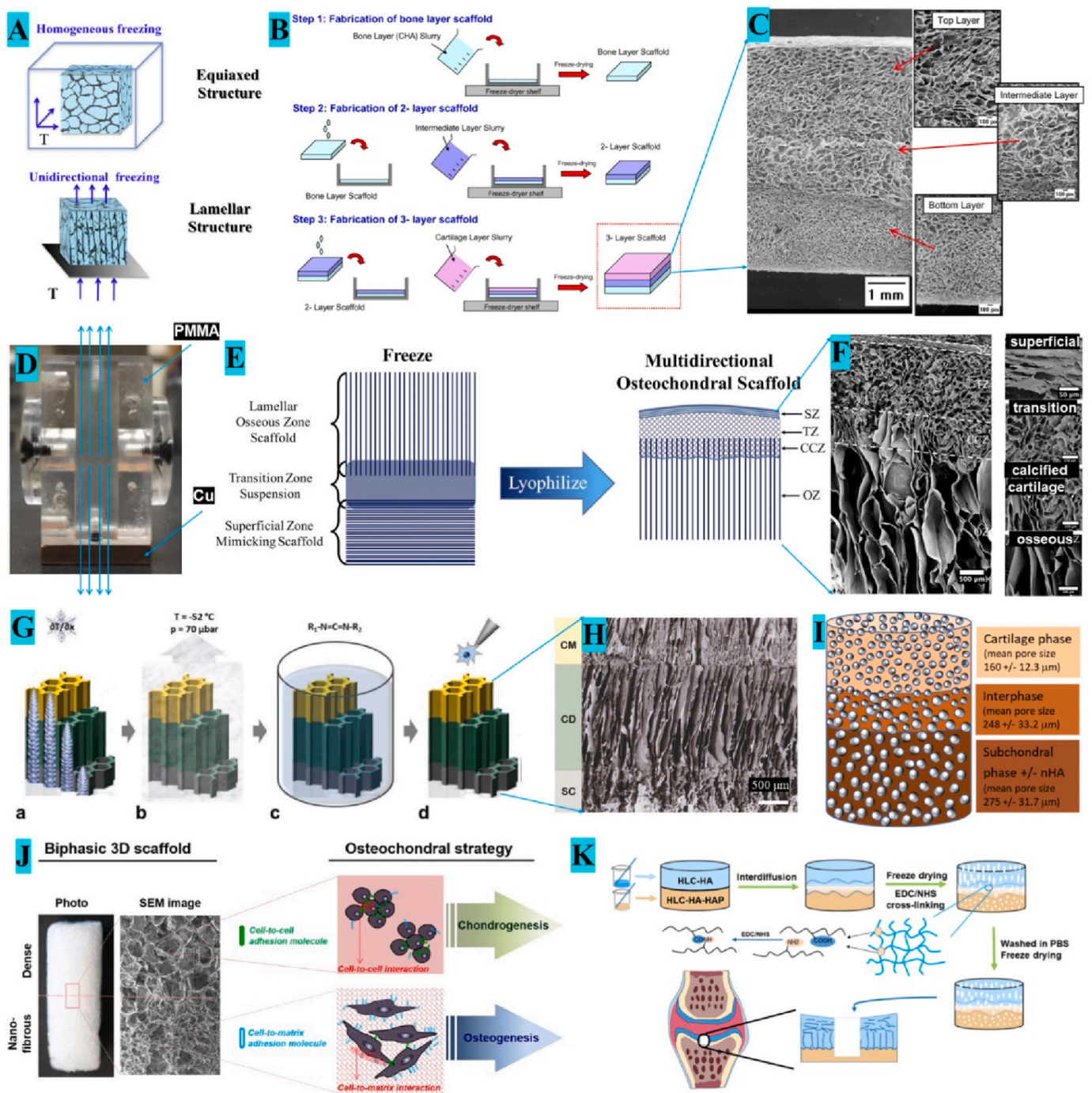
Fig. 5. Representative fabrication processes of MZSs manufactured by multilayered lyophilization or single layered lyophilization in combination with other techniques. A. Schematic illustration of the preparation of scaffold with different pore structures through lyophilization. Adapted with permission from Ref. [51]. B/C. Schematic illustration of the three-step process of the iterative layering process and SEM images of the three-layered scaffold fabricated by multilayered lyophilization. Adapted with permission from Ref. [113]. D. PMMA mold used to unidirectionally freeze collagen suspensions to fabricate lamellar superficial layer. Adapted with permission from Ref. [22]. E/F. Schematical illustration of the lyophilization bonding process and SEM images of the monolithic MZS with distinct zonal specific fiber orientations. Adapted with permission from Ref. [259]. G/H. Schematic illustration of the process involved in the cryostructuring process for the fabrication of the three-layered osteochondral scaffold. Adapted with permission from Ref. [260]. I. Schematic image shows pore size gradient in different zones of the trilayered scaffold design prepared by lyophilization in combination with a porogen-leaching out method. Adapted with permission from Ref. [59]. J. Schematic illustration of the design and osteochondral strategy of the biphasic scaffold with dense and nanofibrous morphologies fabricated by a combination of lyophilization, leaching out and phase separation methods. Adapted with permission from Ref. [78]. K. Schematic illustration of the methodology used for the preparation of a bilayered OC scaffold using the combination of lyophilization and liquid phase synthesis method. Adapted with permission from Ref. [261].

three-dimentionality produced by the technique, it is a powerful tool to create various MZSs in conjugation with other processing techniques.

Electrospinning has been used to prepare the cartilage layer of MZSs [284], which can be fused together with a bone scaffold using a press-fitted method [284–286]. Briefly, a PCL scaffold containing β-TCP was prepared using fused deposition modeling (FDM) to serve as the bone layer. Meanwhile, a PCL electrospun membrane was produced, acting as the cartilage layer. To create an integrated biphasic scaffold, the bone layer was quickly heated on a hot plate and then instantly press-fitted onto the PCL electrospun membrane, followed by cooling and solidification. A similar attempt was made to create electrospun cartilage layer, where the bone zone was manufactured by other techniques [287]. As shown in Fig. 6A, a porous scaffold consisting of chitosan and Si-substituted nano-HAP was produced to serve as the bone layer of the MZSs using a combination of ultrasonication, centrifugation, and lyophilization. Then the porous structure was fixed on a collector, and a mixture of zein solution and polyhedral oligomeric silsesquioxanes (POSS) was electrospun onto the collector to create an integrated bilayer scaffold. The scanning electronic microscopy (SEM) image shows a typical morphology of the cartilage layer manufactured by electrospinning atop a porous bone scaffold (Fig. 6B).

Since electrospun structures are typically porous 2D sheets or pseudo-3D nanofiber scaffolds, electrospinning is an ideal technique to create a thin interfacial layer (tidemark or CCZ) between the cartilage and bone layers. Chen et al. [283] built an integrated multilayer composite scaffold using electrospinning in combination with chemical synthesis and lyophilization. In this study, coaxial electrospun PCL/PEG short fibers were incorporated vertically into the subchondral bone scaffold to facilitate controlled, sustained release of loaded growth factors. More importantly, a PCL/PEG electrospun fiber membrane (Fig. 3E, layer C) was included between the cartilage calcification layer (Fig. 3E, layer B) and the subchondral bone scaffold (Fig. 3E, layer D) to prevent unwanted cell migrations between the chondral and osseous zones. A similar attempt was made by Mellor and coworkers [94], where an electrospun PCL layer was sandwiched between a 3D-bioploted superficial layer of PCL combined with decellularized articular cartilage ECM (dECM) hydrogel (cartilage layer) and a 3D-bioplotted PCL-β-TCP (bone layer) scaffold (Fig. 3B). The electrospun layer prevented cell migration between the cartilage and the bone layers in vitro and was considered to act as a potential barrier to prevent blood vessel invasion into the cartilage layer while implanted in vivo in a large animal (Yucatan minipigs) OC defect model [74,94].

Scaffolds prepared by a traditional electrospinning technique typically exhibit a thin layer with small pore sizes, which obstruct osteogenesis and are not suitable for 3D bone tissue regeneration. To manufacture the bone layer of MZSs with good osteochondral regeneration, a second processing procedure is generally required to turn the 2D electrospun structure into a 3D construct [292]. For instance, a chemical immobilization process was applied on an electrospun PCL layer to enhance OC repair potential of the scaffold [293]. In another study, a type I collagen layer was coated onto microporous electrospun PLA nanofiber layer and then freeze-dried to form a bilayered scaffold. This second processing step was verified to be effective in promoting osteogenic differentiation of MSCs, accelerating subchondral bone emergence, and enhancing cartilage formation in a rabbit OC defect model [294]. Alternatively, to enhance osteogenic potential of the subchondral bone layer of MZS prepared by electrospinning, plasma treatment can be performed on electrospun PCL/PEO nanofibrous layer by boosting the hydrophilicity of the scaffold [295].

It is also possible to engineer stacked layers by iterative use of the electrospinning technique. For example, a 3D anisotropic multilayered fibrous scaffold with zonal specific fiber orientations was built using two complementary electrospinning set-ups [288]. Fig. 6C schematically illustrates the processes involved in the fabrication of a PCL-graphene oxide (GO)-collagen cartilage scaffold. The superficial and deep layers were fabricated by electrospinning PCL solutions onto a rotating drum

(Fig. 6C–I). Cylinders were cut from the electrospun mesh to make the superficial layer with horizontally oriented fibers (Fig. 6C–II) while rectangles were cut and rolled into spiraled cylinders within a GO-collagen hydrogel to form the deep layer with vertically oriented fibers (Fig. 6C–III). The middle layer with randomly oriented fibers was created using a second electrospinning setup with a bath filled with ethanol and water acting as the collector (Fig. 6C–IV). The three layers were staggered and frozen (Fig. 6-V). Then the frozen construct was immersed into a GO-collagen hydrogel, and eventually lyophilized to form an integrated trilayered scaffold with zonal-specific fiber orientations and appropriate pore sizes (Fig. 6-VI). This study proposed a potential methodology to create multilayered scaffolds via repetitive electrospinning approach. However, it relied on external support (GO-collagen network in this study) to maintain the structural integrity of the scaffold, implying that the intrinsic mechanical strength of the multilayered scaffold is likely weak. Another study also demonstrated that MZSs prepared by stacked electrospinning method was prone to delaminate during implantation as its interfaces were susceptible to shear stress [296].

5.3. 3D printing/bioprinting

3D printing, also called additive manufacturing or rapid prototyping, is perhaps the most versatile process among the many approaches for fabricating MZSs for OC repair. It translates materials (inks) into 3D tangible constructs in a layer-by-layer manner with computer-aided design (CAD) digital models [297]. Based on various printing processes, American Society for Testing and Materials (ASTM) has cataloged 3D printing into seven groups, including binding jetting, directed energy deposition, materials extrusion, materials jetting, powder bed fusion, sheet lamination, and vat photopolymerization [298]. Regardless of the subclassifications, MZSs produced by 3D printing have significantly higher reproducibility than all other aforementioned techniques, and this technique can create customized constructs with precisely controlled shapes, mechanical properties, and physiological heterogeneities [299]. Over the past ten years, a scaffold-based printing approach known as 3D bioprinting, which involves the use of living cells in the ink, has been developed rapidly attributed to the recent advancements in cell biology, materials science, and 3D printing [300]. It naturally entails more complications than acellular 3D printing, such as the selection of cell types and growth factors (discussed in the following section), the biocompatibility of inks, the technical difficulties of using living cells, and the environmental sensitivity of growth factors during printing [301,302]. That said, 3D bioprinting enables the possibility to create MZSs with not only zonal specific compositions and structures, but also zonal spatial distributions of cells and biological and chemical cues during the scaffold fabrication process [303].

Fig. 6D schematically illustrates a few representative contact and noncontact 3D printing techniques that are commonly used to manufacture cellular and acellular scaffolds for tissue engineering [289]. The working principles and detailed mechanisms of these processes have been reported [289,300,304,305]. Thereinto, extrusion-based printing is considered the most prevalently implemented strategy to produce cell-free or cell-laden hydrogels and scaffolds for tissue regeneration and has been gaining momentum in recent years [121,289,305–310]. Fig. 6E depicts an exemplary schematic of an extrusion-based 3D pneumatic printing system [290], and Fig. 6F presents a cell-free trilayered OC scaffold created using a custom-made, multi-nozzle 3D printing system [110]. The subchondral bone layer, interfacial layer, and cartilage layer comprising different combinations of inks were printed layer-by-layer from individual nozzles with different syringe temperatures, extrusion pressures, and layer thicknesses. A UV light source was equipped onto a platform to photo-crosslink the trilayered scaffold during printing. The trilayered scaffold exhibited appropriate swelling ratio, biodegradation rate, and mechanical properties, excellent biocompatibility, and promising osteochondral regeneration capability in repairing a full thickness
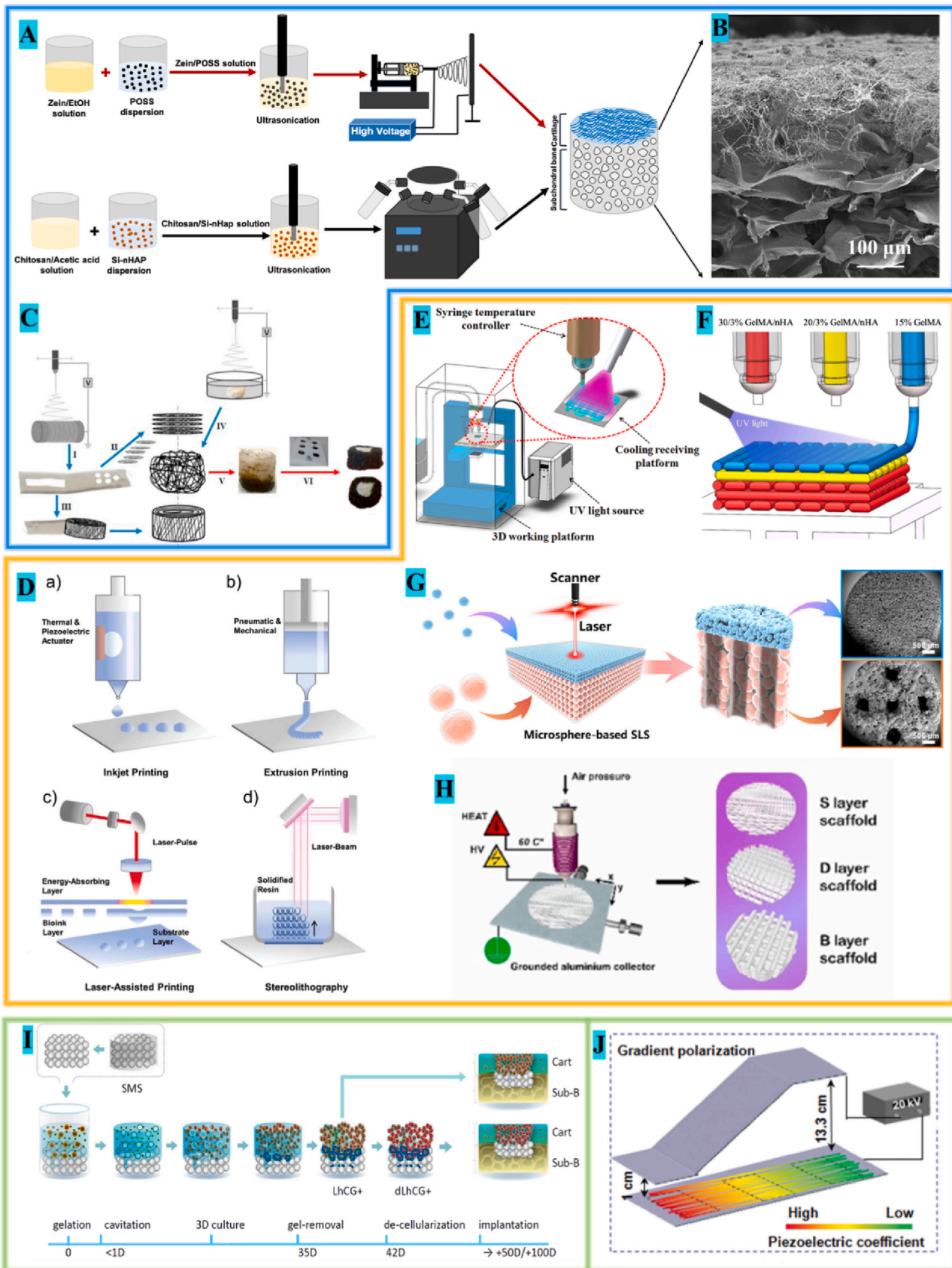
Fig. 6. Representative fabrication processes of MZSs manufactured by electrospinning-based, 3D printing and other strategies. A/B. Schematic process and an SEM image of the chitosan/nHAP porous layer and zein/POSS fiber layer fabricated by a combination of ultrasonication, lyophilization, and electrospinning. Adapted with permission from Ref. [287]. C. Schematical illustration of the process for fabrication of a PCL-GO-collagen scaffold using repeated electrospinning. Adapted with permission from Ref. [288]. D. Schematics of representative 3D printing techniques: a) inkjet, b) extrusion, c) laser-assisted, and d) stereolithography printing. Adapted with permission from Ref. [289]. E. Schematic of advanced extrusion-based 3D pneumatic bioprinting system affiliated with a temperature controller. Adapted with permission from Ref. [290]. F. Schematic of a 3D multi-nozzle pneumatic printing system used to fabricate gelatin methacrylate (GelMA)/nHAP-based scaffold. Adapted with permission from Ref. [110]. G. Schematical diagram of the fabrication processes and SEM images of the bilayered integrated OC scaffold with inconsecutive channels obtained using SLS. Adapted with permission from Ref. [291]. H. Schematic drawing of the MEW setup and the fiber network for fabrication of a trilayered scaffold. Adapted with permission from Ref. [112]. I. schematic illustration of the fabrication process of a full-scale OC graft consisting of natural chondrocytes secreted ECM cartilage layer and sintered microsphere scaffold (SMS) subchondral bone layer. Adapted with permission from Ref. [23]. J. Schematic illustration of the gradient polarization process using a DC electric field to grant uniform scaffolds with gradient piezoelectricity for osteochondral regeneration. Adapted with permission from Ref. [209].

rabbit OC defect. In a recent study, a series of PLA-alginate osteochondral scaffolds, including monophasic, biphasic, triphasic, and gradient (seven zones) ones, were designed and fabricated using extrusion-based 3D printing and bioprinting [63]. Such obtained scaffolds demonstrated precisely controlled spatial hierarchy with tunable zonal specific porosities. High cell viability was found in the top zone of either a cell-laden triphasic or a gradient scaffold, which was realized by concurrent printing chondrocytes loaded alginate hydrogel-PCL scaffolds [63].

Another important 3D printing technique in manufacturing osteochondral MZSs is SLS, which is a subset of powder bed fusion 3D printing. As the name implies, it is a laser-assisted printing technology that selectively sinters powder particles with a high-intensity laser, fusing the particles to form 3D objects in a layer-by-layer fashion [311]. With the aid of sintered fusion, MZSs manufactured by SLS provide a stronger interfacial interlocking to prevent them from delamination during implantation compared to other additive manufacturing techniques. Gu et al. [291] constructed three integrated scaffolds with distinct channel patterns, including non-channel, consecutive-channel (channels pass through both zones), and inconsecutive-channel (channels in bone zone only) using microsphere-based SLS. Fig. 6G depicts the schematic diagram of the process used to fabricate the integrated osteochondral scaffold with inconsecutive channels using SLS, and the SEM images show both the dense cartilage layer and the porous subchondral bone layer. The obtained scaffolds exhibited excellent mechanical properties, the porous bone zone illustrated perforated channels promoted bone ingrowth and vascular remodeling, and the dense cartilage zone inhibited the invasion of vascularization in a rabbit OC defect model. A similar attempt was made by Du et al. [97], where a multilayer osteochondral scaffold consisting of PCL and HA/PCL microspheres was constructed using SLS. This MZS was able to produce outstanding neo-native tissue integration and accelerate early subchondral bone healing in a rabbit OC defect model.

In general, 3D printing techniques suffer from limited spatial resolution and lack of the ability to construct scaffold with submicron features to closely mimic the native OC tissue [296,312]. Combining the advantages of solution electrospinning and 3D printing, MEW has recently emerged as a high-resolution, 3D printing approach to create precisely controlled tissue engineering scaffolds with a few micrometers to submicronmeter ranged structural details [313–315]. For example, Fig. 6H presents the schematic diagram of the preparation processes of a gelatin methacrylate (GelMA)-based trilayered osteochondral scaffold, which was created by MEW in combination with FDM (an extrusion-based printing) using a single MEW device [112]. Poly(ε-caprolactone)-*block*-poly(ethylene glycol)-block-poly(ε-caprolactone) (PCL-*b*-PEG-*b*-PCL, PCEC) fibers with depth-dependent spatial organizations were fabricated via MEW to mimic the collagen fiber orientations in natural OC tissue. The printed fibers were continuous and well stacked along the constructs with depth-dependent diameters, spacings, lay-down patterns, and orientations. Also, the use of PCEC fibers significantly increased the mechanical strength of the GelMA hydrogel. In follow-up studies, a series of multilayer scaffolds with different compositions and pore sizes were fabricated using MEW alone or in

combination with other techniques, such as inkjet printing, FDM, and lyophilization [73,253,316].

Overall, 3D printing multizonal scaffolds can be easily constructed into defect-specific shapes according to the architecture of different osteochondral lesions, making it possible to create customized tissue engineering scaffolds. The newly emerged 3D bioprinting technique provides a longer tether to treat these defects by creating personalized zonal-specific, cell-laden scaffolds. Nevertheless, the high cost associated with such products might be one of the main barriers that prevents it from being widely used in clinics. In addition, the printability requirement of materials has also obstructed 3D printing from being widely used in tissue engineering. For example, most of the natural polymers, such as collagen and chitosan, have limited printability or have strict requirements of the physicochemical conditions during printing [317,318], and unlikely to be used as the main components in constructing 3D printed scaffolds thus far. Furthermore, some specific 3D printing techniques have their own limitations. For examples, the extrusion-based printing or bioprinting has limited ability to construct scaffolds with submicronmeter level microstructures; the materials used for MEW should be mostly thermoplastics; and the SLS and stereolithography equipment are very expensive.

5.4. Other strategies

Other than the aforementioned techniques, there are also some routes that can engineer integrated OC multizonal scaffolds or generate gradient properties and bioactive cues in uniformed structures to direct the zonal regeneration of OC tissue. This can be achieved by prefabricating a support layer and then produce cell-derived layers to create a multilayered scaffold [23,319]. Alternatively, it can be simply realized by applying external forces such as DC electric field [209] or magnetic field [254,320] to redistribute the prefabricated uniformed constructs with gradient properties, forming a "fake" osteochondral MZS. Here the "fake" MZSs can be defined as those without obvious layered or gradient compositions and architectures but have gradient properties or bioactive signals from top-to-bottom of the spatial coordinates in the defect area to induce zonal-specific, chondrogenic/osteogenic differentiation and osteochondral regeneration.

In a work conducted by Nie et al. [23], a full-scaled osteochondral graft consisting of a sintered microsphere scaffold (SMS) subchondral bone layer, a natural ECM cartilage layer secreted by chondrocytes, and a transitional interconnecting network layer, was manufactured by a biofabrication method. As illustrated in Fig. 6I, sintered PLGA microspheres were heated in a silicon mold to prepare the subchondral bone layer, on top of which porcine chondrocytes and gelatin microspheres were added to an alginate solution allowing for in situ gelation with the addition of Ca^{2+}. Then the whole construct was cultured in vitro allowing for sufficient secretion of ECM by chondrocytes before the alginate gel was revoked. The biologically developed ECM deposition was considered the cartilage layer of the OC graft. Between the two layers, there was a transitional interface layer formed by the migration and ingrowth of chondrocytes in the porous SMS zone, forming a continuous interconnecting network. The whole structure was

decellularized to achieve a longer shelf life. Such prepared multilayered scaffolds (with or without decellularization) demonstrated excellent in vivo tissue regeneration as evaluated in a rabbits OC defect model [23]. Similarly, Jin and coworkers [319] constructed a multilayered (twelve layers) scaffold, in which PCL-gelatin electrospun fibrous meshes were integrated with a number of bio-derived cell sheets. They found that the fibrous meshes were able to act as supporting substrates to induce BM-MSCs to differentiate into osteo- and chondral-linages in chondrogenic and osteogenic inductive media, respectively [321,322]. In particular, three cell sheets, including cartilage, calcified cartilage, and bone layers, were respectively produced atop the fibrous meshes in different media. Then, these pre-differentiated cell sheets and meshes were stacked layer by layer and incubated in vitro for 7 days to form a well-bonded, integrated, gradient 3D construct to mimic the cartilage-to-bone transition. Such prepared bio-fabricated multilayer scaffold was proved to favor OC repair in a rabbit full-thickness OC defect.

Regarding the "fake" osteochondral MZSs, the key point is to direct zonal-specific tissue repair by exerting the spatial property gradient rather than the compositional and structural variations. Inspired by the gradually varied piezoelectric properties of native osteochondral unit, Liu et al. [209] recently designed a biomimetic electrospun PLLA nanofibrous mat (single layer) with gradient piezoelectric properties to induce OC differentiation. As shown in Fig. 6J, an electrospun nanofibrous mat was polarized under a DC electric field with linear variation of strength to generate gradient piezoelectricity along the depth of the scaffold. In the meantime, cell adhesion generated enough forces to trigger piezoelectricity and therefore induced a self-stimulated selective differentiation of MSCs with different piezoelectricity voltages at different spatial coordinates. In particular, it was found that MSCs attached on the surface of the top region of the scaffold had a lower piezoelectricity voltage that promoted chondrogenesis, while those in the bottom region of the scaffold showed a higher piezoelectricity voltage favoring osteogenesis. In addition, a smooth transition from chondrogenic to osteogenic differentiation was observed between the two regions. Other than electric field, an external magnetic field was also used to generate a chondrogenic precondition for enhanced OC repair [320]. Citric acid-coated magnetic nanoparticles (NPs) (CAG) were incorporated into electrospun gelatin nanofibers and seeded with MSCs. The cells within the CAG scaffolds were then stimulated mechanically as a result of spatial confinement and fluid flow while the scaffolds were driven up and down by a rotating magnetic field. These treatments significantly enhanced chondrogenesis of MSCs and such an in vitro preconditioning could achieve superior osteochondral repair in rabbit knee osteochondral defects. Alternatively, the use of magnetic field could pattern a spatial biochemical gradients in uniformed hydrogels or even scaffold-free systems by pre-loading magnetic NPs with chondrogenic or osteogenic growth factors (discussed in the following section), and therefore obtain region-specific cell differentiations and eventually simultaneous bone and cartilage regeneration [254, 323]. Compared to other strategies, the use of these "fake" MZSs in treating OC lesions clearly simplifies the manufacturing processes of MZSs and lessens the concerns of MZSs delamination. Nevertheless, such a strategy usually involves a sophisticated pretreatment or an exquisite design to manipulate the spatial distributions of gradient properties and bioactive signals, which may in turn complicate the overall treatment in in vivo settings and clinical trials.

6. Cell sources and growth factors in MZSs

There are four continuous and overlapping stages involving with the regeneration of both the bone and the cartilage tissues, including hemostasis, inflammation, repair, and remodeling (Fig. 7A) [324]. Tissue engineering strategies with the use of MZSs for OC regeneration mainly play direct roles in the latter two stages. That said, to realize simultaneous bone and cartilage regenerations, cells and growth factors can be introduced into MZSs to regulate all the four stages directly or indirectly by impacting many important immune molecules and signaling as described in Fig. 7A. Therefore, in addition to advanced scaffold design, appropriate selections of cell sources and GFs are the remaining two major factors impacting the outcomes of osteochondral repair using MZSs.

6.1. Cell sources for osteochondral regeneration

The major types of cells resident in different zones of the OC tissue is depicted in Fig. 7B [325]. Consequently, chondrocytes, osteoblasts, chondroprogenitor cells, and stem cells with chondrogenic or osteogenic potentials have been used in osteochondral regeneration. As the main cell type resident in articular cartilage, chondrocytes were once the dominate cell source in the field. However, they are prone to dedifferentiate into fibroblasts and have limited proliferation ability during expansion [326]. Although osteoblasts have been found to possess some potential to differentiate into chondrocyte-like cells [327], they are usually cocultured in the lower zone of OC unit with other types of cells to primarily promote the subchondral bone regeneration [71,103,122]. Chondroprogenitor cells have been considered a promising candidate for cartilage repair due to their inherent nature of chondrogenesis potential and low possibility of hypertrophic cartilage formation [312,328, 329]. But these cells especially their immunogenic properties still have not been well identified and their exact contribution to OC repair remains obscure [330]. To optimize the use of chondroprogenitor cells for osteochondral regeneration, a better understanding needs to be developed on how to enhance chondrogenesis of chondroprogenitors while maintaining their minimal hypertrophic tendency [331].

Alternative options are the use of stem cells, including adult stem cells (ASCs), embryonic stem cells (ESCs), and induced pluripotent stem cells (iPSCs) [334]. ASCs are found in different adult body tissues. Among various ASCs, MSCs derived from adipose tissue (AT-MSCs), peripheral blood (PB-MSCs), joint synovium (JS-MSCs), and especially bone marrow (BM-MSCs), are the most commonly used forms in osteochondral tissue engineering due to their ease of isolation and high availability compared to other types of stem cells [335–337]. As BM-MSCs have long been used for bone regeneration due to their high potential of osteogenic differentiation and bone formation [269,338, 339], they can be a good cell source to stimulate subchondral bone regeneration in MZS. Although BM-MSCs have shown some chondrogenic potential, they produce cartilage only after external induction with extensive environmental cues, which may cause concerns on hypertrophic cartilage formation and subsequent calcification [340,341]. Recent studies have recognized the osteogenic and chondrogenic potentials of activated skeletal stem cells (SSCs), which can be found in many different skeletal tissues [342,343]. Fig. 7C depicts multiple anatomical sites of mice postnatal long bone where SSCs reside [332]. But like other species of ASCs, their application in clinics may be restricted by their low population and low proliferation rate in aged patients. And they have to be activated by certain procedures to enhance their differentiation capacity [342]. Although ESCs from mammalian embryo have been considered the most suitable type for osteochondral repair due to their unlimited self-renew ability and pluripotency, their use is still ethically controversial [344]. The use of iPSCs, which can be genetically reprogrammed from somatic cells, has therefore been gaining momentum since their discovery in 2006 as they possess similar self-renew potential and pluripotency of ESCs but have no ethical complications [345–347]. For example, Nam et al. [348] found that human iPSCs derived from cord blood cell showed high expression of chondrogenic markers, such as ACAN, COMP, Col2, SOX9, but low expression of fibrotic and hypertrophic cartilage makers, Col1 and Col10. Zhang et al. [349] successfully induced iPSCs to differentiate into chondrogenic mesoderm lineage and the resulted cartilaginous pellets were found to be capable of promoting bone/cartilage regeneration in vivo. iPSCs have also demonstrated obvious tissue regeneration in large
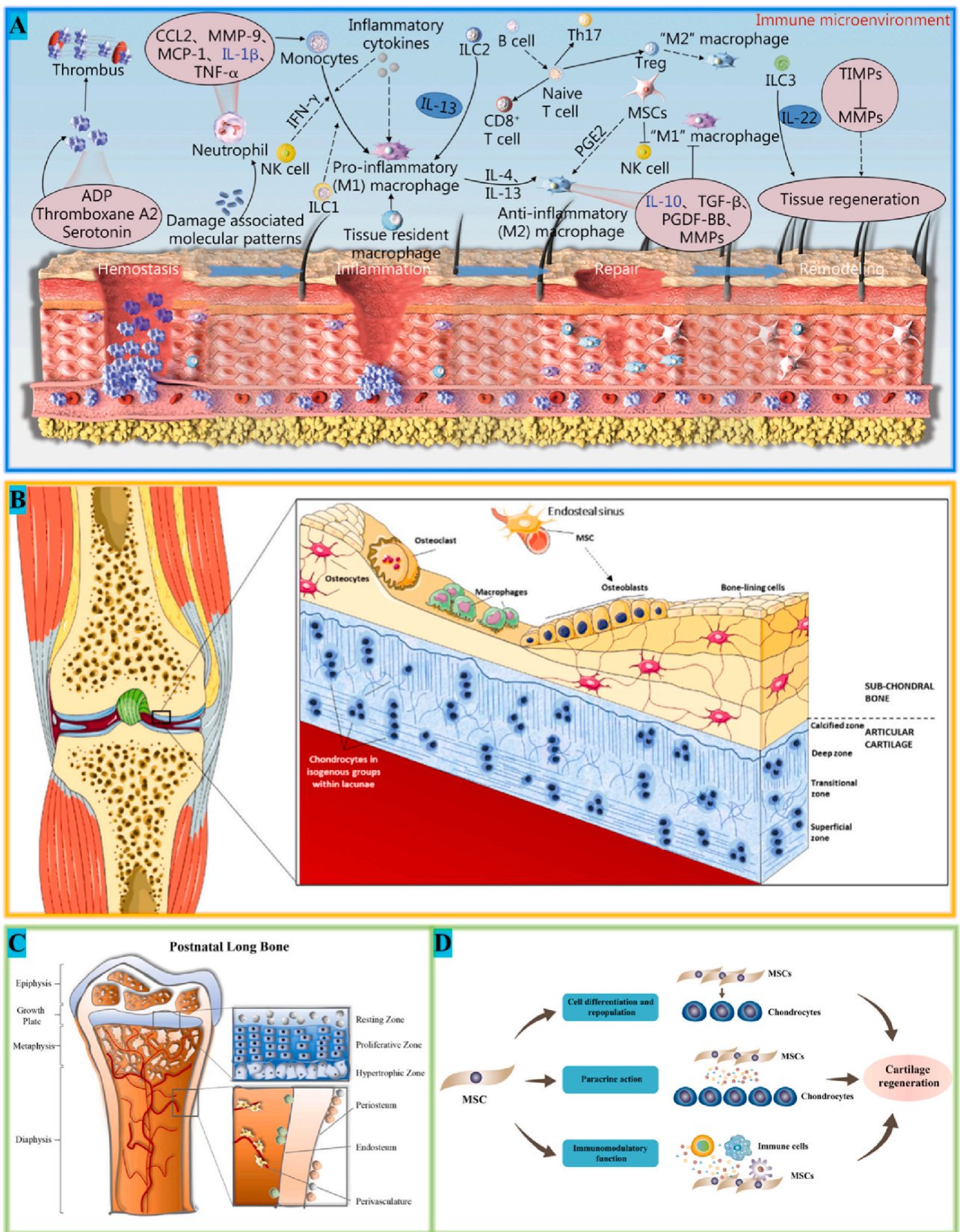
Fig. 7. A. Four continuous and overlapping stages involved with bone/cartilage tissue regeneration and important immune molecules and signaling during tissue regeneration. Adapted with permission from Ref. [324]. B. Anatomical illustration of major types of cells residing in osteochondral tissue. Adapted with permission from Ref. [325]. C. Multiple anatomical sites of long bone skeletal stem cells in mice. Adapted with permission from Ref. [332]. D. Different mechanisms of cartilage regeneration promoted by MSCs. Adapted with permission from Ref. [333].

animal OC defect model, such as pigs, when they are loaded into a tissue engineering scaffolds [350]. Despite these exciting findings of iPSCs for OC regeneration, as a relative new cell type, there still lacks a gold standard to control the directional differentiation of iPSCs toward osteogenesis or chondrogenesis, and the production of hyaline cartilage from iPSCs is highly dependent on their surrounding microenvironment [351,352]. A recent study revealed that even the chondrocytes derived from the same iPSCs but through mesodermal and ectomesodermal differentiations could induce totally different outcomes [353]. Besides, it is noted that both ESCs and iPSCs are of safety risks as the residual undifferentiated cells can have a tumorigenic potential [354].

Therefore, selection of appropriate cell sources for osteochondral regeneration remains a challenge as each type of cell has its pros and cons. Table 3 summarizes the major advantages and disadvantages of these cells and their applications in osteochondral regeneration. Regardless of the cell types, it is believed that stem cells contribute to osteochondral repair mainly via three mechanisms: (1) They directly differentiate into either cartilage or bone lineage under suitable environmental cues; (2) With the revealing that the newly regenerated OC tissue consisted of no DNA of donor MSCs [355], researchers have proven that the paracrine secretome from exogenous donor stem cells play important roles in homing, proliferation, differentiation, metabolism, and inflammatory processes of host cells to facilitate osteochondral repair [356–359]. (3) They participate in immunomodulatory functions by interacting with immune cells. Fig. 7D specifies the diverse mechanisms of MSCs in regenerating cartilage tissue [333]. To differentiate donor cell contribution to tissue regeneration, our group recently used progenitor cells harboring different colors of fluorescent makers from host transgenic mice [53,267]. The results showed that no donor fluorescence was detected from the newly regenerated bone or cartilage

tissue, which indicated that the tissue formation was mainly contributed by host cells. Overall, we believe that the donor cells contributed to tissue regeneration more likely via secreting active paracrine factors or playing active roles in immune reactions instead of directly differentiating into targeted cell lineages.

6.2. Growth factors for osteochondral repair

Addition of natural or synthetic GFs is an alternative approach to regulate the microenvironment for effective OC tissue repair [362]. GFs can be administered through systemic delivery, but their half-life in blood stream is typically short [19]. To effectively address this issue, growth factors have been loaded into MZSs to enable a localized and sustained release, as illustrated in Fig. 8. Natural growth factors used for osteochondral repair mainly include transforming growth factor-β (TGFβ) superfamily, platelet-derived growth factors (PDGFs), insulin-like growth factors (IGFs), fibroblast growth factors (FGFs), and angiogenesis-related GFs such as the pro-angiogenesis vascular endothelial growth factors (VEGFs) and anti-angiogenesis thrombospondins (TSPs) [334,363,364]. Due to the low availability and high cost of these natural GFs, synthetic molecules, such as dexamethasone (DEX), kartogenin (KGN), and Bevacizumab, have also become popular payloads to stimulate OC repair [365,366].

Bone morphological proteins (BMPs), which are a group of cytokines belonging to the TGFβ superfamily, have long been used for bone and cartilage regeneration as they involve in a series of embryonic development processes, such as skeletal morphogenesis, hematopoietic, and epithelial cell differentiation [367,368]. They are distinguished from other TGFβ members by the presence of conserved cysteines in the mature region [368]. BMP2 has been investigated the most as it is

Table 3
Comparison of different cell sources for osteochondral regeneration.

| Types of Cells	Types of layers	Pros for osteochondral regeneration	Cons for osteochondral regeneration	Ref.
Chondrocytes	CL	Major cell type in articular cartilage. High tolerance in the low oxygen tension environment of avascular tissue such as cartilage.	Prone to dedifferentiate into fibroblasts. Poor self-healing property. Limited in vitro proliferation ability. Low overall differentiation capacity.	[325,326]
Osteoblasts	BL	High availability. Osteogenic capability.	Limited chondrogenic potential. Potential of vascular invasion into cartilage. Low overall differentiation capacity.	[71,103,122, 325,327]
Chondroprogenitor cells (descendants of stem cells with bias toward chondrocytes)	CL	High chondrogenic ability. In vitro expansion does not alter differentiation. Low hypertrophic cartilage formation.	Low population. Extensive expansion is necessary for clinical use. No standard isolation protocols. Immunogenic reaction unclear.	[312,328–330, 354,360]
MSCs (multipotent)	BL/CL	Abundant sources (can be obtained from different tissues such as adipose tissue, joint synovium, peripheral blood, bone marrow). High potential of both osteogenesis and chondrogenesis. Good anti-inflammatory and immunomodulatory properties.	Potential of hypertrophic cartilage formation. Potential of cartilage calcification. Difficult to ascertain their contributions and reveal specific mechanisms to symptomatic improvement.	[269,335–342, 361]
SSCs (multipotent)	BL/CL	Abundant sources (Fig. 7C). High self-renew ability. High potentials of both osteogenesis and chondrogenesis. Recruiting of SSCs into injured sites can be triggered by localized and acute injuries.	Low population in aged patients. Differentiation capacity has to be activated by certain procedures.	[332,342,353]
ESCs (pluripotent)	BL/CL	Unlimited self-renew ability. Theoretically the most suitable cell type for OC repair. High potentials of both osteogenesis and chondrogenesis.	Ethical concerns. Safety concerns (tumorigenic potential of undifferentiated cells).	[344,354]
iPSCs (pluripotent)	BL/CL	High availability. Unlimited self-renew ability. High potentials of both osteogenesis and chondrogenesis. Superior for clinical use than ESCs.	Safety concerns (tumorigenic potential of undifferentiated cells). Highly sensitive to surrounding microenvironment.	[345–354]
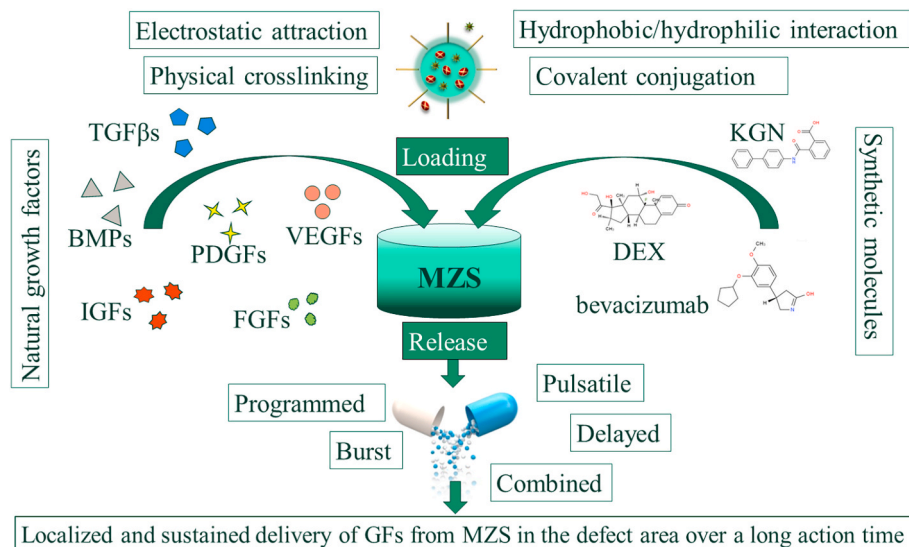
Fig. 8. Illustration of typical loading routes and release patterns of natural and synthetic growth factors for osteochondral repair.

currently the only BMP that has been approved by the Food and Drug Administration (FDA) and has shown both osteogenic and chondrogenic potentials [369,370]. Still, its applications in clinics were associated with various side effects, such as swelling, seroma, increased cancer risk, and hypertrophy tissue formation [371]. Besides, convincing clinical data, which offer valuable knowledge regarding the BMP2 dosage, time-course, loading carrier, and controlled release pattern, remain a dearth [372]. BMP7, also known as osteogenic protein 1 (OP1), was once considered a potent bone inducing agent and showed some initial functions in cartilage homeostasis and repair [373,374]. However, it is no longer an option for bone and cartilage repair in clinic as it failed to get ultimate approval from the FDA and its products had been withdrawn from the market [375,376]. With that being said, researchers are still actively investigating BMP7, alone or combing with other growth factors, in MZSs to stimulate osteochondral defect regeneration [112, 253,377]. BMP3 is the most abundant BMPs and acts as a negative regulator of bone density [378]. Thus, it is commonly used as an antagonist to reduce the chance of hypertrophy induced by osteogenic BMPs, such as BMP2. BMP4, BMP6, and BMP9 are other commonly seen BMPs for bone and cartilage repair. They have shown to induce bone mineralization, orthotopic ossification, chondrocyte maturation, and chondrogenic differentiation [379–383].

Other members of the TGFβ superfamily include activins, inhibins, and TGFβs [367]. TGFβ factors were initially isolated from platelets, and they were lately found extremely rich in bone as osteoblasts have a high concentration of TGFβ receptors [384–386]. Three isoforms of TGFβ (β1, β2, β3) present in human beings and play important roles in cell replication, cartilage/bone formation, and fibrosis [387]. Among them, TGFβ1 and TGFβ2 are associated with metabolism of proteoglycans and formation of stabilized aggregates of link proteins in articular cartilage, while TGFβ3 is believed to regulate collagen synthesis and promote hyaline cartilage formation [386–390]. As a result, all three of them are commonly used to stimulate chondrogenesis of stem cells and articular cartilage tissue regeneration [391–393]. To mediate osteochondral damage, TGFβs are usually co-delivered to the defect area with other osteogenic growth factors. For example, it has been a long tradition that TGFβ1 was loaded to the chondral zones, while BMP2 was added to the osseous zones of MZS to simultaneously stimulate cartilage and bone regeneration [275,394–398].

Besides TGFβ, there is another important family of grow factors that can be isolated from platelets, called PDGFs. Human PDGF was identified as two different disulfide-bonded polypeptide chains, A and B, which give three isoforms of PDGFs including PDGF-AA, PDGF-AB, and PDGF-BB [399,400]. Since PDGFs are stored primarily in platelets, they play fundamental roles in the wound healing cascade [401]. Recombinant human PDGF-BB (rhPDGF-BB) has received FDA approval for the treatment of periodontal, orthopedic bone defects, and dermal wound healing [402]. Although cartilage is an avascular tissue, PDGFs are believed to promote cartilage tissue regeneration as they are potent mitogenic and chemotactic factors for various cells, including MSCs, fibroblasts, osteoblasts, osteoclasts, and chondrocytes [401,403]. HA hydrogels loaded with rhPDGF-BB have shown significant improvement of the anabolism of collagen type II and inhibition of the catabolism of chondrocytes in a rat knee OA model [404]. Meanwhile, rhPDGF-BB could be used to alleviate the level of inflammation in chondrocytes and decrease the apoptosis rate of chondrocytes [405]. It has also been demonstrated that collagen sponge impregnated with PDGF was able to repair full-thickness osteochondral defect of New Zealand while rabbits [406]. Very recently, Luo et al. [407] found that continuous release of PDGF from SF-HAP-based MZS could significantly increase the adhesion, proliferation, and chondrogenic differentiation of SJ-MSCs and largely improve the repair process of rabbit critical-size osteochondral defect.

IGFs include both IGF1 and IGF2, which are named after their similar protein sequencing to insulin. IGF1 is a protein participating in many biological activities and thus is closely associated with a series of severe diseases, such as congestive heart failure, Huntington's disease, and Alzheimer's disease [408–410]. It is the main anabolic growth factor for articular cartilage and primarily produced by livers and it reaches cartilage through the synovial fluid [401,411]. As a result, it plays an important role in cartilage homeostasis by balancing the synthesis and breakdown of proteoglycan via chondrocytes [412]. The decrease of serum level of IGF1 is believed to be associated with increased risk of rheumatoid arthritis [413]. In osteochondral tissue engineering, sustained release of IGF1 from a coacervate-mediated hydrogel has been reported to effectively induce chondrogenic differentiation of AD-MSCs and significantly augment tissue repair in a rabbit full thickness OC model [414]. Localized delivery of IGF1 enhanced the migration, adhesion, growth, and cartilaginous matrix production of chondrocytes, and improved the cartilage-graft integration in rats [415]. A co-delivery of IGF1 and TGFβ1 accelerated osteochondral defect healing in a rabbit OC defect model [416,417]. Besides cartilage, IGF1 has also been shown to enhance osteogenic capability of aged BM-MSCs and stimulate mouse longitudinal bone growth [418,419]. IGF2 can be a possible mediator influencing tumor growth and cardiovascular diseases with some inconclusive initial evidences, but it has rarely been used in OC tissue

engineering [420,421].

FGFs are important in bone and cartilage development and repair as mutations of FGFs in patients may ultimately result in various skeletal abnormalities, such as chondrodysplasia syndromes, skeletal overgrowth, and craniosynostosis syndromes [334,422]. They can regulate limb bud development and formation of mesenchymal condensation, and play important roles in mediating chondrogenesis, osteogenesis, and bone and mineral homeostasis [422]. Among the discovered 22 species of FGFs, FGF-2, also known as basic FGF (bFGF), is the most broadly used form for treating osteochondral damages as it is widely distributed in the body, including most organs, tissues, and cells and possesses strong cell-promoting ability [423]. It has been demonstrated that targeted delivery of FGF2 to subchondral bone could enhance the repair of rabbit articular cartilage defect via BMP signaling pathway [424]. Moreover, FGF2 was evidenced to regenerate both bone and cartilage tissues when treating large OC defects in rabbits and sheep [425–427]. Other members of FGFs, including FGF8 [428,429], FGF9 [430,431], and FGF18 [430,432–434], were found effective in treating OC defects. FGF8 is known as androgen-induced growth factor (AIGF) and was found to play key roles in early embryonic development, brain formation, and limb development, and therefore has been used to direct MSCs to differentiate into osteogenic linages and stimulate new bone formation [428,429]. FGF9 and FGF18 were reported to stimulate early chondrogenesis, augment ECM production, and delay terminal hypertrophy of MSCs [430]. Intra-articular injection of exogenous FGF9 has been shown to delay articular cartilage degradation while aggravating osteophyte formation in post-traumatic OA [431]. FGF18 has also been used to stimulate repair of damaged cartilage and decrease articular cartilage degradation [432,433]. Recently, it has been applied to enhance the healing of microfracture-induced cartilage [434].

As mentioned above, healthy cartilage tissue is avascular and aneural. However, blood vessels may breach into the tidemark and invade cartilage from the subchondral bone while OA is developed [435]. Thus, angiogenesis must be avoided in chondrogenesis to prevent associated structural damage and pain in cartilage [436–438]. However, angiogenesis is a prerequisite to osteogenesis as insufficient neovascularization in bone defect leads to hypoxia and cellular necrosis, ultimately leading to the failure of bone regeneration [436,439]. Therefore, it is important to manage the angiogenetic effects in different zones of MZSs to achieve zonal specific tissue repair of osteochondral defects via addition of either pro- or anti-angiogenetic GFs. VEGFs are considered major inducers of angiogenesis that can be secreted from chondrocytes. The family of VEGFs contains seven members, including VEGF-A-F, and placental growth factor (PlGF), among which VEGF-A is the most prominent in angiogenesis, being known as VEGF [440]. Controlled release of VEGF from tissue engineering scaffolds has been shown to effectively enhance osteogenic differentiation and bone regeneration [441–444]. In an in vivo study conducted by Sakata et al. [445], the early-stage osteochondral regeneration process was found to be highly related to the level of VEGF expression. It was found that obvious bone ingrowth was achieved in the deep zone of the scaffolds as a result of continuous VEGF expression, while cartilage formation was observed in the superficial zone of the scaffolds with decreased VEGF expression in a rabbit osteochondral defect filled with a bioresorbable poly(DL-lactide-co-glycolide) scaffold. In contrast, VEGF localization covered the entire defect area in the group without scaffold implanted, resulting in delayed cartilage regeneration [445]. Significantly higher levels of VEGF and its receptors were also observed from chondrocytes and cartilage tissues of OA patients compared to those of healthy ones, further revealing the direct relationship between VEGF and cartilage damage [446–448]. As a result, creating an avascular environment in cartilage zone by effectively blocking VEGF signals could be a promising strategy in treating OA and improving cartilage repair [440,448,449]. Alternatively, this can be achieved by using antiangiogenic factors, such as angiostatin, endostatin, and most of the primarily TSPs including TSP1, TSP2, TSP4, and TSP5 [329,364,450–453]. In summary, to

effectively treat biphasic OC defects using angiogenetic factors, it remains a challenge to balance their roles in promoting bone regeneration while deteriorating cartilage lesion.

Besides these natural growth factors, synthetic molecules have also been drawn attention to the treatment of OC defects owing to their low cost and high availability. As mentioned above, creating a vascular-free microenvironment by the addition of antiangiogenic molecules could be an effective way to enhance articular cartilage regeneration. As the first antiangiogenic antibody that was approved by the FDA in 2004, bevacizumab, also known by its brand name as Avastin, has been used extensively to inhibit osteoarthritis and improve articular cartilage repair through its anti-VEGF effect in animals [454–456]. Recently, Utsunomiya et al. [438] revealed that intra-articular injection of bevacizumab could significantly enhance the quality and quantity of regenerated hyaline cartilage in a rabbit OC defect model. However, it still lacked convincing evidence in clinics or even in large animal models to prove the efficiency of bevacizumab in treating OA or OC defects. DEX, a synthetic glucocorticoid with broad anti-inflammatory activities, has been used in clinics to treat a wide range of diseases. It is noted that DEX is the first drug to show life-saving effect in patients infected with COVID-19, decreasing mortality by 35% of those with severe symptoms. This is due to that DEX has potent anti-inflammatory effect to reduce the chance of hyperinflammation, an overreaction of the immune system which can ultimately cause organ failures and fatalities [457–459]. OA or OC defects are always associated with joint inflammation and pain. DEX has therefore been orally or intravenously administrated to control inflammation and reduce joint damage [460–463]. It has also long been used as a supplement of cell culture medium to induce chondrogenic differentiation of cells [134,464,465]. It was discovered that localized and sustained release of low-dose DEX from an acellular agarose hydrogel could enhance osteochondral repair through a dual pro-anabolic and anti-catabolic effect to attenuate inflammation and support the functional integrity between the acellular graft material and host tissue in a preclinical canine OC autograft model [466]. DEX also showed enhanced OC repair in rats when it was loaded in a MZS made of alginate, chitosan and β-TCP [467]. It was found that the OC healing potential of such treated MZS was even better than a commercial product, Maioregen® [467]. KGN is another example of synthetic molecule that has positive impacts on cartilage regeneration. It has drawn significant attention since its discovery in 2012 by Johnson et al. [468]. It has been proven to be a chondrogenic and chondroprotective agent and be able to induce cartilage regeneration in many forms, such as to be a supplement of chondrogenic medium [469–471], a drug in an intra-articular injection [472–474], or incorporation in drug delivery thermogels and scaffolds [475–479]. Similarly, in multilayered hydrogels and MZSs, KGN has been used solely or in combination with other GFs such as BMP2 to promote chondrogenic differentiation and OC defect repair [188,480–482]. The clinical application of KGN is however limited by its hydrophobicity and low water solubility as it forms precipitates in cells, leading to ineffective chondrogenic stimulation [483]. Although encapsulating KGN into other carriers, such as nanoparticles [472,484], exosomes [483], nanographene oxide (NGO) [485], has shown to be a good strategy to address this issue in animal models, the safety of these carrier materials are still concerns in clinics. Besides, as a newly discovered molecule for cartilage repair, its long-term in vivo and clinical effects remain to be better understood.

We summarize the major characteristics, functions, and applications of various growth factors used for osteochondral regeneration in Table 4. Regardless of the species of numerous natural or synthetic GFs for bone and cartilage regeneration, one of the largest challenges affecting the stimulation efficiency of OC repair is their effective dose. A low dose might not provide sufficient repair, while a high dose could cause severe side effects, such as bone/cartilage hypertrophy and organ toxicity. Therefore, comparing to GF selection, facilitating a stable loading and controlled release pattern of GFs from MZSs is equally important. Generally, GFs can be loaded onto MZS through directly

Table 4
Comparison of different growth factors for osteochondral regeneration.

Families of growth factors	Major characteristics and functions	Main members for osteochondral regeneration	Types of layers incorporated	Applications for osteochondral regeneration	Ref
BMPs	Involved in embryonic development such as skeletal morphogenesis, hematopoietic and epithelial cell differentiation.	BMP2	BL	It is the only BMP that has received FDA approval for bone graft substitutes. Its application is associated with a series side effects including swelling, seroma, risk of cancer, and hypertrophy bone formation.	[367–371]
		BMP7 (OP1)	BL	It was considered a high potential osteogenic agent and showed some initial functions for cartilage homeostasis and repair. Its related products had been withdrawn from the market as they failed to receive final FDA approval.	[373–376]
		BMP3	BL	It is the most abundant BMP that acts as a negative regulator of bone density and therefore is used to reduce the side effects of other BMPs.	[378]
		BMP4, 6, 9	BL/CL	It induces bone mineralization, orthotopic ossification, chondrocyte maturation, and chondrogenic differentiation.	[379–383]
TGFβs	Extremely rich in bone as osteoblasts have a high concentration of TGFβ receptors; play roles in cell replication, bone/cartilage formation and fibrosis.	TGFβ1, 2	CL	It is associated with metabolism of proteoglycans and stabilized aggregates of link proteins in articular cartilage. It is usually co-delivered with BMP to simultaneously stimulate bone and cartilage regeneration.	[275, 384–387, 394–398]
		TGFβ3	CL	It regulates collagen synthesis and promotes hyaline cartilage formation.	[388–390]
PDGFs	Stored primarily in platelets and play fundamental roles in would healing cascade.	PDGF-BB	CL	It has received FDA approval for use in periodontal, orthopedic bone defects, and dermal wound healing. It improves the anabolism of collagen type II and inhibition of the catabolism of chondrocytes, and it also alleviates inflammation in chondrocytes and decreases chondrocytes apoptosis.	[401,402, 404,405]
		PDGF-AA/AB/BB	BL/CL	Commercially available PDGFs are usually a mix of all three isoforms of PDGFs that have shown to repair full thickness of OC defects.	[406,407]
IGFs	associated with a series of life-threaten diseases; the main anabolic GF for articular cartilage and play important role in cartilage homeostasis	IGF1	BL/CL	Its decrease is associated with increased risk of rheumatoid arthritis. Its sustained release can enhance the migration, adhesion, growth, and cartilaginous matrix production of chondrocytes, induce chondrogenic differentiation of MSCs, and repair full thickness OC defect. It has also been shown to promote osteogenesis of MSCs and stimulate bone growth.	[401, 408–419]
FGFs	Regulate limb bud development and formation of mesenchymal condensation, and play important roles in mediating chondrogenesis, osteogenesis, and bone and mineral homeostasis	FGF2	BL/CL	It is known as the basic FGF (bFGF), which is the most broadly used member of FGFs. It can enhance the regeneration of both bone and cartilage owing to its strong cell-promoting ability.	[422–427]
		FGF8	BL	It is known as androgen-induced GF (AIGF) and plays key roles in early embryonic development, brain formation, and limb development. It induces osteogenesis of MSCs and stimulates bone regeneration.	[428,429]
		FGF9, 18	CL	It stimulates early chondrogenesis, augments ECM production, delays terminal hypertrophy of MSCs, and delays and decreases articular degradation.	[430–434]
Angiogenesis-related GFs (VEGFs/TSPs)	Angiogenesis is a prerequisite to osteogenesis while it has to be avoided in chondrogenesis.	VEGF-A	BL/CL	It is known as VEGF, the most prominent in angiogenesis. OA patients usually have higher expressions of both VEGF and its receptors. Its increase can enhance bone regeneration while its decrease can enhance cartilage formation.	[440–448]
		TSPs (TSP1, 2, 4, 5)	BL/CL	It acts as a reverse role of VEGFs as antiangiogenic factors.	[329,364, 450–453]
		Bevacizumab	BL/CL	It is known by its brand name, Avastin, the first antiangiogenic antibody to receive FDA approval for OA treatment. Its synthetic molecule has similar effect of antiangiogenic factors.	[438, 454–456]
Other synthetic molecules	N/A	DEX	BL/CL	It is a synthetic glucocorticoid that regulates biological activities with broad anti-inflammatory effects. It also induces chondrogenic differentiation of various cells as	[134, 464–467]

(continued on next page)

Table 4 (*continued*)

Families of growth factors	Major characteristics and functions	Main members for osteochondral regeneration	Types of layers incorporated	Applications for osteochondral regeneration	Ref
		KGN	CL	a supplement in cell culture medium. It enhances OC repair through a dual pro-anabolic and anti-catabolic effect to attenuate inflammation. It acts as a chondrogenic and chondroprotective agent to induce cartilage regeneration, but its clinical application is limited by its hydrophobicity and low water solubility as it forms precipitates in cells, leading to ineffective chondrogenic stimulation.	[188, 469–482]

dropping onto the surface of the scaffolds (physical crosslinking), electrostatic attraction, hydrophobic or hydrophilic interactions, and covalent conjugation. The release patterns of GFs can be diverse, such as programmed, delayed, pulsatile, burst, and combining a few patterns, depending upon binding mechanisms and properties of the scaffold material (Fig. 8). GF loading and release kinetics have been carefully reviewed by Qasim et al. [334]. Overall, enabling a sustained and localized release of GFs over a relative long working time from MZSs is an important criterion for evaluating the effectiveness of MZSs in OC repair.

7. Challenges and future directions

Although painstaking efforts have been made by a large cadre of researchers actively seeking for advanced strategies to treat OC defects in the last a few decades, it is still a huge challenge today that OC defects and OA account for a large portion of the patients suffering from long-term chronic pains in the world. The development of tissue engineering strategy and particularly the usage of MZSs have open new opportunities for not only palliating the short-term symptomatic pains of the patients, but also aiming for a long-term cure by providing a regenerative treatment. That being said, it is currently impossible to fabricate a scaffold with all required features to effectively treat OC defects and OA clinically. Considering the multiphasic complexity of natural OC tissue in structure, composition, property, and function, several future perspectives are proposed here to provide some insight to address the current challenges in the field.

As the integration between the osseous and chondral zones has been shown to be a critical factor influencing the treatment efficiency [92, 486], it is one of the most indispensable needs in the future to explore more advanced strategies to improve the interfacial bonding strength between two adjacent layers within MZSs. Besides, the transition layer should have ideal porosity and pore sizes to 1) allow for nutrient and waste transportation between osseous and chondral zones; 2) prevent differentiated cells from crossing the interface; 3) act as a barrier to prevent the regenerated blood vessels and nerves of subchondral bone from invading into the articular cartilage zone; and 4) bear proper biomechanics for appropriate stress distribution. Below are a few strategies we believe may be the future directions to address the integration problem of MZSs. Researchers from Massachusetts Institute of Technology have recently developed a dry double-sided tape made from a combination of a biopolymer (gelatin or chitosan) and crosslinked poly (acrylic acid) grafted with N-hydrosuccinimide ester, which provides strong adhesion between wet tissues and devices [487]. This may offer an opportunity to enhance the interfacial bonding of stratified MZSs for OC regeneration if the permeability of this tape can be improved. Alternatively, some studies have demonstrated that continuous gradient scaffolds offer more promising results than the stratified ones as they more closely mimic the structure of native OC tissue compared to other MZS designs. To this end, Niu et al. [488] recently proposed to use a single technique, such as electrospinning or 3D printing, to fabricate the whole integrated gradient tissue engineering osteochondral scaffolds (IGTEOS). This may potentially mitigate the concerns regarding poor shear properties of layered MZSs. Besides, considering the pseudo 3D structures generated by electrospinning, advanced techniques such as MEW, which combines the advantages of electrospinning and 3D printing, could be an ideal candidate for manufacturing MZSs with controlled submicron 3D architecture, good shear property, desired stress distribution, and capability to load zonal-specific GFs and cells for OC defect repair.

Selection of biomaterials is another challenge. For example, as the main organic and inorganic components in native OC tissue, collagen and calcium phosphate should be of the top priority for consideration. However, collagen is extremely reactive to the surrounding environment and prone to denaturation, which significantly reduces its processibility for MZSs. Besides, its low printability further limits its possibility to be manufactured using advanced processing techniques, such as MEW, to fabricate integrated MZSs and continuous gradient scaffolds. To adapt to advanced processing techniques, it is key to improve the printability of natural polymers via either modifying their rheological properties or combining them with other highly printable polymers. For example, processing collagen into hydrolyzed collagen through proteolytic enzymes could result in lower viscosity and higher solubility compared to the native collagen counterpart as the molecular weight of the processed collagen significantly decreased [489,490]. Also, the addition of chitosan was proved to improve the printability of collagen [317]. More interestingly, it was found that improved printability of collagen-based bioinks could be achieved with a high cell density [491]. Other than the printability, there are concerns on the purity and reproductivity of collagen. The collagen source, no matter whether it is from fish, bovine, rat, porcine or any other animals, can introduce impurities and thus cannot maintain the structural integrity as a biomimetic material. Additionally, collagen properties may vary significantly from batch to batch, which further lowers the reproducibility of the material. To mitigate these concerns, future study may need to focus on how to develop a global standard for natural polymer extraction and how to improve the purity and reproductivity of these extracted materials. Regarding the inorganic component in MZSs, although the inclusion of nanosized calcium phosphate particles (especially HAP) in the bone layer of MZSs has been proven to be effective for osteogenic differentiation, subchondral bone regeneration, and reduction of biodegradability, additional studies are required to optimize their contents, which ranges from 0.5 to 70 wt% in existing studies. Another aspect that needs to be addressed in biomaterial selection for OC regeneration is the biodegradability of these materials. Ideally, MZSs should have a biodegradation rate that matches the rate of bone and cartilage regeneration in each zone.

Another less apparent but nonetheless important characteristic of OC tissue is its intrafibrillar mineralization feature of collagen fibers in the subchondral bone. Zuo et al. [492] revealed that clear periodic banding patterns (D-banding) were observable in the subchondral bone sample of grade I (mild OA) patients, whereas only random and undulated

arrangement of minerals were detected along the collagen fibrils from the subchondral bone of grade IV (severe OA) patients. This suggests that the occurrence of OA might be associated with the demineralization of collagen fibrils, and intrafibrillar mineralization is a unique characteristic of native subchondral bone, which has unfortunately been neglected in the design of existed MZSs for OC regeneration. Intrafibrillar mineralized collagen fibrils have demonstrated superior mechanical properties, osteoconductivity, and biocompatibility compared to those without mineralization or with only extrafibrillar mineralization [53,493,494]. Therefore, it is crucial to replicate this feature while designing the subchondral bone region of future MZSs to better recapitulate the zonal characteristic of natural OC tissues.

Although some cell-free and GF-free strategies have demonstrated good initial results in repairing OC defects, cell-laden constructs have demonstrated the most promising outcomes. To this end, cells, signals (GFs or bioactive factors), and scaffolds constitute the three fundamental components of OC repair strategy. Cells directly differentiate into zonal-specific (bone or cartilage) linages and secrete appropriate ECMs, or release paracrine secretome, and thus facilitate the homing and differentiation of host cells to accelerate tissue regeneration; signals provide the biological and environmental cues to guide the differentiation of both host and donor cells; and finally scaffolds offer the temporary spatial substrate for cell attachment and zonal specific proliferation and differentiation [495,496]. To reiterate, since differentiation of iPSCs is sensitive to environmental cues, it may provide opportunities for researchers to design a desirable MZS to simultaneously induce iPSCs to differentiate into zonal-specific lineages in corresponding zones. In addition, ideal MZSs should also have the capability to load zonal specific GFs and generate a sustained and controlled delivery of GFs. For example, BMP2 has been widely used as a GF for bone regeneration, while its overdosage could result in significant off-target side effects, such as extopic bone formation and tissue hypertrophy [497,498]. Moreover, GFs are generally vulnerable and easy to degrade. Future studies should also focus on how to control the loading efficiency and release patterns of GFs while maintaining their bioactivity so that they can drive the zonal-specific differentiation of cells for a relatively longer period. The zonal-specific delivery of GFs can be achieved by introducing a durable CCL, and chondrogenic and osteogenic GFs can be loaded into specific regions of MZSs. Besides, encapsulating GFs into micro particles, NPs, mesoporous NPs, or polymers (such as the gap zone of collagen fibers, PLGA, SF, etc.) is of great potential to obtain a sustained delivery of GFs. Before this strategy can be widely adopted, the bioactivity, bioavailability, and long-term performance of the released GFs in regenerating OC tissue must be established.

8. Conclusions

Osteochondral tissue engineering is a fast-growing research topic that has drawn considerable attention since its emergence in the 1990s. Due to the sophisticated multiphasic hierarchies of nature OC tissue, the use of MZSs has been gaining massive momentum especially over the past decade. In this review, the advantages of the tissue engineering strategy particularly involving the use of MZSs over the current clinical interventions on OC repair have been discussed. By presenting the zonal-specific hierarchical architectures of OC tissue, such as the orientations of collagen fibers, morphologies of chondrocytes, and distributions of blood vessels and nerves, we concluded and compared the pros and cons of different biomimetic designs of MZSs, including bilayered, trilayered, multilayered, and gradient (continuous and discontinuous) ones. Further, key factors influencing the overall treatment efficiency, including the selections of biomaterials, cells, growth factors, and processing techniques for producing cell-laden and/or GF-incorporated tissue engineering MZSs for OC regeneration, have been reviewed in detail. Finally, the current major challenges and future perspectives of the field have been discussed and proposed. While we are doing our best

to encompass as much information as we could, due to the delicacy of OC tissue and the complexity of the topic itself, we apologize for any omissions and oversights.

Ethics approval and consent to participate

This work contains no clinical study. No ethics approval and consent are required.

Declaration of competing interest

The authors declare no conflicts of interest.

Abbreviations

adipose derived mesenchymal stem cell (AD-MSCs)
adult stem cells (ASCs)
American Society for Testing and Materials (ASTM)
androgen-induced growth factor (AIGF)
basic FGF (bFGF)
bone layer (BL)
bone marrow mesenchymal stem cells (BM-MSCs)
bone morphological protein (BMP)
calcified cartilage layer (CCL)
calcified cartilage zone (CCZ)
calcium phosphates (CaPs)
cartilage layer (CL)
citric acid-coated magnetic NPs (CAG)
computer-aided design (CAD)
decellularized articular cartilage ECM (dECM)
decellularized bone ECM (DBM)
decellularized cartilage ECM (DCM)
deep chondral zone (CD)
deep zone (DZ)
dexamethasone (DEX)
embryonic stem cells (ESCs)
extracellular matrix (ECM)
fibroblast growth factors (FGFs)
Food and Drug Administration (FDA)
fused deposition modeling (FDM)
gelatin methacrylate (GelMA)
glycosaminoglycans (GAGs)
graphene oxide (GO)
growth factors (GFs)
hyaluronic acid (HA)
hydroxyapatite (HAP)
induced pluripotent stem cells (iPSCs)
insulin-like growth factors (IGFs)
integrated gradient tissue engineering osteochondral scaffolds
       (IGTEOS)
Interleukin-4 (IL4)
joint synovium MSCs (JS-MSCs)
kartogenin (KGN)
melt electrowriting (MEW)
mesenchymal stem cells (MSCs)
mesoporous bioactive glasses (MBG)
methacrylated hyaluronic acid (MeHA)
methylcellulose (MC)
microribbons (μRBs)
middle chondral zone (MZ)
middle layer (ML)
multizonal scaffolds (MZSs)
N-acryloyl 6-aminocaproic acid (A6ACA)
nanographene oxide (NGO)
nano-hydroxyapatite (nHAP)
nanoparticles (NPs)

octacalcium phosphate (OCP)
osseous zone (OZ)
osteoarthritis (OA)
osteochondral (OC)
osteogenic protein 1 (OP1)
PCL-b-PEG-b-PCL (PCEC)
peripheral blood MSCs (PB-MSCs)
placental growth factor (PlGF)
platelet-derived growth factors (PDGFs)
poly(ethylene glycol) (PEG)
poly(glycerol sebacate) (PGS)
poly(L/D-lactide acid) (PLDLA)
poly(lactide-coglycolide) acid (PLGA)
poly(L-lactic acid) (PLLA)
poly(methyl methacrylate) (PMMA)
polycaprolactone (PCL)
polydopamine (PDA)
polyethylene glycol diacrylate (PEGDA)
polyethylene oxide (PEO)
polyglycolic acid (PGA)
polyhedral oligomeric silsesquioxanes (POSS)
polylactic acid (PLA)
polyvinyl alcohol (PVA)
scanning electronic microscopy (SEM)
selective laser sintering (SLS)
silk fibroin (SF)
sintered microsphere scaffold (SMS)
skeletal stem cells (SSCs)
subchondral zone (SC)
superficial zone (SZ)
tantalum (Ta)
thermally-induced phase separation (TIPS)
thrombospondins (TSPs)
titanium (Ti)

References

[1] C.J.L. Murray, A.D. Lopez, O. World Health, B. World, H. Harvard, School of Public, the Global burden of disease : a comprehensive assessment of mortality and disability from diseases, injuries, and risk factors, in: Christopher J. L. Murray, Alan D. Lopez (Eds.), In 1990 and Projected to 2020 : Summary/, World Health Organization, Geneva, 1996.

[2] R.F. Loeser, Age-related changes in the musculoskeletal system and the development of osteoarthritis, Clin. Geriatr. Med. 26 (2010) 371–386.

[3] eumusc.net, Musculoskeletal Health in Europe, Report v5.0.

[4] C. Baumann, B. Hinckel, C. Bozynski, J. Farr, Articular Cartilage: Structure and Restoration, A Clinical Casebook, 2019, pp. 3–24.

[5] C. Deng, C. Xu, Q. Zhou, Y. Cheng, Advances of Nanotechnology in Osteochondral Regeneration, vol. 11, Wiley Interdiscip Rev Nanomed Nanobiotechnol, 2019, e1576.

[6] D.R. Pereira, R.L. Reis, J.M. Oliveira, Layered scaffolds for osteochondral tissue engineering, Adv. Exp. Med. Biol. 1058 (2018) 193–218.

[7] D.D. Frisbie, S. Morisset, C.P. Ho, W.G. Rodkey, J.R. Steadman, C.W. McIlwraith, Effects of calcified cartilage on healing of chondral defects treated with microfracture in horses, Am. J. Sports Med. 34 (2006) 1824–1831.

[8] M. Drobnic, D. Radosavljevic, A. Cör, M. Brittberg, K. Strazar, Debridement of cartilage lesions before autologous chondrocyte implantation by open or transarthroscopic techniques: a comparative study using post-mortem materials, J Bone Joint Surg Br 92 (2010) 602–608.

[9] H. Madry, M. Ochi, M. Cucchiarini, D. Pape, R. Seil, Large animal models in experimental knee sports surgery: focus on clinical translation, Journal of Experimental Orthopaedics 2 (2015).

[10] C. Erggelet, P. Vavken, Microfracture for the treatment of cartilage defects in the knee joint – a golden standard? Journal of Clinical Orthopaedics and Trauma 7 (2016) 145–152.

[11] J.A. Buckwalter, H.J. Mankin, Articular cartilage repair and transplantation, Arthritis Rheum. 41 (1998) 1331–1342.

[12] J.R. Steadman, K.K. Briggs, J.J. Rodrigo, M.S. Kocher, T.J. Gill, W.G. Rodkey, Outcomes of microfracture for traumatic chondral defects of the knee: average 11-year follow-up, Arthroscopy 19 (2003) 477–484.

[13] J.R. Steadman, B.S. Miller, S.G. Karas, T.F. Schlegel, K.K. Briggs, R.J. Hawkins, The microfracture technique in the treatment of full-thickness chondral lesions of the knee in National Football League players, J. Knee Surg. 16 (2003) 83–86.

[14] M.-C. Killen, C.P. Charalambous, Chapter 6 - advances in cartilage restoration techniques, in: W. Ahmed, D.A. Phoenix, M.J. Jackson, C.P. Charalambous (Eds.) Advances in Medical and Surgical Engineering, Academic Press2020, pp. 71-83.

[15] J.S. Temenoff, A.G. Mikos, Review: tissue engineering for regeneration of articular cartilage, Biomaterials 21 (2000) 431–440.

[16] E.B. Hunziker, Articular cartilage repair: are the intrinsic biological constraints undermining this process insuperable? Osteoarthritis Cartilage 7 (1999) 15–28.

[17] A.E. Gross, W. Kim, F. Las Heras, D. Backstein, O. Safir, K.P. Pritzker, Fresh osteochondral allografts for posttraumatic knee defects: long-term followup, Clin. Orthop. Relat. Res. 466 (2008) 1863–1870.

[18] M. Marcacci, G. Filardo, E. Kon, Treatment of cartilage lesions: what works and why? Injury 44 (2013) S11–S15.

[19] C. Deng, J. Chang, C. Wu, Bioactive scaffolds for osteochondral regeneration, Journal of Orthopaedic Translation 17 (2019) 15–25.

[20] M.H. Flynn Jm, Springfield DS, Osteoarticular allografts to treat distal femoral osteonecrosis, Clin Orthop Re1 Res 303 (1994) 38–43.

[21] H. Kang, Y. Zeng, S. Varghese, Functionally graded multilayer scaffolds for in vivo osteochondral tissue engineering, Acta Biomater. 78 (2018) 365–377.

[22] D. Clearfield, A. Nguyen, M. Wei, Biomimetic multidirectional scaffolds for zonal osteochondral tissue engineering via a lyophilization bonding approach, J. Biomed. Mater. Res. 106 (2018) 948–958.

[23] X. Nie, Y.J. Chuah, P. He, D.-A. Wang, Engineering a multiphasic, integrated graft with a biologically developed cartilage–bone interface for osteochondral defect repair, J. Mater. Chem. B 7 (2019) 6515–6525.

[24] T. Wang, W. Xu, X. Zhao, B. Bai, Y. Hua, J. Tang, F. Chen, Y. Liu, Y. Wang, G. Zhou, Y. Cao, Repair of osteochondral defects mediated by double-layer scaffolds with natural osteochondral-biomimetic microenvironment and interface, Mater Today Bio 14 (2022), 100234. -100234.

[25] N.H. Dormer, C.J. Berkland, M.S. Detamore, Emerging techniques in stratified designs and continuous gradients for tissue engineering of interfaces, Ann. Biomed. Eng. 38 (2010) 2121–2141.

[26] L. Fu, Z. Yang, C. Gao, H. Li, Z. Yuan, F. Wang, X. Sui, S. Liu, Q. Guo, Advances and prospects in biomimetic multilayered scaffolds for articular cartilage regeneration, Regenerative biomaterials 7 (2020) 527–542.

[27] H. Xiao, W. Huang, K. Xiong, S. Ruan, C. Yuan, G. Mo, R. Tian, S. Zhou, R. She, P. Ye, B. Liu, J. Deng, Osteochondral repair using scaffolds with gradient pore sizes constructed with silk fibroin, chitosan, and nano-hydroxyapatite, Int. J. Nanomed. 14 (2019) 2011–2027.

[28] A.R. Poole, T. Kojima, T. Yasuda, F. Mwale, M. Kobayashi, S. Laverty, Composition and Structure of Articular Cartilage: a Template for Tissue Repair, Clin Orthop Relat Res, 2001, pp. S26–S33.

[29] E.J. Chung, N. Shah, R.N. Shah, 11 - nanomaterials for cartilage tissue engineering, in: A.K. Gaharwar, S. Sant, M.J. Hancock, S.A. Hacking (Eds.), Nanomaterials in Tissue Engineering, Woodhead Publishing, 2013, pp. 301–334.

[30] A.L. Mescher, Junqueira's Basic Histology: Text and Atlas, thirteenth ed., McGraw-Hill Medical, New York, 2013.

[31] J.A. Buckwalter, Articular cartilage, Instr. Course Lect. 32 (1983) 349–370.

[32] A.M. Bhosale, J.B. Richardson, Articular cartilage: structure, injuries and review of management, Br. Med. Bull. 87 (2008) 77–95.

[33] M. Huber, S. Trattnig, F. Lintner, Anatomy, biochemistry, and physiology of articular cartilage, Invest. Radiol. 35 (2000) 573–580.

[34] C.B. Knudson, W. Knudson, Cartilage proteoglycans, Semin. Cell Dev. Biol. 12 (2001) 69–78.

[35] D. Eyre, Collagen of articular cartilage, Arthritis Res. 4 (2002) 30–35.

[36] W. Wei, H. Dai, Articular cartilage and osteochondral tissue engineering techniques: recent advances and challenges, Bioact. Mater. 6 (2021) 4830–4855.

[37] V.C. Mow, S.C. Kuei, W.M. Lai, C.G. Armstrong, Biphasic creep and stress relaxation of articular cartilage in compression? Theory and experiments, J. Biomech. Eng. 102 (1980) 73–84.

[38] V.C. Mow, X.E. Guo, Mechano-electrochemical properties of articular cartilage: their inhomogeneities and anisotropies, Annu. Rev. Biomed. Eng. 4 (2002) 175–209.

[39] J. Mansour, in: C.A. Oatis (Ed.), Biomechanics of Cartilage, Lippincott Williams & Wilkins, Baltimore, Md, USA, 2003.

[40] J. Eschweiler, N. Horn, B. Rath, M. Betsch, A. Baroncini, M. Tingart, F. Migliorini, The biomechanics of cartilage-an overview, Life 11 (2021) 302.

[41] K.A. Athanasiou, M. Rosenwasser, J. Buckwalter, T. Malinin, V.C. Mow, Interspecies comparisons of in situ intrinsic mechanical properties of distal femoral cartilage, J. Orthop. Res. 9 (1991) 330–340.

[42] F.C. Boschetti, M; Peretti, GM; Fraschini, G; Pietrabissa, R, Direct Annd Indirect Measurement of Human Articular Cartilage Permeability, Orthopaedic Research Society, 0293.

[43] S. Ansari, S. Khorshidi, A. Karkhaneh, Engineering of gradient osteochondral tissue: from nature to lab, Acta Biomater. 87 (2019) 41–54.

[44] S. Lee, M. Porter, S. Wasko, G. Lau, P.Y. Chen, E. Novitskaya, A. Tomsia, A. Almutairi, J. McKittrick, Potential bone replacement materials prepared by two methods, MRS Proceedings 1418 (2012).

[45] C.J. Little, N.K. Bawolin, X. Chen, Mechanical properties of natural cartilage and tissue-engineered constructs, Tissue Eng. B Rev. 17 (2011) 213–227.

[46] A.J. Sophia Fox, A. Bedi, S.A. Rodeo, The basic science of articular cartilage: structure, composition, and function, Sport Health 1 (2009) 461–468.

[47] J.M. Lane, C. Weiss, Review of articular cartilage collagen research, Arthritis Rheum. 18 (1975) 553–562.

[48] Y. Li, Z. Yuan, H. Yang, H. Zhong, W. Peng, R. Xie, Recent advances in understanding the role of cartilage lubrication in osteoarthritis, Molecules 26 (2021).

[49] J.C. Mansfield, V. Mandalia, A. Toms, C.P. Winlove, S. Brasselet, Collagen reorganization in cartilage under strain probed by polarization sensitive second harmonic generation microscopy, J. R. Soc. Interface 16 (2019), 20180611.

[50] D.A. Grande, A.S. Breitbart, J. Mason, C. Paulino, J. Laser, R.E. Schwartz, Cartilage tissue engineering: current limitations and solutions, Clin. Orthop. Relat. Res. 367 (1999) S176–S185.

[51] Z. Xia, X. Yu, X. Jiang, H.D. Brody, D.W. Rowe, M. Wei, Fabrication and characterization of biomimetic collagen-apatite scaffolds with tunable structures for bone tissue engineering, Acta Biomater. 9 (2013) 7308–7319.

[52] Z. Xia, M.M. Villa, M. Wei, A biomimetic collagen–apatite scaffold with a multi-level lamellar structure for bone tissue engineering, J. Mater. Chem. B 2 (2014) 1998–2007.

[53] L. Yu, D.W. Rowe, I.P. Perera, J. Zhang, S.L. Suib, X. Xin, M. Wei, Intrafibrillar mineralized collagen–hydroxyapatite-based scaffolds for bone regeneration, ACS Appl. Mater. Interfaces 12 (2020) 18235–18249.

[54] S. Weiner, H.D. Wagner, The material bone: structure-mechanical function relations, Annu. Rev. Mater. Sci. 28 (1998) 271–298.

[55] A.M. Mohamed, An overview of bone cells and their regulating factors of differentiation, Malays. J. Med. Sci. 15 (2008) 4–12.

[56] B. Zhang, J. Huang, R.J. Narayan, Gradient scaffolds for osteochondral tissue engineering and regeneration, J. Mater. Chem. B 8 (2020) 8149–8170.

[57] L. Shang, B. Ma, F. Wang, J. Li, S. Shen, X. Li, H. Liu, S. Ge, Nanotextured silk fibroin/hydroxyapatite biomimetic bilayer tough structure regulated osteogenic/chondrogenic differentiation of mesenchymal stem cells for osteochondral repair, Cell Prolif 53 (2020), e12917.

[58] I.A.D. Mancini, S. Schmidt, H. Brommer, B. Pouran, S. Schäfer, J. Tessmar, A. Mensinga, M.H.P. van Rijen, J. Groll, T. Blunk, R. Levato, J. Malda, P.R. van Weeren, A composite hydrogel-3D printed thermoplast osteochondral anchor as example for a zonal approach to cartilage repair: *in vivo* performance in a long-term equine model, Biofabrication 12 (2020), 035028.

[59] K.A. Pitrolino, R.M. Felfel, L.M. Pellizzeri, J. Mlaren, A.A. Popov, V. Sottile, C. A. Scotchford, B.E. Scammell, G.A.F. Roberts, D.M. Grant, Development and in vitro assessment of a bi-layered chitosan-nano-hydroxyapatite osteochondral scaffold, Carbohydr. Polym. 282 (2022), 119126.

[60] D.J. Huey, J.C. Hu, K.A. Athanasiou, Unlike bone, cartilage regeneration remains elusive, Science 338 (2012) 917–921.

[61] P. Orth, M. Cucchiarini, D. Kohn, H. Madry, Alterations of the subchondral bone in osteochondral repair–translational data and clinical evidence, Eur. Cell. Mater. 25 (2013) 299–316. ; discussion 314-296.

[62] Q.L. Loh, C. Choong, Three-dimensional scaffolds for tissue engineering applications: role of porosity and pore size, Tissue Eng. B Rev. 19 (2013) 485–502.

[63] A. Golebiowska, S.P. Nukavarapu, Bio-inspired Zonal-Structured Matrices for Bone-Cartilage Interface Engineering, Biofabrication, 2022.

[64] Z. Li, S. Jia, Z. Xiong, Q. Long, S. Yan, F. Hao, J. Liu, Z. Yuan, 3D-printed scaffolds with calcified layer for osteochondral tissue engineering, J. Biosci. Bioeng. 126 (2018) 389–396.

[65] T. Chen, J. Bai, J. Tian, P. Huang, H. Zheng, J. Wang, A single integrated osteochondral in situ composite scaffold with a multi-layered functional structure, Colloids and surfaces, B, Biointerfaces 167 (2018) 354–363.

[66] T. Wang, W. Xu, X. Zhao, B. Bai, J. Hua, J. Tang, F. Chen, Y. Liu, Y. Wang, G. Zhou, Y. Cao, Repair of osteochondral defects mediated by double-layer scaffolds with natural osteochondral-biomimetic microenvironment and interface, Materials Today Bio 14 (2022), 100234.

[67] S.-J. Seo, C. Mahapatra, R.K. Singh, J.C. Knowles, H.-W. Kim, Strategies for osteochondral repair: focus on scaffolds, J. Tissue Eng. 5 (2014), 2041731414541850. -2041731414541850.

[68] P. Duan, Z. Pan, L. Cao, J. Gao, H. Yao, X. Liu, R. Guo, X. Liang, J. Dong, J. Ding, Restoration of osteochondral defects by implanting bilayered poly(lactide-co-glycolide) porous scaffolds in rabbit joints for 12 and 24 weeks, Journal of Orthopaedic Translation 19 (2019) 68–80.

[69] A.E. Erickson, J. Sun, S.K. Lan Levengood, S. Swanson, F.-C. Chang, C.T. Tsao, M. Zhang, Chitosan-based composite bilayer scaffold as an in vitro osteochondral defect regeneration model, Biomed. Microdevices 21 (2019) 34.

[70] L. Gong, J. Li, J. Zhang, Z. Pan, Y. Liu, F. Zhou, Y. Hong, Y. Hu, Y. Gu, H. Ouyang, X. Zou, S. Zhang, An interleukin-4-loaded bi-layer 3D printed scaffold promotes osteochondral regeneration, Acta Biomater. 117 (2020) 246–260.

[71] V.P. Ribeiro, S. Pina, J.B. Costa, I.F. Cengiz, L. García-Fernández, M.d. M. Fernández-Gutiérrez, O.C. Paiva, A.L. Oliveira, J. San-Román, J.M. Oliveira, R. L. Reis, Enzymatically cross-linked silk fibroin-based hierarchical scaffolds for osteochondral regeneration, ACS Appl. Mater. Interfaces 11 (2019) 3781–3799.

[72] F. Gao, Z. Xu, Q. Liang, B. Liu, H. Li, Y. Wu, Y. Zhang, Z. Lin, M. Wu, C. Ruan, W. Liu, Direct 3D printing of high strength biohybrid gradient hydrogel scaffolds for efficient repair of osteochondral defect, Adv. Funct. Mater. 28 (2018), 1706644.

[73] Y. Han, B. Jia, M. Lian, B. Sun, Q. Wu, B. Sun, Z. Qiao, K. Dai, High-precision, gelatin-based, hybrid, bilayer scaffold using melt electro-writing to repair cartilage injury, Bioact. Mater. 6 (2021) 2173–2186.

[74] R.C. Nordberg, P. Huebner, K.G. Schuchard, L.F. Mellor, R.A. Shirwaiker, E. G. Loboa, J.T. Spang, The evaluation of a multiphasic 3D-bioplotted scaffold seeded with adipose derived stem cells to repair osteochondral defects in a porcine model, J. Biomed. Mater. Res. B Appl. Biomater. 109 (2021) 2246–2258.

[75] X. Liu, Y. Wei, C. Xuan, L. Liu, C. Lai, M. Chai, Z. Zhang, L. Wang, X. Shi, A biomimetic biphasic osteochondral scaffold with layer-specific release of stem cell differentiation inducers for the reconstruction of osteochondral defects, Advanced healthcare materials 9 (2020), 2000076.

[76] X. Ding, J. Gao, X. Yu, J. Shi, J. Chen, L. Yu, S. Chen, J. Ding, 3D-Printed porous scaffolds of hydrogels modified with TGF-β1 binding peptides to promote in vivo cartilage regeneration and animal gait restoration, ACS Appl. Mater. Interfaces 14 (2022) 15982–15995.

[77] A.B.M. Natarajan, V.P.D. Sivadas, P. Nair, 3D-printed biphasic scaffolds for the simultaneous regeneration of osteochondral tissues, Biomed. Mater. (Bristol, U. K.) 16 (2021).

[78] C. Mahapatra, J.-J. Kim, J.-H. Lee, G.-Z. Jin, J.C. Knowles, H.-W. Kim, Differential chondro- and osteo-stimulation in three-dimensional porous scaffolds with different topological surfaces provides a design strategy for biphasic osteochondral engineering, J. Tissue Eng. 10 (2019), 2041731419826433. -2041731419826433.

[79] D. Lin, B. Cai, L. Wang, L. Cai, Z. Wang, J. Xie, Q.-x. Lv, Y. Yuan, C. Liu, S.F. Shen, A viscoelastic PEGylated poly(glycerol sebacate)-based bilayer scaffold for cartilage regeneration in full-thickness osteochondral defect, Biomaterials 253 (2020), 120095.

[80] R. Cao, A. Zhan, Z. Ci, C. Wang, Y. She, Y. Xu, K. Xiao, H. Xia, L. Shen, D. Meng, C. Chen, A biomimetic biphasic scaffold consisting of decellularized cartilage and decalcified bone matrixes for osteochondral defect repair, Front. Cell Dev. Biol. 9 (2021), 639006.

[81] S.L. Sing, S. Wang, S. Agarwala, F.E. Wiria, T.M.H. Ha, W.Y. Yeong, Fabrication of titanium based biphasic scaffold using selective laser melting and collagen immersion, International journal of bioprinting 3 (2017) 7.

[82] T. Yang, M. Tamaddon, L. Jiang, J. Wang, Z. Liu, Z. Liu, H. Meng, Y. Hu, J. Gao, X. Yang, Y. Zhao, Y. Wang, A. Wang, Q. Wu, C. Liu, J. Peng, X. Sun, Q. Xue, Bilayered scaffold with 3D printed stiff subchondral bony compartment to provide constant mechanical support for long-term cartilage regeneration, J Orthop Translat 30 (2021) 112–121.

[83] M. Tamaddon, G. Blunn, R. Tan, P. Yang, X. Sun, S.-M. Chen, J. Luo, Z. Liu, L. Wang, D. Li, R. Donate, M. Monzón, C. Liu, In Vivo Evaluation of Additively Manufactured Multi-Layered Scaffold for the Repair of Large Osteochondral Defects, Bio-Design and Manufacturing, 2022.

[84] C. Zhai, Q. Zuo, K. Shen, J. Zhou, J. Chen, X. Zhang, C. Luo, H. Fei, W. Fan, Utilizing an integrated tri-layered scaffold with Titanium-Mesh-Cage base to repair cartilage defects of knee in goat model, Mater. Des. 193 (2020), 108766.

[85] X. Wei, B. Liu, G. Liu, F. Yang, F. Cao, X. Dou, W. Yu, B. Wang, G. Zheng, L. Cheng, Z. Ma, Y. Zhang, J. Yang, Z. Wang, J. Li, D. Cui, W. Wang, H. Xie, L. Li, F. Zhang, W.C. Lineaweaver, D. Zhao, Mesenchymal stem cell-loaded porous tantalum integrated with biomimetic 3D collagen-based scaffold to repair large osteochondral defects in goats, Stem Cell Res. Ther. 10 (2019) 72.

[86] D.L. Dorcemus, H.S. Kim, S.P. Nukavarapu, Gradient scaffold with spatial growth factor profile for osteochondral interface engineering, Biomed. Mater. (Bristol, U. K.) 16 (2021).

[87] X. Li, J. Ding, J. Wang, X. Zhuang, X. Chen, Biomimetic biphasic scaffolds for osteochondral defect repair, Regenerative Biomaterials 2 (2015) 221–228.

[88] E.J. Sheehy, T. Vinardell, C.T. Buckley, D.J. Kelly, Engineering osteochondral constructs through spatial regulation of endochondral ossification, Acta Biomater. 9 (2013) 5484–5492.

[89] J. Guo, Q. Li, R. Zhang, B. Li, J. Zhang, L. Yao, Z. Lin, L. Zhang, X. Cao, B. Duan, Loose pre-cross-linking mediating cellulose self-assembly for 3D printing strong and tough biomimetic scaffolds, Biomacromolecules 23 (2022) 877–888.

[90] E.B. Hunziker, I.M.K. Driesang, Functional barrier principle for growth-factor-based articular cartilage repair, Osteoarthritis Cartilage 11 (2003) 320–327.

[91] S. Critchley, E.J. Sheehy, G. Cunniffe, P. Diaz-Payno, S.F. Carroll, O. Jeon, E. Alsberg, P.A.J. Brama, D.J. Kelly, 3D printing of fibre-reinforced cartilaginous templates for the regeneration of osteochondral defects, Acta Biomater. 113 (2020) 130–143.

[92] R. Choe, E. Devoy, B. Kuzemchak, M. Sherry, E. Jabari, J.D. Packer, J.P. Fisher, Computational investigation of interface printing patterns within 3D printed multilayered scaffolds for osteochondral tissue engineering, Biofabrication 14 (2022), 025015.

[93] V. Kesireddy, F.K. Kasper, Approaches for building bioactive elements into synthetic scaffolds for bone tissue engineering, J. Mater. Chem. B 4 (2016) 6773–6786.

[94] L.F. Mellor, R.C. Nordberg, P. Huebner, M. Mohiti-Asli, M.A. Taylor, W. Efird, J. T. Oxford, J.T. Spang, R.A. Shirwaiker, E.G. Loboa, Investigation of multiphasic 3D-bioplotted scaffolds for site-specific chondrogenic and osteogenic differentiation of human adipose-derived stem cells for osteochondral tissue engineering applications, J. Biomed. Mater. Res. B Appl. Biomater. 108 (2020) 2017–2030.

[95] E.F. Chan, I.-L. Liu, E.J. Semler, H.M. Aberman, T.M. Simon, A.C. Chen, K. G. Truncale, R.L. Sah, Association of 3-dimensional cartilage and bone structure with articular cartilage properties in and adjacent to autologous osteochondral grafts after 6 and 12 Months in a goat, Model 3 (2012) 255–266.

[96] H. Zhou, L. Yuan, Z. Xu, X. Yi, X. Wu, C. Mu, L. Ge, D. Li, Mimicking the composition and structure of the osteochondral tissue to fabricate a heterogeneous three-layer scaffold for the repair of osteochondral defects, ACS Appl. Bio Mater. 5 (2022) 734–746.

[97] Y. Du, H. Liu, Q. Yang, S. Wang, J. Wang, J. Ma, I. Noh, A.G. Mikos, S. Zhang, Selective laser sintering scaffold with hierarchical architecture and gradient composition for osteochondral repair in rabbits, Biomaterials 137 (2017) 37–48.

[98] Y. Luo, X. Cao, J. Chen, J. Gu, H. Yu, J. Sun, J. Zou, Platelet-derived growth factor-functionalized scaffolds for the recruitment of synovial mesenchymal stem cells for osteochondral repair, Stem Cell. Int. 2022 (2022), 2190447.

[99] B. Pouran, A. Raoof, D.M. de Winter, V. Arbabi, R.L. Bleys, F.J. Beekman, A. A. Zadpoor, J. Malda, H. Weinans, Topographic features of nano-pores within the

osteochondral interface and their effects on transport properties–a 3D imaging and modeling study, J. Biomech. 123 (2021), 110504.

[100] F. Wang, Z. Ying, X. Duan, H. Tan, B. Yang, L. Guo, G. Chen, G. Dai, Z. Ma, L. Yang, Histomorphometric analysis of adult articular calcified cartilage zone, J. Struct. Biol. 168 (2009) 359–365.

[101] R. Kandel, M. Hurtig, M. Grynpas, Characterization of the mineral in calcified articular cartilagenous tissue formed in vitro, Tissue Eng. 5 (1999) 25–34.

[102] W. Wang, R. Ye, W. Xie, Y. Zhang, S. An, Y. Li, Y. Zhou, Roles of the calcified cartilage layer and its tissue engineering reconstruction in osteoarthritis treatment, Front. Bioeng. Biotechnol. 10 (2022).

[103] J. Yang, Y.S. Zhang, K. Yue, A. Khademhosseini, Cell-laden hydrogels for osteochondral and cartilage tissue engineering, Acta Biomater. 57 (2017) 1–25.

[104] S. Jia, J. Wang, T. Zhang, W. Pan, Z. Li, X. He, C. Yang, Q. Wu, W. Sun, Z. Xiong, D. Hao, Multilayered scaffold with a compact interfacial layer enhances osteochondral defect repair, ACS Appl. Mater. Interfaces 10 (2018) 20296–20305.

[105] Y. Huang, H. Fan, X. Gong, L. Yang, F. Wang, Scaffold with natural calcified cartilage zone for osteochondral defect repair in minipigs, Am. J. Sports Med. 49 (2021) 1883–1891.

[106] Y. Zhao, X. Ding, Y. Dong, X. Sun, L. Wang, X. Ma, M. Zhu, B. Xu, Q. Yang, Role of the calcified cartilage layer of an integrated trilayered silk fibroin scaffold used to regenerate osteochondral defects in rabbit knees, ACS Biomater. Sci. Eng. 6 (2020) 1208–1216.

[107] J. Li, X. Zhang, Q. Guo, J. Zhang, Y. Cao, X. Zhang, J. Huang, Q. Wang, X. Liu, C. Hao, Preparation and in vitro evaluation of tissue engineered osteochondral integration of multi-layered scaffold, Zhongguo xiu fu chong jian wai ke za zhi = Zhongguo xiufu chongjian waike zazhi = Chinese journal of reparative and reconstructive surgery 32 (2018) 434–440.

[108] X. Hu, S. Zheng, R. Zhang, Y. Wang, Z. Jiao, W. Li, Y. Nie, T. Liu, K. Song, Dynamic process enhancement on chitosan/gelatin/nano-hydroxyapatite-bone derived multilayer scaffold for osteochondral tissue repair, Mater. Sci. Eng. C (2022), 112662.

[109] C. Gegg, F. Yang, Spatially patterned microribbon-based hydrogels induce zonally-organized cartilage regeneration by stem cells in 3D, Acta Biomater. 101 (2020) 196–205.

[110] J. Liu, L. Li, H. Suo, M. Yan, J. Yin, J. Fu, 3D printing of biomimetic multi-layered GelMA/nHA scaffold for osteochondral defect repair, Mater. Des. 171 (2019), 107708.

[111] E. Amann, A. Amirall, A.R. Franco, P.S.P. Poh, F.J. Sola Dueñas, G. Fuentes Estévez, I.B. Leonor, R.L. Reis, M. van Griensven, E.R. Balmayor, A graded, porous composite of natural biopolymers and octacalcium phosphate guides osteochondral differentiation of stem cells, Advanced healthcare materials 10 (2021), e2001692.

[112] Z. Qiao, M. Lian, Y. Han, B. Sun, X. Zhang, W. Jiang, H. Li, Y. Hao, K. Dai, Bioinspired stratified electrowritten fiber-reinforced hydrogel constructs with layer-specific induction capacity for functional osteochondral regeneration, Biomaterials 266 (2021), 120385.

[113] T.J. Levingstone, A. Matsiko, G.R. Dickson, F.J. O'Brien, J.P. Gleeson, A biomimetic multi-layered collagen-based scaffold for osteochondral repair, Acta Biomater. 10 (2014) 1996–2004.

[114] L. Fu, Z. Yang, C. Gao, H. Li, Z. Yuan, F. Wang, X. Sui, S. Liu, Q. Guo, Advances and prospects in biomimetic multilayered scaffolds for articular cartilage regeneration, Regen Biomater 7 (2020) 527–542.

[115] H. Xiao, W. Huang, K. Xiong, S. Ruan, C. Yuan, G. Mo, R. Tian, S. Zhou, R. She, P. Ye, B. Liu, J. Deng, Osteochondral repair using scaffolds with gradient pore sizes constructed with silk fibroin, chitosan, and nano-hydroxyapatite, Int. J. Nanomed. 14 (2019) 2011–2027.

[116] C. Parisi, L. Salvatore, L. Veschini, M.P. Serra, C. Hobbs, M. Madaghiele, A. Sannino, L. Di Silvio, Biomimetic gradient scaffold of collagen–hydroxyapatite for osteochondral regeneration, J. Tissue Eng. 11 (2020), 2041731419896068.

[117] C. Erisken, D.M. Kalyon, H. Wang, Viscoelastic and biomechanical properties of osteochondral tissue constructs generated from graded polycaprolactone and beta-tricalcium phosphate composites, J. Biomech. Eng. 132 (2010), 091013.

[118] S. Sultan, A.P. Mathew, 3D printed scaffolds with gradient porosity based on a cellulose nanocrystal hydrogel, Nanoscale 10 (2018) 4421–4431.

[119] S.M. Bittner, B.T. Smith, L. Diaz-Gomez, C.D. Hudgins, A.J. Melchiorri, D. W. Scott, J.P. Fisher, A.G. Mikos, Fabrication and mechanical characterization of 3D printed vertical uniform and gradient scaffolds for bone and osteochondral tissue engineering, Acta Biomater. 90 (2019) 37–48.

[120] H. Zhang, H. Huang, G. Hao, Y. Zhang, H. Ding, Z. Fan, L. Sun, 3D printing hydrogel scaffolds with nanohydroxyapatite gradient to effectively repair osteochondral defects in rats, Adv. Funct. Mater. 31 (2021), 2006697.

[121] Y. Sun, Y. You, W. Jiang, B. Wang, Q. Wu, K. Dai, 3D bioprinting dual-factor releasing and gradient-structured constructs ready to implant for anisotropic cartilage regeneration, Sci. Adv. 6 (2020), eaay1422.

[122] J. Radhakrishnan, A. Manigandan, P. Chinnaswamy, A. Subramanian, S. Sethuraman, Gradient nano-engineered in situ forming composite hydrogel for osteochondral regeneration, Biomaterials 162 (2018) 82–98.

[123] X. Hu, W. Li, L. Li, Y. Lu, Y. Wang, R. Parungao, S. Zheng, T. Liu, Y. Nie, H. Wang, K. Song, A biomimetic cartilage gradient hybrid scaffold for functional tissue engineering of cartilage, Tissue Cell 58 (2019) 84–92.

[124] F. Hejazi, S. Bagheri-Khoulenjani, N. Olov, D. Zeini, A. Solouk, H. Mirzadeh, Fabrication of nanocomposite/nanofibrous functionally graded biomimetic scaffolds for osteochondral tissue regeneration, J. Biomed. Mater. Res. 109 (2021) 1657–1669.

[125] Y. Li, Y. Xu, Y. Liu, Z. Wang, W. Chen, L. Duan, D. Gu, Decellularized cartilage matrix scaffolds with laser-machined micropores for cartilage regeneration and

articular cartilage repair, Materials science & engineering, C, Materials for biological applications 105 (2019), 110139.

[126] C. Deng, C. Xu, Q. Zhou, Y. Cheng, Advances of nanotechnology in osteochondral regeneration 11 (2019) e1576.

[127] F. Hejazi, S. Bagheri-Khoulenjani, N. Olov, D. Zeini, A. Solouk, H. Mirzadeh, Fabrication of nanocomposite/nanofibrous functionally graded biomimetic scaffolds for osteochondral tissue regeneration 109 (2021) 1657–1669.

[128] M.O. Wang, C.E. Vorwald, M.L. Dreher, E.J. Mott, M.-H. Cheng, A. Cinar, H. Mehdizadeh, S. Somo, D. Dean, E.M. Brey, J.P. Fisher, Evaluating 3D-printed biomaterials as scaffolds for vascularized, Bone Tissue Engineering 27 (2015) 138–144.

[129] R.A. Perez, G. Mestres, Role of pore size and morphology in musculo-skeletal tissue regeneration, Mater. Sci. Eng. C 61 (2016) 922–939.

[130] X. Guo, C. Wang, C. Duan, M. Descamps, Q. Zhao, L. Dong, S. Lü, K. Anselme, J. Lu, Y.Q. Song, Repair of osteochondral defects with autologous chondrocytes seeded onto bioceramic scaffold in sheep, Tissue Eng. 10 (2004) 1830–1840.

[131] J.S. Temenoff, A.G. Mikos, Review: tissue engineering for regeneration of articular cartilage, Biomaterials 21 (2000) 431–440.

[132] Y. Takahashi, Y. Tabata, Effect of the fiber diameter and porosity of non-woven PET fabrics on the osteogenic differentiation of mesenchymal stem cells, J. Biomater. Sci. Polym. Ed. 15 (2004) 41–57.

[133] P. Duan, Z. Pan, L. Cao, Y. He, H. Wang, Z. Qu, J. Dong, J. Ding, The effects of pore size in bilayered poly(lactide-co-glycolide) scaffolds on restoring osteochondral defects in rabbits, J. Biomed. Mater. Res. 102 (2014) 180–192.

[134] J.A.M. Steele, A.C. Moore, J.-P. St-Pierre, S.D. McCullen, A.J. Gormley, C. C. Horgan, C.R.M. Black, C. Meinert, T. Klein, S. Saifzadeh, R. Steck, J. Ren, M. A. Woodruff, M.M. Stevens, In vitro and in vivo investigation of a zonal microstructured scaffold for osteochondral defect repair, Biomaterials 286 (2022), 121548.

[135] R. Dwivedi, S. Kumar, R. Pandey, A. Mahajan, D. Nandana, D.S. Katti, D. Mehrotra, Polycaprolactone as biomaterial for bone scaffolds: review of literature, Journal of Oral Biology and Craniofacial Research 10 (2020) 381–388.

[136] R. Jin, L.S. Teixeira, P.J. Dijkstra, C.A. van Blitterswijk, M. Karperien, J. Feijen, Enzymatically-crosslinked injectable hydrogels based on biomimetic dextran-hyaluronic acid conjugates for cartilage tissue engineering, Biomaterials 31 (2010) 3103–3113.

[137] D. Seliktar, Designing cell-compatible hydrogels for biomedical applications, Science 336 (2012) 1124–1128.

[138] I.C. Liao, F.T. Moutos, B.T. Estes, X. Zhao, F. Guilak, Composite three-dimensional woven scaffolds with interpenetrating network hydrogels to create functional synthetic articular cartilage, Adv. Funct. Mater. 23 (2013) 5833–5839.

[139] Y. Wu, S. Joseph, N.R. Aluru, Effect of cross-linking on the diffusion of water, ions, and small molecules in hydrogels, J. Phys. Chem. B 113 (2009) 3512–3520.

[140] I.L. Kim, R.L. Mauck, J.A. Burdick, Hydrogel design for cartilage tissue engineering: a case study with hyaluronic acid, Biomaterials 32 (2011) 8771–8782.

[141] A.J. Engler, S. Sen, H.L. Sweeney, D.E. Discher, Matrix elasticity directs stem cell lineage specification, Cell 126 (2006) 677–689.

[142] M. Li, P. Song, W. Wang, Y. Xu, J. Li, L. Wu, X. Gui, Z. Zeng, Z. Zhou, M. Liu, Q. Kong, Y. Fan, X. Zhang, C. Zhou, L. Liu, Preparation and characterization of biomimetic gradient multi-layer cell-laden scaffolds for osteochondral integrated repair, J. Mater. Chem. B 10 (2022) 4172–4188.

[143] B. Arzi, G.D. DuRaine, C.A. Lee, D.J. Huey, D.L. Borjesson, B.G. Murphy, J.C. Y. Hu, N. Baumgarth, K.A. Athanasiou, Cartilage immunoprivilege depends on donor source and lesion location, Acta Biomater. 23 (2015) 72–81.

[144] F. Alihosseini, 10 - plant-based compounds for antimicrobial textiles, in: G. Sun (Ed.), Antimicrobial Textiles, Woodhead Publishing, 2016, pp. 155–195.

[145] K. Schlichting, H. Schell, R.U. Kleemann, A. Schill, A. Weiler, G.N. Duda, D. R. Epari, Influence of scaffold stiffness on subchondral bone and subsequent cartilage regeneration in an ovine model of osteochondral defect, Healing 36 (2008) 2379–2391.

[146] C. Ding, Z. Qiao, W. Jiang, H. Li, J. Wei, G. Zhou, K. Dai, Regeneration of a goat femoral head using a tissue-specific, biphasic scaffold fabricated with CAD/CAM technology, Biomaterials 34 (2013) 6706–6716.

[147] D.E. Shepherd, B.B. Seedhom, Thickness of human articular cartilage in joints of the lower limb, Ann. Rheum. Dis. 58 (1999) 27–34.

[148] F. Guilak, W.R. Jones, H.P. Ting-Beall, G.M. Lee, The deformation behavior and mechanical properties of chondrocytes in articular cartilage, Osteoarthritis Cartilage 7 (1999) 59–70.

[149] L.A. McMahon, F.J. O'Brien, P.J. Prendergast, Biomechanics and mechanobiology in osteochondral tissues, Regen. Med. 3 (2008) 743–759.

[150] A.J. Kerin, M.R. Wisnom, M.A. Adams, The compressive strength of articular cartilage 212 (1998) 273–280.

[151] K. Rezwan, Q.Z. Chen, J.J. Blaker, A.R. Boccaccini, Biodegradable and bioactive porous polymer/inorganic composite scaffolds for bone tissue engineering, Biomaterials 27 (2006) 3413–3431.

[152] S. Stratton, N.B. Shelke, K. Hoshino, S. Rudraiah, S.G. Kumbar, Bioactive polymeric scaffolds for tissue engineering, Bioact. Mater. 1 (2016) 93–108.

[153] H.-p. Lee, L. Gu, D.J. Mooney, M.E. Levenston, O. Chaudhuri, Mechanical confinement regulates cartilage matrix formation by chondrocytes, Nat. Mater. 16 (2017) 1243–1251.

[154] O. Chaudhuri, L. Gu, D. Klumpers, M. Darnell, S.A. Bencherif, J.C. Weaver, N. Huebsch, H.-P. Lee, E. Lippens, G.N. Duda, D.J. Mooney, Hydrogels with tunable stress relaxation regulate stem cell fate and activity, Nat. Mater. 15 (2016) 326–334.

[155] O. Chaudhuri, L. Gu, M. Darnell, D. Klumpers, S.A. Bencherif, J.C. Weaver, N. Huebsch, D.J. Mooney, Substrate stress relaxation regulates cell spreading, Nat. Commun. 6 (2015) 6365.

[156] J. Malda, J. Visser, F.P. Melchels, T. Jüngst, W.E. Hennink, W.J.A. Dhert, J. Groll, D.W. Hutmacher, 25th Anniversary Article: Engineering Hydrogels for Biofabrication 25 (2013) 5011–5028.

[157] H. Muir, The chondrocyte, architect of cartilage. Biomechanics, structure, function and molecular biology of cartilage matrix macromolecules, Bioessays : news and reviews in molecular, cellular and developmental biology 17 (1995) 1039–1048.

[158] V. Irawan, T.-C. Sung, A. Higuchi, T. Ikoma, Collagen scaffolds in cartilage tissue engineering and relevant approaches for future development, Tissue engineering and regenerative medicine 15 (2018) 673–697.

[159] L.-P. Yan, Y.-J. Wang, L. Ren, G. Wu, S.G. Caridade, J.-B. Fan, L.-Y. Wang, P.-H. Ji, J.M. Oliveira, J.T. Oliveira, J.F. Mano, R.L. Reis, Genipin-cross-linked collagen/chitosan biomimetic scaffolds for articular cartilage tissue engineering applications 95A (2010) 465–475.

[160] W. Friess, Collagen–biomaterial for drug delivery, Eur. J. Pharm. Biopharm. : official journal of Arbeitsgemeinschaft fur Pharmazeutische Verfahrenstechnik e. V 45 (1998) 113–136.

[161] R. Cao, Y. Xu, Y. Xu, D.D. Brand, G. Zhou, K. Xiao, H. Xia, J.T. Czernuszka, Development of tri-layered biomimetic atelocollagen scaffolds with interfaces for osteochondral tissue engineering, Advanced healthcare materials 11 (2022), e2101643.

[162] K.Y. Lee, D.J. Mooney, Hydrogels for tissue engineering, Chem. Rev. 101 (2001) 1869–1879.

[163] J.W. Nichol, S.T. Koshy, H. Bae, C.M. Hwang, S. Yamanlar, A. Khademhosseini, Cell-laden microengineered gelatin methacrylate hydrogels, Biomaterials 31 (2010) 5536–5544.

[164] W. Schuurman, P.A. Levett, M.W. Pot, P.R. van Weeren, W.J.A. Dhert, D. W. Hutmacher, F.P.W. Melchels, T.J. Klein, J. Malda, Gelatin-Methacrylamide Hydrogels as Potential Biomaterials for Fabrication of Tissue-Engineered Cartilage Constructs, vol. 13, 2013, pp. 551–561.

[165] D. Loessner, C. Meinert, E. Kaemmerer, L.C. Martine, K. Yue, P.A. Levett, T. J. Klein, F.P.W. Melchels, A. Khademhosseini, D.W. Hutmacher, Functionalization, preparation and use of cell-laden gelatin methacryloyl–based hydrogels as modular tissue culture platforms, Nat. Protoc. 11 (2016) 727–746.

[166] A. Erdem, M.A. Darabi, R. Nasiri, S. Sangabathuni, Y.N. Ertas, H. Alem, V. Hosseini, A. Shamloo, A.S. Nasr, S. Ahadian, M.R. Dokmeci, A. Khademhosseini, N. Ashammakhi, 3D Bioprinting of Oxygenated Cell-Laden Gelatin Methacryloyl Constructs 9 (2020), 1901794.

[167] B. Kundu, R. Rajkhowa, S.C. Kundu, X. Wang, Silk fibroin biomaterials for tissue regenerations, Adv. Drug Deliv. Rev. 65 (2013) 457–470.

[168] P.-H.G. Chao, S. Yodmuang, X. Wang, L. Sun, D.L. Kaplan, G. Vunjak-Novakovic, Silk hydrogel for cartilage tissue engineering, J. Biomed. Mater. Res. B Appl. Biomater. 95 (2010) 84–90.

[169] R. Naomi, J. Ratanavaraporn, M.B. Fauzi, Comprehensive review of hybrid collagen and silk fibroin for cutaneous wound healing, Materials 13 (2020) 3097.

[170] L.P. Yan, J.M. Oliveira, A.L. Oliveira, S.G. Caridade, J.F. Mano, R.L. Reis, Macro/microporous silk fibroin scaffolds with potential for articular cartilage and meniscus tissue engineering applications, Acta Biomater. 8 (2012) 289–301.

[171] N.R. Raia, B.P. Partlow, M. McGill, E.P. Kimmerling, C.E. Ghezzi, D.L. Kaplan, Enzymatically crosslinked silk-hyaluronic acid hydrogels, Biomaterials 131 (2017) 58–67.

[172] Y. Lu, S. Zhang, X. Liu, S. Ye, X. Zhou, Q. Huang, L. Ren, Silk/agarose scaffolds with tunable properties via SDS assisted rapid gelation, RSC Adv. 7 (2017) 21740–21748.

[173] X. Zhang, Y. Liu, Q. Zuo, Q. Wang, Z. Li, K. Yan, T. Yuan, Y. Zhang, K. Shen, R. Xie, W. Fan, 3D bioprinting of biomimetic bilayered scaffold consisting of decellularized extracellular matrix and silk fibroin for osteochondral repair, International journal of bioprinting 7 (2021) 401.

[174] S.K.L. Levengood, M. Zhang, Chitosan-based scaffolds for bone tissue engineering, J. Mater. Chem. B 2 (2014) 3161–3184.

[175] F. Croisier, C. Jérôme, Chitosan-based biomaterials for tissue engineering, Eur. Polym. J. 49 (2013) 780–792.

[176] K.M. Vårum, M.M. Myhr, R.J.N. Hjerde, O. Smidsrød, In vitro degradation rates of partially N-acetylated chitosans in human serum, Carbohydr. Res. 299 (1997) 99–101.

[177] S.M. Ahsan, M. Thomas, K.K. Reddy, S.G. Sooraparaju, A. Asthana, I. Bhatnagar, Chitosan as biomaterial in drug delivery and tissue engineering, Int. J. Biol. Macromol. 110 (2018) 97–109.

[178] A. Oryan, S. Sahvieh, Effectiveness of chitosan scaffold in skin, bone and cartilage healing, Int. J. Biol. Macromol. 104 (2017) 1003–1011.

[179] A.R. Costa-Pinto, V.M. Correlo, P.C. Sol, M. Bhattacharya, P. Charbord, B. Delorme, R.L. Reis, N.M. Neves, Osteogenic differentiation of human bone marrow mesenchymal stem cells seeded on melt based chitosan scaffolds for bone tissue engineering applications, Biomacromolecules 10 (2009) 2067–2073.

[180] A.R. Costa-Pinto, A.J. Salgado, V.M. Correlo, P. Sol, M. Bhattacharya, P. Charbord, R.L. Reis, N.M. Neves, Adhesion, proliferation, and osteogenic differentiation of a mouse mesenchymal stem cell line (BMC9) seeded on novel melt-based chitosan/polyester 3D porous scaffolds, Tissue engineering, Part. Accel. 14 (2008) 1049–1057.

[181] S.J. Florczyk, D.J. Kim, D.L. Wood, M. Zhang, Influence of processing parameters on pore structure of 3D porous chitosan-alginate polyelectrolyte complex scaffolds, J. Biomed. Mater. Res. 98 (2011) 614–620.

[182] S.J. Florczyk, K. Wang, S. Jana, D.L. Wood, S.K. Sytsma, J. Sham, F.M. Kievit, M. Zhang, Porous chitosan-hyaluronic acid scaffolds as a mimic of glioblastoma microenvironment ECM, Biomaterials 34 (2013) 10143–10150.

[183] C.R. Lee, A.J. Grodzinsky, M. Spector, The effects of cross-linking of collagen-glycosaminoglycan scaffolds on compressive stiffness, chondrocyte-mediated contraction and biosynthesis, Biomaterials 22 (2001) 3145–3154.

[184] G. Kim, M. Okumura, T. Ishiguro, T. Kadosawa, T. Fujinaga, Preventive effect of hyaluronic acid on the suppression of attachment and migration abilities of bovine chondrocytes by IL-1alpha in vitro, J. Vet. Med. Sci. 65 (2003) 427–430.

[185] H.S. Yoo, E.A. Lee, J.J. Yoon, T.G. Park, Hyaluronic acid modified biodegradable scaffolds for cartilage tissue engineering, Biomaterials 26 (2005) 1925–1933.

[186] J.A. Burdick, C. Chung, X. Jia, M.A. Randolph, R. Langer, Controlled degradation and mechanical behavior of photopolymerized hyaluronic acid networks, Biomacromolecules 6 (2005) 386–391.

[187] J. Hauptstein, T. Böck, M. Bartolf-Kopp, L. Forster, P. Stahlhut, A. Nadernezhad, G. Blahetek, A. Zernecke-Madsen, R. Detsch, T. Jüngst, J. Groll, J. Teßmar, T. Blunk, Hyaluronic acid-based bioink composition enabling 3D bioprinting and improving, Quality of Deposited Cartilaginous Extracellular Matrix 9 (2020), 2000737.

[188] Y. Liu, L. Peng, L. Li, C. Huang, K. Shi, X. Meng, P. Wang, M. Wu, L. Li, H. Cao, K. Wu, Q. Zeng, H. Pan, W.W. Lu, L. Qin, C. Ruan, X. Wang, 3D-bioprinted BMSC-laden biomimetic multiphasic scaffolds for efficient repair of osteochondral defects in an osteoarthritic rat model, Biomaterials 279 (2021), 121216.

[189] J.M. Kemppainen, S.J. Hollister, Tailoring the mechanical properties of 3D-designed poly(glycerol sebacate) scaffolds for cartilage applications, J. Biomed. Mater. Res. 94 (2010) 9–18.

[190] D. Kilian, T. Ahlfeld, A.R. Akkineni, A. Bernhardt, M. Gelinsky, A. Lode, 3D Bioprinting of osteochondral tissue substitutes - in vitro-chondrogenesis in multi-layered mineralized constructs, Sci. Rep. 10 (2020) 8277.

[191] E. Saygili, P. Saglam-Metiner, E. Cakmak, E. Alarcin, G. Beceren, P. Tulum, Y.-W. Kim, K. Gunes, G.G. Eren-Ozcan, D. Akakin, J.-Y. Sun, O. Yesil-Celiktas, Bilayered laponite/alginate-poly(acrylamide) composite hydrogel for osteochondral injuries enhances macrophage polarization: an in vivo study, Biomaterials Advances 134 (2022), 112721.

[192] H. Seddiqi, E. Oliaei, H. Honarkar, J. Jin, L.C. Geonzon, R.G. Bacabac, J. Klein-Nulend, Cellulose and its derivatives: towards biomedical applications, Cellulose 28 (2021) 1893–1931.

[193] R.B. Arote, D. Jere, H.L. Jiang, Y.K. Kim, Y.J. Choi, M.H. Cho, C.S. Cho, 10 - injectable polymeric carriers for gene delivery systems, in: B. Vernon (Ed.), Injectable Biomaterials, Woodhead Publishing, 2011, pp. 235–259.

[194] S.T. Bendtsen, M. Wei, In vitro evaluation of 3D bioprinted tri-polymer network scaffolds for bone tissue regeneration, J. Biomed. Mater. Res. 105 (2017) 3262–3272.

[195] S.T. Bendtsen, S.P. Quinnell, M. Wei, Development of a novel alginate-polyvinyl alcohol-hydroxyapatite hydrogel for 3D bioprinting bone tissue engineered scaffolds, J. Biomed. Mater. Res. 105 (2017) 1457–1468.

[196] K. Schütz, A.M. Placht, B. Paul, S. Brüggemeier, M. Gelinsky, A. Lode, Three-dimensional plotting of a cell-laden alginate/methylcellulose blend: towards biofabrication of tissue engineering constructs with clinically relevant dimensions, Journal of tissue engineering and regenerative medicine 11 (2017) 1574–1587.

[197] J.C. Middleton, A.J. Tipton, Synthetic biodegradable polymers as orthopedic devices, Biomaterials 21 (2000) 2335–2346.

[198] M.A. Woodruff, D.W. Hutmacher, The return of a forgotten polymer—polycaprolactone in the 21st century, Prog. Polym. Sci. 35 (2010) 1217–1256.

[199] A.D. Olubamiji, Z. Izadifar, J.L. Si, D.M.L. Cooper, B.F. Eames, D.X.B. Chen, Modulating mechanical behaviour of 3D-printed cartilage-mimetic PCL scaffolds: influence of molecular weight and pore geometry, Biofabrication 8 (2016), 025020.

[200] H. Sun, L. Mei, C. Song, X. Cui, P. Wang, The in vivo degradation, absorption and excretion of PCL-based implant, Biomaterials 27 (2006) 1735–1740.

[201] J.J.D. Henry, J. Yu, A. Wang, R. Lee, J. Fang, S. Li, Engineering the mechanical and biological properties of nanofibrous vascular grafts for in situ vascular tissue engineering, Biofabrication 9 (2017), 035007.

[202] H.K. Makadia, S.J. Siegel, Poly lactic-co-glycolic acid (PLGA) as biodegradable controlled drug delivery carrier, Polymers 3 (2011) 1377–1397.

[203] C. Shasteen, Y.B. Choy, Controlling degradation rate of poly(lactic acid) for its biomedical applications, Biomedical Engineering Letters 1 (2011) 163.

[204] Z. Pan, J. Ding, Poly(lactide-co-glycolide) porous scaffolds for tissue engineering and regenerative medicine 2 (2012) 366–377.

[205] G. Asensio, L. Benito-Garzón, R.A. Ramírez-Jiménez, Y. Guadilla, J. Gonzalez-Rubio, C. Abradelo, J. Parra, M.R. Martín-López, M.R. Aguilar, B. Vázquez-Lasa, L. Rojo, Biomimetic gradient scaffolds containing hyaluronic acid and Sr/Zn folates for osteochondral tissue engineering, Polymers 14 (2021).

[206] M. Tahriri, F. Moztarzadeh, Preparation, characterization, and in vitro biological evaluation of PLGA/nano-fluorohydroxyapatite (FHA) microsphere-sintered scaffolds for biomedical applications, Appl. Biochem. Biotechnol. 172 (2014) 2465–2479.

[207] Y. Dai, T. Shen, L. Ma, D. Wang, C. Gao, Regeneration of osteochondral defects in vivo by a cell-free cylindrical poly(lactide-co-glycolide) scaffold with a radially oriented microstructure 12 (2018) e1647–e1661.

[208] X. Liang, Y. Qi, Z. Pan, Y. He, X. Liu, S. Cui, J. Ding, Design and preparation of quasi-spherical salt particles as water-soluble porogens to fabricate hydrophobic porous scaffolds for tissue engineering and tissue regeneration, Mater. Chem. Front. 2 (2018) 1539–1553.

[209] Q. Liu, S. Xie, D. Fan, T. Xie, G. Xue, X. Gou, X. Li, Integrated osteochondral differentiation of mesenchymal stem cells on biomimetic nanofibrous mats with cell adhesion-generated piezopotential gradients, Nanoscale 14 (2022) 3865–3877.

[210] E. Dawson, G. Mapili, K. Erickson, S. Taqvi, K. Roy, Biomaterials for stem cell differentiation, Adv. Drug Deliv. Rev. 60 (2008) 215–228.

[211] X.S. Wu, N. Wang, Synthesis, characterization, biodegradation, and drug delivery application of biodegradable lactic/glycolic acid polymers. Part II: biodegradation, Journal of biomaterials science, Polymer edition 12 (2001) 21–34.

[212] S. Abedin Dargoush, H. Hanaee ahvaz, S. Irani, M. Soleimani, M. Khatami, A. Naderi Sohi, A composite bilayer scaffold functionalized for osteochondral tissue regeneration in rat animal model, Journal of tissue engineering and regenerative medicine 16 (2022).

[213] S.N.S. Alconcel, A.S. Baas, H.D. Maynard, FDA-approved poly(ethylene glycol)–protein conjugate drugs, Polym. Chem. 2 (2011) 1442–1448.

[214] J.S. Suk, Q. Xu, N. Kim, J. Hanes, L.M. Ensign, PEGylation as a strategy for improving nanoparticle-based drug and gene delivery, Adv. Drug Deliv. Rev. 99 (2016) 28–51.

[215] L. Vogt, F. Ruther, S. Salehi, A.R. Boccaccini, Poly(Glycerol sebacate) in biomedical, Applications—A Review of the Recent Literature 10 (2021), 2002026.

[216] J.L. Guo, Y.S. Kim, G.L. Koons, J. Lam, A.M. Navara, S. Barrios, V.Y. Xie, E. Watson, B.T. Smith, H.A. Pearce, E.A. Orchard, J. van den Beucken, J. A. Jansen, M.E. Wong, A.G. Mikos, Bilayered, peptide-biofunctionalized hydrogels for in vivo osteochondral tissue repair, Acta Biomater. 128 (2021) 120–129.

[217] P.J. Emans, F. Spaapen, D.A. Surtel, K.M. Reilly, A. Cremers, L.W. van Rhijn, S. K. Bulstra, J.W. Voncken, R. Kuijer, A novel in vivo model to study endochondral bone formation; HIF-1alpha activation and BMP expression, Bone 40 (2007) 409–418.

[218] M.T. Islam, R.M. Felfel, E.A. Abou Neel, D.M. Grant, I. Ahmed, K.M.Z. Hossain, Bioactive calcium phosphate–based glasses and ceramics and their biomedical applications, Review 8 (2017), 2041731417719170.

[219] H. Zhou, J. Lee, Nanoscale hydroxyapatite particles for bone tissue engineering, Acta Biomater. 7 (2011) 2769–2781.

[220] S.C. Goel, D. Singh, A. Rastogi, V. Kumaraswamy, A. Gupta, N. Sharma, Role of tricalcium phosphate implant in bridging the large osteoperiosteal gaps in rabbits, Indian J. Exp. Biol. 51 (2013) 375–380.

[221] X. Li, M. Liu, F. Chen, Y. Wang, M. Wang, X. Chen, Y. Xiao, X. Zhang, Design of hydroxyapatite bioceramics with micro-/nano-topographies to regulate the osteogenic activities of bone morphogenetic protein-2 and bone marrow stromal cells, Nanoscale 12 (2020) 7284–7300.

[222] R. Zhao, P. Xie, K. Zhang, Z. Tang, X. Chen, X. Zhu, Y. Fan, X. Yang, X. Zhang, Selective effect of hydroxyapatite nanoparticles on osteoporotic and healthy bone formation correlates with intracellular calcium homeostasis regulation, Acta Biomater. 59 (2017) 338–350.

[223] N.J. Castro, J. O'Brien, L.G. Zhang, Integrating biologically inspired nanomaterials and table-top stereolithography for 3D printed biomimetic osteochondral scaffolds, Nanoscale 7 (2015) 14010–14022.

[224] G.M. Cunniffe, C.M. Curtin, E.M. Thompson, G.R. Dickson, F.J. O'Brien, Content-dependent osteogenic response of nanohydroxyapatite: an in vitro and in vivo assessment within collagen-based scaffolds, ACS Appl. Mater. Interfaces 8 (2016) 23477–23488.

[225] Z. Sheikh, C. Sima, M. Glogauer, Bone replacement materials and techniques used for achieving vertical alveolar, Bone Augmentation 8 (2015) 2953–2993.

[226] S. Weiner, H.D. Wagner, THE MATERIAL BONE: Structure-Mechanical Function Relations 28 (1998) 271–298.

[227] J. Lu, M. Descamps, J. Dejou, G. Koubi, P. Hardouin, J. Lemaitre, J.P. Proust, The biodegradation mechanism of calcium phosphate biomaterials in bone, J. Biomed. Mater. Res.: An Official Journal of The Society for Biomaterials, The Japanese Society for Biomaterials, and The Australian Society for Biomaterials and the Korean Society for Biomaterials 63 (2002) 408–412.

[228] P. Ducheyne, Q. Qiu, Bioactive ceramics: the effect of surface reactivity on bone formation and bone cell function, Biomaterials 20 (1999) 2287–2303.

[229] B.L. Taylor, T. Andric, J.W. Freeman, Recent advances in bone graft technologies, Recent Pat. Biomed. Eng. 6 (2013) 40–46.

[230] H. Oonishi, L.L. Hench, J. Wilson, F. Sugihara, E. Tsuji, S. Kushitani, H. Iwaki, Comparative bone growth behavior in granules of bioceramic materials of various sizes, J. Biomed. Mater. Res. 44 (1999) 31–43.

[231] S. Kargozar, M. Montazerian, S. Hamzehlou, H.W. Kim, F. Baino, Mesoporous bioactive glasses: promising platforms for antibacterial strategies, Acta Biomater. 81 (2018) 1–19.

[232] M.N. Rahaman, D.E. Day, B.S. Bal, Q. Fu, S.B. Jung, L.F. Bonewald, A.P. Tomsia, Bioactive glass in tissue engineering, Acta Biomater. 7 (2011) 2355–2373.

[233] D. Lin, Y. Chai, Y. Ma, B. Duan, Y. Yuan, C. Liu, Rapid initiation of guided bone regeneration driven by spatiotemporal delivery of IL-8 and BMP-2 from hierarchical MBG-based scaffold, Biomaterials 196 (2019) 122–137.

[234] A.J. Sutherland, G.L. Converse, R.A. Hopkins, M.S. Detamore, The bioactivity of cartilage extracellular matrix in articular cartilage regeneration, Advanced healthcare materials 4 (2015) 29–39.

[235] S.P. Grogan, S.F. Duffy, C. Pauli, J.A. Koziol, A.I. Su, D.D. D'Lima, M.K. Lotz, Zone-specific gene expression patterns in articular cartilage, Arthritis Rheum. 65 (2013) 418–428.

[236] B. He, J.P. Wu, T.B. Kirk, J.A. Carrino, C. Xiang, J. Xu, High-resolution measurements of the multilayer ultra-structure of articular cartilage and their translational potential, Arthritis Res. Ther. 16 (2014) 205.

[237] K.I. Bohsali, A.J. Bois, M.A. Wirth, Complications of Shoulder Arthroplasty 99 (2017) 256–269.

[238] J. Farr, G.C. Gracitelli, N. Shah, E.Y. Chang, A.H. Gomoll, High failure rate of a decellularized osteochondral allograft for the treatment of cartilage, Lesions 44 (2016) 2015–2022.

[239] S. Schwarz, A.F. Elsaesser, L. Koerber, E. Goldberg-Bockhorn, A.M. Seitz, C. Bermueller, L. Dürselen, A. Ignatius, R. Breiter, N. Rotter, Processed xenogenic cartilage as innovative biomatrix for cartilage tissue engineering: effects on chondrocyte differentiation and function 9 (2015) E239–E251.

[240] D.C. Browe, P.J. Díaz-Payno, F.E. Freeman, R. Schipani, R. Burdis, D.P. Ahern, J. M. Nulty, S. Guler, L.D. Randall, C.T. Buckley, P.A.J. Brama, D.J. Kelly, Bilayered extracellular matrix derived scaffolds with anisotropic pore architecture guide tissue organization during osteochondral defect repair, Acta Biomater. 143 (2022) 266–281.

[241] C.-C. Wong, C.-H. Chen, W.P. Chan, L.-H. Chiu, W.-P. Ho, F.-J. Hsieh, Y.-T. Chen, T.-L. Yang, Single-stage cartilage repair using platelet-rich fibrin scaffolds with autologous, Cartilaginous Grafts 45 (2017) 3128–3142.

[242] S. Liu, Y.C. Shin, Additive manufacturing of Ti6Al4V alloy: a review, Mater. Des. 164 (2019), 107552.

[243] E. Chlebus, B. Kuźnicka, T. Kurzynowski, B. Dybała, Microstructure and mechanical behaviour of Ti–6Al–7Nb alloy produced by selective laser melting, Mater. Char. 62 (2011) 488–495.

[244] H. Rotaru, G. Armencea, D. Spîrchez, C. Berce, T. Marcu, D. Leordean, S.G. Kim, S. W. Lee, C. Dinu, G. Băciuţ, M. Băciuţ, In vivo behavior of surface modified Ti6Al7Nb alloys used in selective laser melting for custom-made implants. A preliminary study, Romanian journal of morphology and embryology = Revue roumaine de morphologie et embryologie 54 (2013) 791–796.

[245] L. Yu, T.M. Silva Santisteban, Q. Liu, C. Hu, J. Bi, M. Wei, Effect of three-dimensional porosity gradients of biomimetic coatings on their bonding strength and cell behavior, J. Biomed. Mater. Res. 109 (2021) 615–626.

[246] W. Zhang, Z. Yuan, X. Meng, J. Zhang, T. Long, Z. Yaochao, C. Yang, R. Lin, B. Yue, Q. Guo, Y. Wang, Preclinical evaluation of a mini-arthroplasty implant based on polyetheretherketone and Ti6Al4V for treatment of a focal osteochondral defect in the femoral head of the hip, Biomed. Mater. (Bristol, U. K.) 15 (2020), 055027.

[247] M. Niinomi, Mechanical properties of biomedical titanium alloys, Mater. Sci. Eng. 243 (1998) 231–236.

[248] Y. Torres, P. Trueba, J. Pavón, I. Montealegre, J.A. Rodríguez-Ortiz, Designing, processing and characterisation of titanium cylinders with graded porosity: an alternative to stress-shielding solutions, Mater. Des. 63 (2014) 316–324.

[249] E.H. Mrosek, J.C. Schagemann, H.W. Chung, J.S. Fitzsimmons, M.J. Yaszemski, R. M. Mardones, S.W. O'Driscoll, G.G. Reinholz, Porous tantalum and poly-epsilon-caprolactone biocomposites for osteochondral defect repair: preliminary studies in rabbits, J. Orthop. Res. : official publication of the Orthopaedic Research Society 28 (2010) 141–148.

[250] A.K. Harrison, T.J. Gioe, C. Simonelli, P.J. Tatman, M.C. Schoeller, Do porous tantalum implants help preserve bone?: evaluation of tibial bone density surrounding tantalum tibial implants in TKA, Clin. Orthop. Relat. Res. 468 (2010) 2739–2745.

[251] M. Stiehler, M. Lind, T. Mygind, A. Baatrup, A. Dolatshahi-Pirouz, H. Li, M. Foss, F. Besenbacher, M. Kassem, C. Bünger, Morphology, proliferation, and osteogenic differentiation of mesenchymal stem cells cultured on titanium, tantalum, and chromium surfaces, J. Biomed. Mater. Res. 86 (2008) 448–458.

[252] Y.-L. Zhou, M. Niinomi, T. Akahori, H. Nakai, H. Fukui, Comparison of various properties between titanium-tantalum alloy and pure titanium for biomedical applications, Mater. Trans. 48 (2007) 380–384.

[253] Y. Han, H. Lian, B. Sun, B. Jia, Q. Wu, Z. Qiao, K. Dai, Preparation of high precision multilayer scaffolds based on Melt Electro-Writing to repair cartilage injury, Theranostics 10 (2020), 10214.

[254] C. Li, J.P. Armstrong, I.J. Pence, W. Kit-Anan, J.L. Puetzer, S.C. Carreira, A. C. Moore, M.M. Stevens, Glycosylated superparamagnetic nanoparticle gradients for osteochondral tissue engineering, Biomaterials 176 (2018) 24–33.

[255] W.M. Groen, P. Diloksumpan, P.R. van Weeren, R. Levato, J. Malda, From intricate to integrated: biofabrication of articulating joints, J. Orthop. Res. 35 (2017) 2089–2097.

[256] C. Liu, Z. Han, J. Czernuszka, Gradient collagen/nanohydroxyapatite composite scaffold: development and characterization, Acta Biomater. 5 (2009) 661–669.

[257] X. Liu, L.A. Smith, J. Hu, P.X. Ma, Biomimetic nanofibrous gelatin/apatite composite scaffolds for bone tissue engineering, Biomaterials 30 (2009) 2252–2258.

[258] A. Arora, A. Kothari, D.S. Katti, Pore orientation mediated control of mechanical behavior of scaffolds and its application in cartilage-mimetic scaffold design, J. Mech. Behav. Biomed. Mater. 51 (2015) 169–183.

[259] D. Clearfield, A. Nguyen, M. Wei, Biomimetic multidirectional scaffolds for zonal osteochondral tissue engineering via a lyophilization bonding approach, J. Biomed. Mater. Res. 106 (2018) 948–958.

[260] K. Stuckensen, A. Schwab, M. Knauer, E. Muiños-López, F. Ehlicke, J. Reboredo, F. Granero-Moltó, U. Gbureck, F. Prósper, H. Walles, Tissue mimicry in morphology and composition promotes hierarchical matrix remodeling of invading stem cells in osteochondral and meniscus scaffolds, Adv. Mater. 30 (2018), 1706754.

[261] K. Liu, Y. Liu, Z. Duan, X. Ma, D. Fan, A biomimetic bi-layered tissue engineering scaffolds for osteochondral defects repair, Sci. China Technol. Sci. 64 (2021) 793–805.

[262] T.J. Levingstone, E. Thompson, A. Matsiko, A. Schepens, J.P. Gleeson, F. J. O'Brien, Multi-layered collagen-based scaffolds for osteochondral defect repair in rabbits, Acta Biomater. 32 (2016) 149–160.

[263] T.J. Levingstone, A. Ramesh, R.T. Brady, P.A. Brama, C. Kearney, J.P. Gleeson, F. J. O'Brien, Cell-free multi-layered collagen-based scaffolds demonstrate layer specific regeneration of functional osteochondral tissue in caprine joints, Biomaterials 87 (2016) 69–81.

[264] D. Clearfield, M. Wei, Investigation of structural collapse in unidirectionally freeze cast collagen scaffolds, J. Mater. Sci. Mater. Med. 27 (2016) 15.

[265] C. Hu, L. Yu, M. Wei, Biomimetic intrafibrillar silicification of collagen fibrils through a one-step collagen self-assembly/silicification approach, RSC Adv. 7 (2017) 34624–34632.

[266] C. Hu, M. Zilm, M. Wei, Fabrication of intrafibrillar and extrafibrillar mineralized collagen/apatite scaffolds with a hierarchical structure, J. Biomed. Mater. Res. 104 (2016) 1153–1161.

[267] D.S. Clearfield, X. Xin, S. Yadav, D.W. Rowe, M. Wei, Osteochondral differentiation of fluorescent multireporter cells on zonally-organized biomaterials, Tissue Eng. 25 (2019) 468–486.

[268] J.H. Lee, J.-H. Park, Y.-R. Yun, J.-H. Jang, E.-J. Lee, W. Chrzanowski, I.B. Wall, H.-W. Kim, Tethering bi-functional protein onto mineralized polymer scaffolds to regulate mesenchymal stem cell behaviors for bone regeneration, J. Mater. Chem. B 1 (2013) 2731–2741.

[269] L. Yu, S. Qian, Y. Qiao, X. Liu, Multifunctional Mn-containing titania coatings with enhanced corrosion resistance, osteogenesis and antibacterial activity, J. Mater. Chem. B 2 (2014) 5397–5408.

[270] Y. Wang, Y. Xiao, S. Long, Y. Fan, X. Zhang, Role of N-cadherin in a niche-mimicking microenvironment for chondrogenesis of mesenchymal stem cells in vitro, ACS Biomater. Sci. Eng. 6 (2020) 3491–3501.

[271] P. Occhetta, M. Centola, B. Tonnarelli, A. Redaelli, I. Martin, M. Rasponi, High-throughput microfluidic platform for 3D cultures of mesenchymal stem cells, towards engineering developmental processes, Sci. Rep. 5 (2015) 1–12.

[272] B.A. Harley, A.K. Lynn, Z. Wissner-Gross, W. Bonfield, I.V. Yannas, L.J. Gibson, Design of a multiphase osteochondral scaffold III: fabrication of layered scaffolds with continuous interfaces, J. Biomed. Mater. Res. Part A: An Official Journal of The Society for Biomaterials, The Japanese Society for Biomaterials, and The Australian Society for Biomaterials and the Korean Society for Biomaterials 92 (2010) 1078–1093.

[273] Q. Yao, P. Nooeaid, R. Detsch, J.A. Roether, Y. Dong, O.M. Goudouri, D. W. Schubert, A.R. Boccaccini, Bioglass®/chitosan–polycaprolactone bilayered composite scaffolds intended for osteochondral tissue engineering, J. Biomed. Mater. Res. 102 (2014) 4510–4518.

[274] A.E. Erickson, J. Sun, S.K. Lan Levengood, S. Swanson, F.-C. Chang, C.T. Tsao, M. Zhang, Chitosan-based composite bilayer scaffold as an in vitro osteochondral defect regeneration model, Biomed. Microdevices 21 (2019) 1–16.

[275] N. Mohan, N.H. Dormer, K.L. Caldwell, V.H. Key, C.J. Berkland, M.S. Detamore, Continuous gradients of material composition and growth factors for effective regeneration of the osteochondral interface, Tissue Eng. 17 (2011) 2845–2855.

[276] M. Singh, N. Dormer, J.R. Salash, J.M. Christian, D.S. Moore, C. Berkland, M. S. Detamore, Three-dimensional macroscopic scaffolds with a gradient in stiffness for functional regeneration of interfacial tissues, J. Biomed. Mater. Res., Part A 94 (2010) 870–876.

[277] S. Ramakrishna, An Introduction to Electrospinning and Nanofibers, World scientific, 2005.

[278] C. Yang, Q. Shao, Y. Han, Q. Liu, L. He, Q. Sun, S. Ruan, Fibers by electrospinning and their emerging applications in bone tissue engineering, Appl. Sci. 11 (2021) 9082.

[279] F. Barbosa, F.C. Ferreira, J.C. Silva, Piezoelectric electrospun fibrous scaffolds for bone, articular cartilage and osteochondral tissue engineering, Int. J. Mol. Sci. 23 (2022) 2907.

[280] M. Rahmati, D.K. Mills, A.M. Urbanska, M.R. Saeb, J.R. Venugopal, S. Ramakrishna, M. Mozafari, Electrospinning for tissue engineering applications, Prog. Mater. Sci. 117 (2021), 100721.

[281] X. Zhang, L. Li, J. Ouyang, L. Zhang, J. Xue, H. Zhang, W. Tao, Electroactive electrospun nanofibers for tissue engineering, Nano Today 39 (2021), 101196.

[282] H. Ding, Y. Cheng, X. Niu, Y. Hu, Application of electrospun nanofibers in bone, cartilage and osteochondral tissue engineering, J. Biomater. Sci. Polym. Ed. 32 (2020) 536–561.

[283] T. Chen, J. Bai, J. Tian, P. Huang, H. Zheng, J. Wang, A single integrated osteochondral in situ composite scaffold with a multi-layered functional structure, Colloids Surf. B Biointerfaces 167 (2018) 354–363.

[284] J.E. Jeon, C. Vaquette, C. Theodoropoulos, T.J. Klein, D.W. Hutmacher, Multiphasic construct studied in an ectopic osteochondral defect model, J. R. Soc. Interface 11 (2014), 20140184.

[285] C. Vaquette, W. Fan, Y. Xiao, S. Hamlet, D.W. Hutmacher, S. Ivanovski, A biphasic scaffold design combined with cell sheet technology for simultaneous regeneration of alveolar bone/periodontal ligament complex, Biomaterials 33 (2012) 5560–5573.

[286] P.F. Costa, C. Vaquette, Q. Zhang, R.L. Reis, S. Ivanovski, D.W. Hutmacher, Advanced tissue engineering scaffold design for regeneration of the complex hierarchical periodontal structure, J. Clin. Periodontol. 41 (2014) 283–294.

[287] S. Tamburaci, B. Cecen, O. Ustun, B.U. Ergur, H. Havitcioglu, F. Tihminlioglu, Production and characterization of a novel bilayer nanocomposite scaffold composed of chitosan/Si-nHap and zein/POSS structures for osteochondral tissue regeneration, ACS Appl. Bio Mater. 2 (2019) 1440–1455.

[288] A.F. Girão, Â. Semitela, G. Ramalho, A. Completo, P.A. Marques, Mimicking nature: fabrication of 3D anisotropic electrospun polycaprolactone scaffolds for cartilage tissue engineering applications, Compos. B Eng. 154 (2018) 99–107.

[289] S. Wang, S. Zhao, J. Yu, Z. Gu, Y. Zhang, Advances in translational 3D printing for cartilage, bone, and osteochondral tissue engineering, Small (2022), 2201869.

[290] J. Yin, M. Yan, Y. Wang, J. Fu, H. Suo, 3D bioprinting of low-concentration cell-laden gelatin methacrylate (GelMA) bioinks with a two-step cross-linking strategy, ACS Appl. Mater. Interfaces 10 (2018) 6849–6857.

[291] X. Gu, Y. Zha, Y. Li, J. Chen, S. Liu, Y. Du, S. Zhang, J. Wang, Integrated polycaprolactone microsphere-based scaffolds with biomimetic hierarchy and tunable vascularization for osteochondral repair, Acta Biomater. 141 (2022) 190–197.

[292] F. Naghizadeh, A. Solouk, S.B. Khoulenjani, Osteochondral scaffolds based on electrospinning method: general review on new and emerging approaches, International Journal of Polymeric Materials and Polymeric Biomaterials 67 (2018) 913–924.

[293] A. Kabirkoohian, H. Bakhshi, S. Irani, F. Sharifi, Chemical immobilization of carboxymethyl chitosan on polycaprolactone nanofibers as osteochondral scaffolds, Appl. Biochem. Biotechnol. (2022) 1–12.

[294] S. Zhang, L. Chen, Y. Jiang, Y. Cai, G. Xu, T. Tong, W. Zhang, L. Wang, J. Ji, P. Shi, Bi-layer collagen/microporous electrospun nanofiber scaffold improves the osteochondral regeneration, Acta Biomater. 9 (2013) 7236–7247.

[295] H. Hanaee-Ahvaz, S. Irani, M. Soleimani, S. Khatami, A. Sohi, A composite bilayer scaffold functionalized for osteochondral tissue regeneration in rat animal model, Journal of tissue engineering and regenerative medicine 16 (2022) 559–574.

[296] L.F. Mellor, P. Huebner, S. Cai, M. Mohiti-Asli, M.A. Taylor, J. Spang, R. A. Shirwaiker, E.G. Loboa, Fabrication and evaluation of electrospun, 3D-bio-plotted, and combination of electrospun/3D-bioplotted scaffolds for tissue engineering applications, BioMed Res. Int. 2017 (2017).

[297] J. Li, M. Pumera, 3D printing of functional microrobots, Chem. Soc. Rev. 50 (2021) 2794–2838.

[298] A.C.F.o.A.M. Technologies, A.C.F.o.A.M.T.S.F.o. Terminology, Standard Terminology for Additive Manufacturing Technologies, Astm International, 2012.

[299] F. Pati, J. Gantelius, H.A. Svahn, 3D bioprinting of tissue/organ models, Angew. Chem. Int. Ed. 55 (2016) 4650–4665.

[300] J. Li, C. Wu, P.K. Chu, M. Gelinsky, 3D printing of hydrogels: rational design strategies and emerging biomedical applications, Mater. Sci. Eng. R Rep. 140 (2020), 100543.

[301] S. Vijayavenkataraman, W.-C. Yan, W.F. Lu, C.-H. Wang, J.Y.H. Fuh, 3D bioprinting of tissues and organs for regenerative medicine, Adv. Drug Deliv. Rev. 132 (2018) 296–332.

[302] S.V. Murphy, A. Atala, 3D bioprinting of tissues and organs, Nat. Biotechnol. 32 (2014) 773–785.

[303] A.C. Daly, F.E. Freeman, T. Gonzalez-Fernandez, S.E. Critchley, J. Nulty, D. J. Kelly, 3D bioprinting for cartilage and osteochondral tissue engineering, Advanced healthcare materials 6 (2017), 1700298.

[304] F. Ghorbani, D. Li, S. Ni, Y. Zhou, B. Yu, 3D printing of acellular scaffolds for bone defect regeneration: a review, Mater. Today Commun. 22 (2020), 100979.

[305] S.E. Doyle, F. Snow, S. Duchi, C.D. O'connell, C. Onofrillo, C. Di Bella, E. Pirogova, 3D printed multiphasic scaffolds for osteochondral repair: challenges and opportunities, Int. J. Mol. Sci. 22 (2021), 12420.

[306] M. Askari, M.A. Naniz, M. Kouhi, A. Saberi, A. Zolfagharian, M. Bodaghi, Recent progress in extrusion 3D bioprinting of hydrogel biomaterials for tissue regeneration: a comprehensive review with focus on advanced fabrication techniques, Biomater. Sci. 9 (2021) 535–573.

[307] J. Gao, X. Ding, X. Yu, X. Chen, X. Zhang, S. Cui, J. Shi, J. Chen, L. Yu, S. Chen, Cell-free bilayered porous scaffolds for osteochondral regeneration fabricated by continuous 3D-printing using nascent physical hydrogel as ink, Advanced healthcare materials 10 (2021) 2001404.

[308] W. Dai, L. Zhang, Y. Yu, W. Yan, F. Zhao, Y. Fan, C. Cao, Q. Cai, X. Hu, Y. Ao, 3D bioprinting of heterogeneous constructs providing tissue-specific microenvironment based on host–guest modulated dynamic hydrogel bioink for osteochondral regeneration, Adv. Funct. Mater. (2022) 2200710.

[309] C. Qin, J. Ma, L. Chen, H. Ma, H. Zhuang, M. Zhang, Z. Huan, J. Chang, N. Ma, C. Wu, 3D Bioprinting of Multicellular Scaffolds for Osteochondral Regeneration, Materials Today, 2021.

[310] C. Deng, Q. Yang, X. Sun, L. Chen, C. Feng, J. Chang, C. Wu, Bioactive scaffolds with Li and Si ions-synergistic effects for osteochondral defects regeneration, Appl. Mater. Today 10 (2018) 203–216.

[311] F. Fina, S. Gaisford, A.W. Basit, Powder Bed Fusion: the Working Process, Current Applications and Opportunities, 3D printing of pharmaceuticals, 2018, pp. 81–105.

[312] P. Diloksumpan, M. de Ruijter, M. Castilho, U. Gbureck, T. Vermonden, P.R. Van Weeren, J. Malda, R. Levato, Combining multi-scale 3D printing technologies to engineer reinforced hydrogel-ceramic interfaces, Biofabrication 12 (2020), 025014.

[313] F.M. Wunner, M.L. Wille, T.G. Noonan, O. Bas, P.D. Dalton, E.M. De-Juan-Pardo, D.W. Hutmacher, Melt electrospinning writing of highly ordered large volume scaffold architectures, Adv. Mater. 30 (2018), 1706570.

[314] A. Hrynevich, B.Ş. Elçi, J.N. Haigh, R. McMaster, A. Youssef, C. Blum, T. Blunk, G. Hochleitner, J. Groll, P.D. Dalton, Dimension-based design of melt electrowritten scaffolds, Small 14 (2018), 1800232.

[315] G. Hochleitner, T. Jüngst, T.D. Brown, K. Hahn, C. Moseke, F. Jakob, P.D. Dalton, J. Groll, Additive manufacturing of scaffolds with sub-micron filaments via melt electrospinning writing, Biofabrication 7 (2015), 035002.

[316] Y. Han, M. Lian, Q. Wu, Z. Qiao, B. Sun, K. Dai, Effect of pore size on cell behavior using melt electrowritten scaffolds, Front. Bioeng. Biotechnol. 9 (2021) 495.

[317] H. Suo, J. Zhang, M. Xu, L. Wang, Low-temperature 3D printing of collagen and chitosan composite for tissue engineering, Mater. Sci. Eng. C 123 (2021) 111963.

[318] J. Stepanovska, M. Supova, K. Hanzalek, A. Broz, R. Matejka, Collagen bioinks for bioprinting: a systematic review of hydrogel properties, bioprinting parameters, protocols, and bioprinted structure cellular characteristics, Biomedicines 9 (2021) 1137.

[319] L. Jin, W. Zhao, B. Ren, L. Li, X. Hu, X. Zhang, Q. Cai, Y. Ao, X. Yang, Osteochondral tissue regenerated via a strategy by stacking pre-differentiated BMSC sheet on fibrous mesh in a gradient, Biomed. Mater. 14 (2019), 065017.

[320] J. Zhang, M. Zhang, R. Lin, Y. Du, L. Wang, Q. Yao, A. Zannettino, H. Zhang, Chondrogenic preconditioning of mesenchymal stem/stromal cells within a magnetic scaffold for osteochondral repair, Biofabrication 14 (2022), 025020.

[321] Z. Ren, S. Ma, L. Jin, Z. Liu, D. Liu, X. Zhang, Q. Cai, X. Yang, Repairing a bone defect with a three-dimensional cellular construct composed of a multi-layered cell sheet on electrospun mesh, Biofabrication 9 (2017), 025036.

[322] C.-Y. Gao, Z.-H. Huang, W. Jing, P.-F. Wei, L. Jin, X.-H. Zhang, Q. Cai, X.-L. Deng, X.-P. Yang, Directing osteogenic differentiation of BMSCs by cell-secreted decellularized extracellular matrixes from different cell types, J. Mater. Chem. B 6 (2018) 7471–7485.

[323] W. Zhang, G. Yang, X. Wang, L. Jiang, F. Jiang, G. Li, Z. Zhang, X. Jiang, Magnetically controlled growth-factor-immobilized multilayer cell sheets for complex tissue regeneration, Adv. Mater. 29 (2017), 1703795.

[324] Y. Xiong, B.-B. Mi, Z. Lin, Y.-Q. Hu, L.-K. Zha, A.C. Panayi, T. Yu, L. Chen, Z.-P. Liu, The role of the immune microenvironment in bone, cartilage, and soft tissue regeneration: from mechanism to therapeutic opportunity, Military Medical Research 9 (2022) 1–29.

[325] P. Morouço, C. Fernandes, W. Lattanzi, Challenges and innovations in osteochondral regeneration: insights from biology and inputs from bioengineering toward the optimization of tissue engineering strategies, J. Funct. Biomater. 12 (2021) 17.

[326] V. Graceffa, C. Vinatier, J. Guicheux, M. Stoddart, M. Alini, D.I. Zeugolis, Chasing Chimeras–The elusive stable chondrogenic phenotype, Biomaterials 192 (2019) 199–225.

[327] D.J. Munoz-Pinto, R.E. McMahon, M.A. Kanzelberger, A.C. Jimenez-Vergara, M. A. Grunlan, M.S. Hahn, Inorganic–organic hybrid scaffolds for osteochondral regeneration, J. Biomed. Mater. Res. Part A: An Official Journal of The Society for Biomaterials, The Japanese Society for Biomaterials, and The Australian Society for Biomaterials and the Korean Society for Biomaterials 94 (2010) 112–121.

[328] E. Vinod, S.M. Amirtham, U. Kachroo, A. Goyal, O. Ozbey, J.V. James, S. Sathishkumar, B. Ramasamy, Articular chondroprogenitors in platelet rich plasma for treatment of osteoarthritis and osteochondral defects in a rabbit knee model, Knee 30 (2021) 51–62.

[329] S.Y. Jeong, D.H. Kim, J. Ha, H.J. Jin, S.J. Kwon, J.W. Chang, S.J. Choi, W. Oh, Y. S. Yang, G. Kim, Thrombospondin-2 secreted by human umbilical cord blood-derived mesenchymal stem cells promotes chondrogenic differentiation, Stem Cell. 31 (2013) 2136–2148.

[330] S. Khorshidi, A. Karkhaneh, A review on gradient hydrogel/fiber scaffolds for osteochondral regeneration, Journal of tissue engineering and regenerative medicine 12 (2018) e1974–e1990.

[331] E. Vinod, R. Parameswaran, B. Ramasamy, U. Kachroo, Pondering the potential of hyaline cartilage–derived chondroprogenitors for tissue regeneration: a systematic review, Cartilage 13 (2021) 34S–52S.

[332] T.H. Ambrosi, M.T. Longaker, C.K. Chan, A revised perspective of skeletal stem cell biology, Front. Cell Dev. Biol. 7 (2019) 189.

[333] K. Zha, X. Li, Z. Yang, G. Tian, Z. Sun, X. Sui, Y. Dai, S. Liu, Q. Guo, Heterogeneity of mesenchymal stem cells in cartilage regeneration: from characterization to application, NPJ Regenerative Medicine 6 (2021) 1–15.

[334] M. Qasim, D.S. Chae, N.Y. Lee, Bioengineering strategies for bone and cartilage tissue regeneration using growth factors and stem cells, J. Biomed. Mater. Res. 108 (2020) 394–411.

[335] P. Saeedi, R. Halabian, A.A.I. Fooladi, A revealing review of mesenchymal stem cells therapy, clinical perspectives and Modification strategies, Stem Cell Invest. 6 (2019).

[336] P. Neybecker, C. Henrionnet, E. Pape, L. Grossin, D. Mainard, L. Galois, D. Loeuille, P. Gillet, A. Pinzano, Respective stemness and chondrogenic potential of mesenchymal stem cells isolated from human bone marrow, synovial membrane, and synovial fluid, Stem Cell Res. Ther. 11 (2020) 1–12.

[337] H. Le, W. Xu, X. Zhuang, F. Chang, Y. Wang, J. Ding, Mesenchymal stem cells for cartilage regeneration, J. Tissue Eng. 11 (2020), 2041731420943839.

[338] L. Yu, Y. Tian, Y. Qiao, X. Liu, Mn-containing titanium surface with favorable osteogenic and antimicrobial functions synthesized by PIII&D, Colloids Surf. B Biointerfaces 152 (2017) 376–384.

[339] D. Jiao, A. Zheng, Y. Liu, X. Zhang, X. Wang, J. Wu, W. She, K. Lv, L. Cao, X. Jiang, Bidirectional differentiation of BMSCs induced by a biomimetic procallus based on a gelatin-reduced graphene oxide reinforced hydrogel for rapid bone regeneration, Bioact. Mater. 6 (2021) 2011–2028.

[340] A. Dickhut, K. Pelttari, P. Janicki, W. Wagner, V. Eckstein, M. Egermann, W. Richter, Calcification or dedifferentiation: requirement to lock mesenchymal stem cells in a desired differentiation stage, J. Cell. Physiol. 219 (2009) 219–226.

[341] Y. Zhu, L. Kong, F. Farhadi, W. Xia, J. Chang, Y. He, H. Li, An injectable continuous stratified structurally and functionally biomimetic construct for enhancing osteochondral regeneration, Biomaterials 192 (2019) 149–158.

[342] M.P. Murphy, L.S. Koepke, M.T. Lopez, X. Tong, T.H. Ambrosi, G.S. Gulati, O. Marecic, Y. Wang, R.C. Ransom, M.Y. Hoover, Articular cartilage regeneration by activated skeletal stem cells, Nat. Med. 26 (2020) 1583–1592.

[343] O. Duchamp de Lageneste, A. Julien, R. Abou-Khalil, G. Frangi, C. Carvalho, N. Cagnard, C. Cordier, S.J. Conway, C. Colnot, Periosteum contains skeletal stem cells with high bone regenerative potential controlled by Periostin, Nat. Commun. 9 (2018) 1–15.

[344] M.T. Rodrigues, M.E. Gomes, R.L. Reis, Current strategies for osteochondral regeneration: from stem cells to pre-clinical approaches, Curr. Opin. Biotechnol. 22 (2011) 726–733.

[345] K. Takahashi, S. Yamanaka, Induction of pluripotent stem cells from mouse embryonic and adult fibroblast cultures by defined factors, Cell 126 (2006) 663–676.

[346] Y. Xu, C. Chen, P.B. Hellwarth, X. Bao, Biomaterials for stem cell engineering and biomanufacturing, Bioact. Mater. 4 (2019) 366–379.

[347] R. Castro Viñuelas, C. Sanjurjo-Rodríguez, M. Piñeiro-Ramil, T. Hermida Gómez, I.M. Fuentes Boquete, F.J.d. Toro Santos, F.J. Blanco García, S. Díaz-Prado, Induced pluripotent stem cells for cartilage repair: current status and future perspectives, Eur. Cell. Mater. 36 (2018) 96–109.

[348] Y. Nam, Y.A. Rim, S.M. Jung, J.H. Ju, Cord blood cell-derived iPSCs as a new candidate for chondrogenic differentiation and cartilage regeneration, Stem Cell Res. Ther. 8 (2017) 1–13.

[349] M. Zhang, J. Shi, M. Xie, J. Wen, K. Niibe, X. Zhang, J. Luo, R. Yan, Z. Zhang, H. Egusa, Recapitulation of cartilage/bone formation using iPSCs via biomimetic 3D rotary culture approach for developmental engineering, Biomaterials 260 (2020) 120334.

[350] S. Uto, S. Nishizawa, A. Hikita, T. Takato, K. Hoshi, Application of induced pluripotent stem cells for cartilage regeneration in CLAWN miniature pig osteochondral replacement model, Regenerative Therapy 9 (2018) 58–70.

[351] C. Murphy, A. Mobasheri, Z. Táncos, J. Kobolák, A. Dinnyés, The potency of induced pluripotent stem cells in cartilage regeneration and osteoarthritis treatment, Cell Biology and Translational Medicine 1 (2017) 55–68.

[352] M.S. Lach, M.A. Rosochowicz, M. Richter, I. Jagiełło, W.M. Suchorska, T. Trzeciak, The induced pluripotent stem cells in articular cartilage regeneration and disease modelling: are we ready for their clinical use? Cells 11 (2022) 529.

[353] M.-S. Lee, M.J. Stebbins, H. Jiao, H.-C. Huang, E.M. Leiferman, B.E. Walczak, S. P. Palecek, E.V. Shusta, W.-J. Li, Comparative evaluation of isogenic mesodermal and ectomesodermal chondrocytes from human iPSCs for cartilage regeneration, Sci. Adv. 7 (2021), eabf0907.

[354] I. Urlić, A. Ivković, Cell sources for cartilage repair—biological and clinical perspective, Cells 10 (2021) 2496.

[355] T.S. de Windt, L.A. Vonk, I.C. Slaper-Cortenbach, M.P. van den Broek, R. Nizak, M.H. van Rijen, R.A. de Weger, W.J. Dhert, D.B. Saris, Allogeneic mesenchymal stem cells stimulate cartilage regeneration and are safe for single-stage cartilage repair in humans upon mixture with recycled autologous chondrons, Stem Cell. 35 (2017) 256–264.

[356] P. Kumar, S. Kandoi, R. Misra, S. Vijayalakshmi, K. Rajagopal, R.S. Verma, The mesenchymal stem cell secretome: a new paradigm towards cell-free therapeutic mode in regenerative medicine, Cytokine Growth Factor Rev. 46 (2019) 1–9.

[357] S. Jiang, G. Tian, X. Li, Z. Yang, F. Wang, Z. Tian, B. Huang, F. Wei, K. Zha, Z. Sun, Research progress on stem cell therapies for articular cartilage regeneration, Stem Cell. Int. 2021 (2021).

[358] M. Lo Monaco, G. Merckx, J. Ratajczak, P. Gervois, P. Hilkens, P. Clegg, A. Bronckaers, J.-M. Vandeweerd, I. Lambrichts, Stem cells for cartilage repair: preclinical studies and insights in translational animal models and outcome measures, Stem Cell. Int. (2018) 2018.

[359] S. Jiang, G. Tian, Z. Yang, X. Gao, F. Wang, J. Li, Z. Tian, B. Huang, F. Wei, X. Sang, Enhancement of acellular cartilage matrix scaffold by Wharton's jelly mesenchymal stem cell-derived exosomes to promote osteochondral regeneration, Bioact. Mater. 6 (2021) 2711–2728.

[360] C.T. Jayasuriya, Q. Chen, Potential benefits and limitations of utilizing chondroprogenitors in cell-based cartilage therapy, Connect. Tissue Res. 56 (2015) 265–271.

[361] J. Galle, A. Bader, P. Hepp, W. Grill, B. Fuchs, J. Kas, A. Krinner, B. MarquaB, K. Muller, J. Schiller, Mesenchymal stem cells in cartilage repair: state of the art and methods to monitor cell growth, differentiation and cartilage regeneration, Curr. Med. Chem. 17 (2010) 2274–2291.

[362] W. Wei, H. Dai, Articular cartilage and osteochondral tissue engineering techniques: recent advances and challenges, Bioact. Mater. 6 (2021) 4830–4855.

[363] H. Kwon, W.E. Brown, C.A. Lee, D. Wang, N. Paschos, J.C. Hu, K.A. Athanasiou, Surgical and tissue engineering strategies for articular cartilage and meniscus repair, Nat. Rev. Rheumatol. 15 (2019) 550–570.

[364] Z. Huang, S.-D. Bao, Roles of main pro-and anti-angiogenic factors in tumor angiogenesis, World J. Gastroenterol. 10 (2004) 463.

[365] G. Chen, N. Kawazoe, Porous Scaffolds for Regeneration of Cartilage, Bone and Osteochondral Tissue, Osteochondral tissue engineering, 2018, pp. 171–191.

[366] W. Zhang, C. Ling, A. Zhang, H. Liu, Y. Jiang, X. Li, R. Sheng, Q. Yao, J. Chen, An all-silk-derived functional nanosphere matrix for sequential biomolecule delivery and in situ osteochondral regeneration, Bioact. Mater. 5 (2020) 832–843.

[367] P.C. Bessa, M. Casal, R. Reis, Bone morphogenetic proteins in tissue engineering: the road from the laboratory to the clinic, part I (basic concepts), Journal of tissue engineering and regenerative medicine 2 (2008) 1–13.

[368] Z. Deng, Y. Li, X. Gao, G. Lei, J. Huard, Bone morphogenetic proteins for articular cartilage regeneration, Osteoarthritis Cartilage 26 (2018) 1153–1161.

[369] R. Vayas, R. Reyes, M.R. Arnau, C. Évora, A. Delgado, Injectable scaffold for bone marrow stem cells and bone morphogenetic protein-2 to repair cartilage, Cartilage 12 (2021) 293–306.

[370] C. Wang, H. Zang, D. Zhou, Bone morphogenetic protein-2 exhibits therapeutic benefits for osteonecrosis of the femoral head through induction of cartilage and bone cells, Exp. Ther. Med. 15 (2018) 4298–4308.

[371] A. Carreira, F. Lojudice, E. Halcsik, R. Navarro, M. Sogayar, J. Granjeiro, Bone morphogenetic proteins: facts, challenges, and future perspectives, J. Dent. Res. 93 (2014) 335–345.

[372] O.P. Gautschi, S.P. Frey, R. Zellweger, Bone morphogenetic proteins in clinical applications, ANZ J. Surg. 77 (2007) 626–631.

[373] S. Chubinskaya, M. Hurtig, D.C. Rueger, OP-1/BMP-7 in cartilage repair, Int. Orthop. 31 (2007) 773–781.

[374] H.K. Kim, J.H. Kim, D.S. Park, K.S. Park, S.S. Kang, J.S. Lee, M.H. Jeong, T. R. Yoon, Osteogenesis induced by a bone forming peptide from the prodomain region of BMP-7, Biomaterials 33 (2012) 7057–7063.

[375] I. El Bialy, W. Jiskoot, M. Reza Nejadnik, Formulation, delivery and stability of bone morphogenetic proteins for effective bone regeneration, Pharmaceut. Res. 34 (2017) 1152–1170.

[376] E.P. Ramly, A.R. Alfonso, R.S. Kantar, M.M. Wang, J.R.D. Siso, A. Ibrahim, P. G. Coelho, R.L. Flores, Safety and efficacy of recombinant human bone morphogenetic protein-2 (rhBMP-2) in craniofacial surgery, Plastic and Reconstructive Surgery Global Open 7 (2019).

[377] J. Sun, J. Lyu, F. Xing, R. Chen, X. Duan, Z. Xiang, A biphasic, demineralized, and Decellularized allograft bone-hydrogel scaffold with a cell-based BMP-7 delivery system for osteochondral defect regeneration, J. Biomed. Mater. Res. 108 (2020) 1909–1921.

[378] A. Daluiski, T. Engstrand, M.E. Bahamonde, L.W. Gamer, E. Agius, S.L. Stevenson, K. Cox, V. Rosen, K.M. Lyons, Bone morphogenetic protein-3 is a negative regulator of bone density, Nat. Genet. 27 (2001) 84–88.

[379] C. Chen, K.J. Grzegorzewski, S. Barash, Q. Zhao, H. Schneider, Q. Wang, M. Singh, L. Pukac, A.C. Bell, R. Duan, An integrated functional genomics screening program reveals a role for BMP-9 in glucose homeostasis, Nat. Biotechnol. 21 (2003) 294–301.

[380] Q. Kang, M.H. Sun, H. Cheng, Y. Peng, A. Montag, A. Deyrup, W. Jiang, H. Luu, J. Luo, J. Szatkowski, Characterization of the distinct orthotopic bone-forming activity of 14 BMPs using recombinant adenovirus-mediated gene delivery, Gene Ther. 11 (2004) 1312–1320.

[381] Y. Shyng, C. Chi, H. Devlin, P. Sloan, Healing of tooth extraction sockets in the streptozotocin diabetic rat model: induction of cartilage by BMP-6, Growth Factors 28 (2010) 447–451.

[382] L.F. Mendes, W.L. Tam, Y.C. Chai, L. Geris, F.P. Luyten, S.J. Roberts, Combinatorial analysis of growth factors reveals the contribution of bone morphogenetic proteins to chondrogenic differentiation of human periosteal cells, Tissue Eng. C Methods 22 (2016) 473–486.

[383] C. Ude, H. Chen, M. Norhamdan, B. Azizi, B. Aminuddin, B. Ruszymah, The evaluation of cartilage differentiations using transforming growth factor beta3 alone and with combination of bone morphogenetic protein-6 on adult stem cells, Cell Tissue Bank. 18 (2017) 355–367.

[384] M.B. Sporn, A.B. Roberts, L.M. Wakefield, B. de Crombrugghe, Some recent advances in the chemistry and biology of transforming growth factor-beta, J. Cell Biol. 105 (1987) 1039–1045.

[385] E. Grimaud, D. Heymann, F. Rédini, Recent advances in TGF-β effects on chondrocyte metabolism: potential therapeutic roles of TGF-β in cartilage disorders, Cytokine Growth Factor Rev. 13 (2002) 241–257.

[386] A. Patil, R. Sable, R. Kothari, An update on transforming growth factor-β (TGF-β): sources, types, functions and clinical applicability for cartilage/bone healing, J. Cell. Physiol. 226 (2011) 3094–3103.

[387] J. Moroco, R. Hinton, P. Buschang, S. Milam, A. Iacopino, Type II collagen and TGF-βs in developing and aging porcine mandibular condylar cartilage: immunohistochemical studies, Cell Tissue Res. 289 (1997) 119–124.

[388] H. Murata, L. Zhou, S. Ochoa, A. Hasan, E. Badiavas, V. Falanga, TGF-β3 stimulates and regulates collagen synthesis through TGF-β1-dependent and independent mechanisms, J. Invest. Dermatol. 108 (1997) 258–262.

[389] Q.O. Tang, K. Shakib, M. Heliotis, E. Tsiridis, A. Mantalaris, U. Ripamonti, E. Tsiridis, TGF-β3: a potential biological therapy for enhancing chondrogenesis, Expet Opin. Biol. Ther. 9 (2009) 689–701.

[390] J. Lee, S. Lee, S.J. Huh, B.J. Kang, H. Shin, Directed regeneration of osteochondral tissue by hierarchical assembly of spatially organized composite spheroids, Adv. Sci. 9 (2022) 2103525.

[391] Q. Sun, L. Zhang, T. Xu, J. Ying, B. Xia, H. Jing, P. Tong, Combined use of adipose derived stem cells and TGF-β3 microspheres promotes articular cartilage regeneration in vivo, Biotech. Histochem. 93 (2018) 168–176.

[392] C. Wang, H. Yue, W. Huang, X. Lin, X. Xie, Z. He, X. He, S. Liu, L. Bai, B. Lu, Cryogenic 3D printing of heterogeneous scaffolds with gradient mechanical strengths and spatial delivery of osteogenic peptide/TGF-β1 for osteochondral tissue regeneration, Biofabrication 12 (2020), 025030.

[393] G.I. Im, Regeneration of articular cartilage using adipose stem cells, J. Biomed. Mater. Res. 104 (2016) 1830–1844.

[394] R. Reyes, A. Delgado, E. Sanchez, A. Fernandez, A. Hernandez, C. Evora, Repair of an osteochondral defect by sustained delivery of BMP-2 or TGFβ1 from a bilayered alginate–PLGA scaffold, Journal of tissue engineering and regenerative medicine 8 (2014) 521–533.

[395] P. Diaz-Rodriguez, J.D. Erndt-Marino, T. Gharat, D.J. Munoz Pinto, S. Samavedi, R. Bearden, M.A. Grunlan, W.B. Saunders, M.S. Hahn, Toward zonally tailored scaffolds for osteochondral differentiation of synovial mesenchymal stem cells, J. Biomed. Mater. Res. B Appl. Biomater. 107 (2019) 2019–2029.

[396] D.L. Dorcemus, H.S. Kim, S.P. Nukavarapu, Gradient scaffold with spatial growth factor profile for osteochondral interface engineering, Biomed. Mater. 16 (2021), 035021.

[397] S. Lu, J. Lam, J.E. Trachtenberg, E.J. Lee, H. Seyednejad, J.J. van den Beucken, Y. Tabata, M.E. Wong, J.A. Jansen, A.G. Mikos, Dual growth factor delivery from bilayered, biodegradable hydrogel composites for spatially-guided osteochondral tissue repair, Biomaterials 35 (2014) 8829–8839.

[398] C. Wang, R.M. Silverman, J. Shen, R.J. O'Keefe, Distinct metabolic programs induced by TGF-β1 and BMP2 in human articular chondrocytes with osteoarthritis, Journal of orthopaedic translation 12 (2018) 66–73.

[399] J. Andrae, R. Gallini, C. Betsholtz, Role of platelet-derived growth factors in physiology and medicine, Genes Dev. 22 (2008) 1276–1312.

[400] C.-H. Heldin, B. Westermark, Mechanism of Action and in Vivo Role of Platelet-Derived Growth Factor, Physiological reviews, 1999.

[401] M. Schmidt, E. Chen, S. Lynch, A review of the effects of insulin-like growth factor and platelet derived growth factor on in vivo cartilage healing and repair, Osteoarthritis Cartilage 14 (2006) 403–412.

[402] L. Tavelli, A. Ravidà, S. Barootchi, L. Chambrone, W. Giannobile, Recombinant human platelet–derived growth factor: a systematic review of clinical findings in oral regenerative procedures, JDR Clinical & Translational Research 6 (2021) 161–173.

[403] S.-Q. Xu, J.-Y. Wei, J. Xie, X.-D. Zhou, The Role of Platelet-Derived Growth Factor-AA in the Pathogenesis and Development of Osteoarthritis, Sichuan da xue xue bao, Yi xue ban= Journal of Sichuan University. Medical science edition 53 (2022) 349–354.

[404] I.G.N.Y. Setiawan, I.K. Suyasa, P. Astawa, I.W.S. Dusak, I.K.S. Kawiyana, I.G.N. W. Aryana, Recombinant platelet derived growth factor-BB and hyaluronic acid effect in rat osteoarthritis models, J. Orthop. 16 (2019) 230–233.

[405] P. Zhu, Z. Wang, Z. Sun, B. Liao, Y. Cai, Recombinant platelet-derived growth factor-BB alleviates osteoarthritis in a rat model by decreasing chondrocyte apoptosis in vitro and in vivo, J. Cell Mol. Med. 25 (2021) 7472–7484.

[406] S. Sarban, H. Tabur, F. Baba, U.E. Işıkan, The positive impact of platelet-derived growth factor on the repair of full-thickness defects of articular cartilage, Joint Diseases and Related Surgery 30 (2019) 91–96.

[407] Y. Luo, X. Cao, J. Chen, J. Gu, H. Yu, J. Sun, J. Zou, Platelet-derived growth factor-functionalized scaffolds for the recruitment of synovial mesenchymal stem cells for osteochondral repair, Stem Cell. Int. 2022 (2022).

[408] L. Lei, Y. Mao, Hormone treatments in congestive heart failure, J. Int. Med. Res. 46 (2018) 2063–2081.

[409] L. Gasparini, H. Xu, Potential roles of insulin and IGF-1 in Alzheimer's disease, Trends Neurosci. 26 (2003) 404–406.

[410] L.M. Cordeiro, M.L. Machado, A.F. da Silva, F.B.O. Baptista, T.L. da Silveira, F.A. A. Soares, L.P. Arantes, Rutin protects Huntington's disease through the insulin/IGF1 (IIS) signaling pathway and autophagy activity: study in Caenorhabditis elegans model, Food Chem. Toxicol. 141 (2020), 111323.

[411] R.E. Miller, A.J. Grodzinsky, K. Cummings, A.H. Plaas, A.A. Cole, R.T. Lee, P. Patwari, Intra-articular injection of HB-IGF-1 sustains delivery of IGF-1 to cartilage through binding to chondroitin sulfate, Arthritis Rheum. 62 (2010) 3686.

[412] D.G. Hickey, S.R. Frenkel, P.E. Di Cesare, Clinical applications of growth factors for articular cartilage repair, Am. J. Orthoped. 32 (2003) 70–76.

[413] J. Yang, Y. Yuan, X. Hu, R. Han, M. Chen, M. Wang, X. Zhang, Y. Ma, M. Wu, Y. Zou, Low serum levels of insulin-like growth factor-1 are associated with an increased risk of rheumatoid arthritis: a systematic review and meta-analysis, Nutr. Res. 69 (2019) 9–19.

[414] H. Cho, J. Kim, S. Kim, Y.C. Jung, Y. Wang, B.-J. Kang, K. Kim, Dual delivery of stem cells and insulin-like growth factor-1 in coacervate-embedded composite hydrogels for enhanced cartilage regeneration in osteochondral defects, J. Contr. Release 327 (2020) 284–295.

[415] M.K. Boushell, C.Z. Mosher, G.K. Suri, S.B. Doty, E.J. Strauss, E.B. Hunziker, H. H. Lu, Polymeric mesh and insulin-like growth factor 1 delivery enhance cell homing and graft– cartilage integration, Ann. N. Y. Acad. Sci. 1442 (2019) 138–152.

[416] M.B. Gugjoo, Amarpal, A. Abdelbaset-Ismail, H.P. Aithal, P. Kinjavdekar, G. S. Kumar, G.T. Sharma, Allogeneic mesenchymal stem cells and growth factors in gel scaffold repair osteochondral defect in rabbit, Regen. Med. 15 (2020) 1261–1275.

[417] M.B. Gugjoo, A. Abdelbaset-Ismail, H.P. Aithal, P. Kinjavdekar, A.M. Pawde, G. S. Kumar, G.T. Sharma, Mesenchymal stem cells with IGF-1 and TGF-β1 in laminin gel for osteochondral defects in rabbits, Biomed. Pharmacother. 93 (2017) 1165–1174.

[418] J.C. Lui, J. Colbert, C.S.F. Cheung, M. Ad, A. Lee, Z. Zhu, K.M. Barnes, D. S. Dimitrov, J. Baron, Cartilage-targeted IGF-1 treatment to promote longitudinal bone growth, Mol. Ther. 27 (2019) 673–680.

[419] C.-Y. Chen, K.-Y. Tseng, Y.-L. Lai, Y.-S. Chen, F.-H. Lin, S. Lin, Overexpression of insulin-like growth factor 1 enhanced the osteogenic capability of aging bone marrow mesenchymal stem cells, Theranostics 7 (2017) 1598.

[420] A. Kasprzak, A. Adamek, Insulin-like growth factor 2 (IGF2) signaling in colorectal cancer—from basic research to potential clinical applications, Int. J. Mol. Sci. 20 (2019) 4915.

[421] D. Bergman, M. Halje, M. Nordin, W. Engström, Insulin-like growth factor 2 in development and disease: a mini-review, Gerontology 59 (2013) 240–249.

[422] D.M. Ornitz, P.J. Marie, Fibroblast growth factor signaling in skeletal development and disease, Genes Dev. 29 (2015) 1463–1486.

[423] J. Zhang, Z. Liu, Y. Li, Q. You, J. Yang, Y. Jin, G. Zou, J. Tang, Z. Ge, Y. Liu, FGF2: a key regulator augmenting tendon-to-bone healing and cartilage repair, Regen. Med. 15 (2020) 2129–2142.

[424] W. Yang, Y. Cao, Z. Zhang, F. Du, Y. Shi, X. Li, Q. Zhang, Targeted delivery of FGF2 to subchondral bone enhanced the repair of articular cartilage defect, Acta Biomater. 69 (2018) 170–182.

[425] H. Maehara, S. Sotome, T. Yoshii, I. Torigoe, Y. Kawasaki, Y. Sugata, M. Yuasa, M. Hirano, N. Mochizuki, M. Kikuchi, Repair of large osteochondral defects in rabbits using porous hydroxyapatite/collagen (HAp/Col) and fibroblast growth factor-2 (FGF-2), J. Orthop. Res. 28 (2010) 677–686.

[426] Y.P. Morscheid, J.K. Venkatesan, G. Schmitt, P. Orth, D. Zurakowski, S. Speicher-Mentges, M.D. Menger, M.W. Laschke, M. Cucchiarini, H. Madry, rAAV-mediated human FGF-2 gene therapy enhances osteochondral repair in a clinically relevant large animal model over time in vivo, Am. J. Sports Med. 49 (2021) 958–969.

[427] A. Vukasovic, M.A. Asnaghi, P. Kostesic, H. Quasnichka, C. Cozzolino, M. Pusic, L. Hails, N. Trainor, C. Krause, E. Figallo, Bioreactor-manufactured cartilage grafts repair acute and chronic osteochondral defects in large animal studies, Cell Prolif 52 (2019), e12653.

[428] H. Chen, Y. Cui, D. Zhang, J. Xie, X. Zhou, The role of fibroblast growth factor 8 in cartilage development and disease, J. Cell Mol. Med. 26 (2022) 990–999.

[429] M.P. Valta, T. Hentunen, Q. Qu, E.M. Valve, A. Harjula, J.A. Seppänen, H. K. Väänänen, P.L. Härkönen, Regulation of osteoblast differentiation: a novel function for fibroblast growth factor 8, Endocrinology 147 (2006) 2171–2182.

[430] D. Correa, R.A. Somoza, P. Lin, S. Greenberg, E. Rom, L. Duesler, J.F. Welter, A. Yayon, A.I. Caplan, Sequential exposure to fibroblast growth factors (FGF) 2, 9 and 18 enhances hMSC chondrogenic differentiation, Osteoarthritis Cartilage 23 (2015) 443–453.

[431] S. Zhou, Z. Wang, J. Tang, W. Li, J. Huang, W. Xu, F. Luo, M. Xu, J. Wang, X. Wen, Exogenous fibroblast growth factor 9 attenuates cartilage degradation and aggravates osteophyte formation in post-traumatic osteoarthritis, Osteoarthritis Cartilage 24 (2016) 2181–2192.

[432] E. Moore, A. Bendele, D. Thompson, A. Littau, K. Waggie, B. Reardon, J. Ellsworth, Fibroblast growth factor-18 stimulates chondrogenesis and cartilage repair in a rat model of injury-induced osteoarthritis, Osteoarthritis Cartilage 13 (2005) 623–631.

[433] Y. Mori, T. Saito, S.H. Chang, H. Kobayashi, C.H. Ladel, H. Guehring, U.-i. Chung, H. Kawaguchi, Identification of fibroblast growth factor-18 as a molecule to protect adult articular cartilage by gene expression profiling, J. Biol. Chem. 289 (2014) 10192–10200.

[434] H. Hendesi, S. Stewart, M.L. Gibison, H. Guehring, D.W. Richardson, G.R. Dodge, Recombinant fibroblast growth factor-18 (sprifermin) enhances microfracture-induced cartilage healing, J. Orthop. Res. 40 (2022) 553–564.

[435] L. Pesesse, C. Sanchez, Y. Henrotin, Osteochondral plate angiogenesis: a new treatment target in osteoarthritis, Joint Bone Spine 78 (2011) 144–149.

[436] L. García-Fernández, Osteochondral Angiogenesis and Promoted Vascularization: New Therapeutic Target, Osteochondral Tissue Engineering, 2018, pp. 315–330.

[437] R. Franses, D. McWilliams, P. Mapp, D. Walsh, Osteochondral angiogenesis and increased protease inhibitor expression in OA, Osteoarthritis Cartilage 18 (2010) 563–571.

[438] H. Utsunomiya, X. Gao, H. Cheng, Z. Deng, G. Nakama, R. Mascarenhas, J. L. Goldman, S.K. Ravuri, J.W. Arner, J.J. Ruzbarsky, Intra-articular injection of bevacizumab enhances bone marrow stimulation–mediated cartilage repair in a rabbit osteochondral defect model, Am. J. Sports Med. 49 (2021) 1871–1882.

[439] S. Suri, D.A. Walsh, Osteochondral alterations in osteoarthritis, Bone 51 (2012) 204–211.

[440] G. Vadalà, F. Russo, M. Musumeci, A. Giacalone, R. Papalia, V. Denaro, Targeting VEGF-A in cartilage repair and regeneration: state of the art and perspectives, J. Biol. Regul. Homeost. Agents 32 (2018) 217–224.

[441] D. Barati, S.R.P. Shariati, S. Moeinzadeh, J.M. Melero-Martin, A. Khademhosseini, E. Jabbari, Spatiotemporal release of BMP-2 and VEGF enhances osteogenic and vasculogenic differentiation of human mesenchymal stem cells and endothelial colony-forming cells co-encapsulated in a patterned hydrogel, J. Contr. Release 223 (2016) 126–136.

[442] B. De la Riva, E. Sánchez, A. Hernández, R. Reyes, F. Tamimi, E. López-Cabarcos, A. Delgado, C. Évora, Local controlled release of VEGF and PDGF from a combined brushite–chitosan system enhances bone regeneration, J. Contr. Release 143 (2010) 45–52.

[443] H. Tian, A. Guo, K. Li, B. Tao, D. Lei, Z. Deng, Effects of a novel self-assembling peptide scaffold on bone regeneration and controlled release of two growth factors, J. Biomed. Mater. Res. 110 (2022) 943–953.

[444] F.E. Freeman, P. Pitacco, L.H. van Dommelen, J. Nulty, D.C. Browe, J.-Y. Shin, E. Alsberg, D.J. Kelly, 3D bioprinting spatiotemporally defined patterns of growth factors to tightly control tissue regeneration, Sci. Adv. 6 (2020), eabb5093.

[445] R. Sakata, T. Kokubu, I. Nagura, N. Toyokawa, A. Inui, H. Fujioka, M. Kurosaka, Localization of vascular endothelial growth factor during the early stages of osteochondral regeneration using a bioabsorbable synthetic polymer scaffold, J. Orthop. Res. 30 (2012) 252–259.

[446] Q. Yuan, L. Sun, J.-J. Li, C.-H. An, Elevated VEGF levels contribute to the pathogenesis of osteoarthritis, BMC Muscoskel. Disord. 15 (2014) 1–8.

[447] K. Lingaraj, C.K. Poh, W. Wang, Vascular endothelial growth factor (VEGF) is expressed during articular cartilage growth and re-expressed in osteoarthritis, Ann. Acad. Med. Singapore 39 (2010) 399.

[448] J.L. Hamilton, M. Nagao, B.R. Levine, D. Chen, B.R. Olsen, H.J. Im, Targeting VEGF and its receptors for the treatment of osteoarthritis and associated pain, J. Bone Miner. Res. 31 (2016) 911–924.

[449] T. Matsumoto, G. Cooper, B. Gharaibeh, L. Meszaros, G. Li, A. Usas, F. Fu, J. Huard, Blocking VEGF as a potential approach to improve cartilage healing after osteoarthritis, J. Musculoskelet. Neuronal Interact. 8 (2008) 316–317.

[450] E.A. Sastre, K. Maly, M. Zhu, J. Witte-Bouma, D. Trompet, A. Böhm, B. Brachvogel, C. van Nieuwenhoven, C. Maes, G. van Osch, Spatiotemporal distribution of thrombospondin-4 and-5 in cartilage during endochondral bone formation and repair, Bone 150 (2021), 115999.

[451] K. Shin, Y. Cha, Y.-H. Ban, D.W. Seo, E.-K. Choi, D. Park, S.K. Kang, J.C. Ra, Y.-B. Kim, Anti-osteoarthritis effect of a combination treatment with human adipose tissue-derived mesenchymal stem cells and thrombospondin 2 in rabbits, World J. Stem Cell. 11 (2019) 1115.

[452] I. Côrtes, R.A. Matsui, M.S. Azevedo, A. Beatrici, K.L. Souza, G. Launay, F. Delolme, J.M. Granjeiro, C. Moali, L.S. Baptista, A scaffold-and serum-free method to mimic human stable cartilage validated by secretome, Tissue Eng. 27 (2021) 311–327.

[453] E. Helgeland, T.O. Pedersen, A. Rashad, A.C. Johannessen, K. Mustafa, A. Rosén, Angiostatin-functionalized collagen scaffolds suppress angiogenesis but do not induce chondrogenesis by mesenchymal stromal cells in vivo, J. Oral Sci. 62 (2020) 371–376.

[454] M. Centola, F. Abbruzzese, C. Scotti, A. Barbero, V. Vadala, V. Denaro, I. Martin, M. Trombetta, A. Rainer, A. Marsano, Scaffold-based delivery of a clinically relevant anti-angiogenic drug promotes the formation of in vivo stable cartilage, Tissue Eng. 19 (2013) 1960–1971.

[455] T. Nagai, M. Sato, M. Kobayashi, M. Yokoyama, Y. Tani, J. Mochida, Bevacizumab, an anti-vascular endothelial growth factor antibody, inhibits osteoarthritis, Arthritis Res. Ther. 16 (2014) 1–12.

[456] T. Nagai, M. Sato, T. Kutsuna, M. Kokubo, G. Ebihara, N. Ohta, J. Mochida, Intravenous administration of anti-vascular endothelial growth factor humanized monoclonal antibody bevacizumab improves articular cartilage repair, Arthritis Res. Ther. 12 (2010) 1–10.

[457] T. Lammers, A.M. Sofias, R. Van der Meel, R. Schiffelers, G. Storm, F. Tacke, S. Koschmieder, T.H. Brümmendorf, F. Kiessling, J.M. Metselaar, Dexamethasone nanomedicines for COVID-19, Nat. Nanotechnol. 15 (2020) 622–624.

[458] R.M. Johnson, J.M. Vinetz, Dexamethasone in the Management of Covid-19, British Medical Journal Publishing Group, 2020.

[459] M. Merad, J.C. Martin, Pathological inflammation in patients with COVID-19: a key role for monocytes and macrophages, Nat. Rev. Immunol. 20 (2020) 355–362.

[460] S. Ashraf, P.I. Mapp, D.A. Walsh, Contributions of angiogenesis to inflammation, joint damage, and pain in a rat model of osteoarthritis, Arthritis Rheum. 63 (2011) 2700–2710.

[461] G. Zhou, W. Liu, L. Cui, X. Wang, T. Liu, Y. Cao, Repair of porcine articular osteochondral defects in non-weightbearing areas with autologous bone marrow stromal cells, Tissue Eng. 12 (2006) 3209–3221.

[462] A.J. Grodzinsky, Y. Wang, S. Kakar, M.S. Vrahas, C.H. Evans, Intra-articular dexamethasone to inhibit the development of post-traumatic osteoarthritis, J. Orthop. Res. 35 (2017) 406–411.

[463] K.D. Huebner, N.G. Shrive, C.B. Frank, Dexamethasone inhibits inflammation and cartilage damage in a new model of post-traumatic osteoarthritis, J. Orthop. Res. 32 (2014) 566–572.

[464] S. Tangtrongsup, J.D. Kisiday, Effects of dexamethasone concentration and timing of exposure on chondrogenesis of equine bone marrow–derived mesenchymal stem cells, Cartilage 7 (2016) 92–103.

[465] S. Camarero-Espinosa, J.J. Cooper-White, Combinatorial presentation of cartilage-inspired peptides on nanopatterned surfaces enables directed differentiation of human mesenchymal stem cells towards distinct articular chondrogenic phenotypes, Biomaterials 210 (2019) 105–115.

[466] R.M. Stefani, A.J. Lee, A.R. Tan, S.S. Halder, Y. Hu, X.E. Guo, A.M. Stoker, G. A. Ateshian, K.G. Marra, J.L. Cook, Sustained low-dose dexamethasone delivery via a PLGA microsphere-embedded agarose implant for enhanced osteochondral repair, Acta Biomater. 102 (2020) 326–340.

[467] D. Algul, A. Gokce, A. Onal, E. Servet, A.I. Dogan Ekici, F.G. Yener, In vitro release and in vivo biocompatibility studies of biomimetic multilayered alginate-chitosan/β-TCP scaffold for osteochondral tissue, J. Biomater. Sci. Polym. Ed. 27 (2016) 431–440.

[468] K. Johnson, S. Zhu, M.S. Tremblay, J.N. Payette, J. Wang, L.C. Bouchez, S. Meeusen, A. Althage, C.Y. Cho, X. Wu, A stem cell–based approach to cartilage repair, Science 336 (2012) 717–721.

[469] E. Music, T. Klein, W. Lott, M. Doran, Transforming growth factor-beta stimulates human bone marrow-derived mesenchymal stem/stromal cell chondrogenesis more so than kartogenin, Sci. Rep. 10 (2020) 1–10.

[470] H. Jing, X. Zhang, M. Gao, K. Luo, W. Fu, M. Yin, W. Wang, Z. Zhu, J. Zheng, X. He, Kartogenin preconditioning commits mesenchymal stem cells to a precartilaginous stage with enhanced chondrogenic potential by modulating JNK and β-catenin–related pathways, Faseb. J. 33 (2019) 5641–5653.

[471] J. Zhang, J.H. Wang, Kartogenin induces cartilage-like tissue formation in tendon–bone junction, Bone research 2 (2014) 1–10.

[472] M.L. Kang, J.-Y. Ko, J.E. Kim, G.-I. Im, Intra-articular delivery of kartogenin-conjugated chitosan nano/microparticles for cartilage regeneration, Biomaterials 35 (2014) 9984–9994.

[473] G. Mohan, S. Magnitsky, G. Melkus, K. Subburaj, G. Kazakia, A.J. Burghardt, A. Dang, N.E. Lane, S. Majumdar, Kartogenin treatment prevented joint degeneration in a rodent model of osteoarthritis: a pilot study, J. Orthop. Res. 34 (2016) 1780–1789.

[474] J.Y. Kwon, S.H. Lee, H.-S. Na, K. Jung, J. Choi, K.H. Cho, C.-Y. Lee, S.J. Kim, S.-H. Park, D.-Y. Shin, Kartogenin inhibits pain behavior, chondrocyte

inflammation, and attenuates osteoarthritis progression in mice through induction of IL-10, Sci. Rep. 8 (2018) 1–11.

[475] C.-Y. Chen, C. Li, C.-J. Ke, J.-S. Sun, F.-H. Lin, Kartogenin enhances chondrogenic differentiation of MSCs in 3D tri-copolymer scaffolds and the self-designed bioreactor system, Biomolecules 11 (2021) 115.

[476] Q. Hu, B. Ding, X. Yan, L. Peng, J. Duan, S. Yang, L. Cheng, D. Chen, Polyethylene glycol modified PAMAM dendrimer delivery of kartogenin to induce chondrogenic differentiation of mesenchymal stem cells, Nanomed. Nanotechnol. Biol. Med. 13 (2017) 2189–2198.

[477] S.-J. Wang, J.-Z. Qin, T.-E. Zhang, C. Xia, Intra-articular injection of kartogenin-incorporated thermogel enhancing osteoarthritis treatment, Front. Chem. (2019) 677.

[478] D. Shi, X. Xu, Y. Ye, K. Song, Y. Cheng, J. Di, Q. Hu, J. Li, H. Ju, Q. Jiang, Photo-cross-linked scaffold with kartogenin-encapsulated nanoparticles for cartilage regeneration, ACS Nano 10 (2016) 1292–1299.

[479] X. Ji, H. Shao, X. Li, M.W. Ullah, G. Luo, Z. Xu, L. Ma, X. He, Z. Lei, Q. Li, Injectable immunomodulation-based porous chitosan microspheres/HPCH hydrogel composites as a controlled drug delivery system for osteochondral regeneration, Biomaterials 285 (2022) 121530.

[480] A.B. Houreh, E. Masaeli, M.H. Nasr-Esfahani, Chitosan/polycaprolactone multilayer hydrogel: a sustained Kartogenin delivery model for cartilage regeneration, Int. J. Biol. Macromol. 177 (2021) 589–600.

[481] L. Zheng, D. Li, W. Wang, Q. Zhang, X. Zhou, D. Liu, J. Zhang, Z. You, J. Zhang, C. He, Bilayered scaffold prepared from a kartogenin-loaded hydrogel and bmp-2-derived peptide-loaded porous nanofibrous scaffold for osteochondral defect repair, ACS Biomater. Sci. Eng. 5 (2019) 4564–4573.

[482] Y. Dong, Y. Liu, Y. Chen, X. Sun, L. Zhang, Z. Zhang, Y. Wang, C. Qi, S. Wang, Q. Yang, Spatiotemporal regulation of endogenous MSCs using a functional injectable hydrogel system for cartilage regeneration, NPG Asia Mater. 13 (2021) 1–17.

[483] X. Xu, Y. Liang, X. Li, K. Ouyang, M. Wang, T. Cao, W. Li, J. Liu, J. Xiong, B. Li, Exosome-mediated delivery of kartogenin for chondrogenesis of synovial fluid-derived mesenchymal stem cells and cartilage regeneration, Biomaterials 269 (2021), 120539.

[484] B. Almeida, Y. Wang, A. Shukla, Effects of nanoparticle properties on kartogenin delivery and interactions with mesenchymal stem cells, Ann. Biomed. Eng. 48 (2020) 2090–2102.

[485] W.-N. Zeng, Y. Zhang, D. Wang, Y.-P. Zeng, H. Yang, J. Li, C.-P. Zhou, J.-L. Liu, Q.-J. Yang, Z.-L. Deng, Intra-articular injection of kartogenin-enhanced bone marrow–derived mesenchymal stem cells in the treatment of knee osteoarthritis in a rat model, Am. J. Sports Med. 49 (2021) 2795–2809.

[486] C. Scotti, D. Wirz, F. Wolf, D.J. Schaefer, V. Bürgin, A.U. Daniels, V. Valderrabano, C. Candrian, M. Jakob, I. Martin, Engineering human cell-based, functionally integrated osteochondral grafts by biological bonding of engineered cartilage tissues to bony scaffolds, Biomaterials 31 (2010) 2252–2259.

[487] H. Yuk, C.E. Varela, C.S. Nabzdyk, X. Mao, R.F. Padera, E.T. Roche, X. Zhao, Dry double-sided tape for adhesion of wet tissues and devices, Nature 575 (2019) 169–174.

[488] X. Niu, N. Li, Z. Du, X. Li, Integrated gradient tissue-engineered osteochondral scaffolds: challenges, current efforts and future perspectives, Bioact. Mater. 20 (2023) 574–597.

[489] A. León-López, A. Morales-Peñaloza, V.M. Martínez-Juárez, A. Vargas-Torres, D. I. Zeugolis, G. Aguirre-Álvarez, Hydrolyzed collagen—sources and applications, Molecules 24 (2019) 4031.

[490] W.W. Chan, D.C.L. Yeo, V. Tan, S. Singh, D. Choudhury, M.W. Naing, Additive biomanufacturing with collagen inks, Bioengineering 7 (2020) 66.

[491] N. Diamantides, C. Dugopolski, E. Blahut, S. Kennedy, L.J. Bonassar, High density cell seeding affects the rheology and printability of collagen bioinks, Biofabrication 11 (2019), 045016.

[492] Q. Zuo, S. Lu, Z. Du, T. Friis, J. Yao, R. Crawford, I. Prasadam, Y. Xiao, Characterization of nano-structural and nano-mechanical properties of osteoarthritic subchondral bone, BMC Muscoskel. Disord. 17 (2016) 1–13.

[493] S.-W. Tsai, F.-Y. Hsu, P.-L. Chen, Beads of collagen–nanohydroxyapatite composites prepared by a biomimetic process and the effects of their surface texture on cellular behavior in MG63 osteoblast-like cells, Acta Biomater. 4 (2008) 1332–1341.

[494] X. Cai, B. Han, Y. Liu, F. Tian, F. Liang, X. Wang, Chlorhexidine-loaded amorphous calcium phosphate nanoparticles for inhibiting degradation and inducing mineralization of type I collagen, ACS Appl. Mater. Interfaces 9 (2017) 12949–12958.

[495] Y.S. Kim, A.G. Mikos, Emerging strategies in reprogramming and enhancing the fate of mesenchymal stem cells for bone and cartilage tissue engineering, J. Contr. Release 330 (2021) 565–574.

[496] D. Parate, N.D. Kadir, C. Celik, E.H. Lee, J.H. Hui, A. Franco-Obregón, Z. Yang, Pulsed electromagnetic fields potentiate the paracrine function of mesenchymal stem cells for cartilage regeneration, Stem Cell Res. Ther. 11 (2020) 1–16.

[497] A.W. James, G. LaChaud, J. Shen, G. Asatrian, V. Nguyen, X. Zhang, K. Ting, C. Soo, A review of the clinical side effects of bone morphogenetic protein-2, Tissue Eng. B Rev. 22 (2016) 284–297.

[498] Y. Dong, X. Sun, Z. Zhang, Y. Liu, L. Zhang, X. Zhang, Y. Huang, Y. Zhao, C. Qi, A. C. Midgley, Regional and sustained dual-release of growth factors from biomimetic tri-layered scaffolds for the repair of large-scale osteochondral defects, Appl. Mater. Today 19 (2020), 100548.